Adaptive MAC protocol for self-deployment of WSNs in restrictive and constrained environment

Moises Nuñez Ochoa

THÈSE

Pour obtenir le grade de

DOCTEUR DE L'UNIVERSITÉ DE GRENOBLE

Spécialité : **Informatique**

Arrêté ministériel : 25 mai 2016

Présentée par

Moisés Nuñez Ochoa

Thèse dirigée par **Andrzej Duda**
et coencadrée par **Mickael Maman**

préparée au sein de
CEA-Leti Grenoble (France),
Laboratoire d'Informatique de Grenoble (LIG),
et de **l'École Doctorale Mathématiques, Sciences et Technologies de l'Information, Informatique (EDMSTII).**

Protocole adaptatif pour un auto-déploiement de réseaux de capteurs dans un environnement contraignant

Thèse soutenue publiquement le **17 juin 2020**,
devant le jury composé de :

M. Vivien Quéma
Professeur, Grenoble INP / ENSIMAG, Président
M. Alexandre Guitton
Professeur, Université Clermont Auvergne, ISIMA, Rapporteur
M. Razvan Stanica
Professeur, INSA Lyon, CITI Lab, INRIA, Rapporteur
Mme. Christelle Caillouet
Professeure, Université Côte d'Azur, I3S Lab, INRIA, Examinatrice
M. Andrzej Duda
Professeur, Université Grenoble Alpes, LIG Lab, Directeur de thèse
M. Mickael Maman (invité)
Ingénieur chercheur, CEA Léti, Co-Encadrant de thèse

I dedicate this thesis to Benjamin and Ivette.

Acknowledgments

This work would not have been possible without the help of many interesting people who guided and inspired me. I would like to express my gratitude to all people who have contributed to the success of this thesis.

First, I would like to express my appreciation to my supervisor, Mickael Maman. I am really thankful for his support and guidance in my research. I would like to thank him for the encouragement, kindness, and patience. I would also like to thank my thesis director, Andrzej Duda, for his advice and guidance.

I would like to thank the jury members, Prof. Alexandre Guitton, Prof. Razvan Stanica, Prof. Christelle Caillouet, and Prof. Vivien Quéma, for reviewing and evaluating my manuscript. Their expert insights have helped me to improve my thesis.

I would like to thank my colleagues in STSF/DRT/CEA-Leti and Drakkar/LIG, for the friendly working environment and facilities to complete my thesis.

Furthermore, I would like to thank my friends for their support, encouragement, kindness, and all the fun we have during the period of my thesis work.

I would like to thank my family for their understanding, continuous encouragement, and support. Thank you for being interested and thinking I did something with the Internet and computers.

I would also like to thank FONDECYT-CONCYTEC of the Peruvian government for the funding.

Finally, I would like to thank all those who contributed from near or far to this work. *¡Muchas gracias!*

Abstract

WSN *(Wireless Sensor Networks)* frequently deployed in harsh environments need to be autonomous with optimized lifetime, reliable connectivity, and robust to interference. The objective of this thesis is to make WSN deployments easier in harsh environments by self-deploying and adapting these networks to the context.

In this thesis, we started by comparing LPWAN technologies and we focused on LoRa offering several degrees of freedom on its communication parameters and making a good candidate for adaptive networks.

Five contributions have been achieved throughout this work.

In the first contribution, we analytically investigated the energy efficiency for different network topologies to improve energy consumption by adapting LoRa communication parameters in star and mesh topologies. The impact on energy consumption of the network density and network coverage is also investigated.

The second contribution is the development of a LoRa network simulator based on WSNet, an event-driven simulator for large scale WSN. It implements the required communication protocol layers and simulates the network behavior with a high level of accuracy. In that sense, we integrated new features of transceivers such as LoRa Semtech and reconfiguration functionalities in the WSNet simulator.

In the third contribution , we investigated performance and limitations of LoRa networks by taking into account only the Physical layer and by including the protocol ADR *(Adaptive Data Rate)* proposed by LoRaWAN. First, we investigated LoRa deployments of nodes with homogeneous parameters. This investigation allows us to obtain the performance of each spreading factor individually to calculate their capacity for each network size assuring a given packet delivery ratio. Second, we investigated LoRa deployments of nodes with heterogeneous parameters. This investigation explores more spreading factor allocation protocols to improve network performance by exploiting LoRa physical layer features such as spreading factor quasi-orthogonality. Finally, we investigated in detail performance analysis of the spreading factor allocation protocol based on the link budget that corresponds to ADR of the LoRaWAN under steady-state assumptions. This analysis allows us to understand the impact of allocating the spreading factor using ADR on the network performance in several aspects: (i) network deployment, (ii) environment, (iii) multiple channels, and (iv) bidirectional communications.

In the fourth contribution, we propose enhancements by allocating spreading factors optimally to improve reliability and fairness taking into account deployment constraints and exploiting LoRa properties. The objective is to avoid the strong impact of the network deployment on network performance. We proposed several strategies to deploy LoRa networks by adapting the parameter spreading factor at the initialization when all nodes join the network. We also proposed improvements to the classical spreading factor allocation, the ADR mechanism that depends on the network deployment impacting the network performance. They improve the network capacity and transmission quality in terms of packet delivery ratio.

In the last contribution, we proposed a strategy to self-deploy LoRa networks by adapting the spreading factor parameter over time when nodes join progressively the network. The strategy is based on the link, network, and distribution metrics of previous joined end-devices to set up the configuration of joining end-devices to self-deploy LoRa networks according to the context. We can use current network performance metrics to configure an end-device joining the network.

Contents

List of Figures

Introduction

Context

During the last years, the number of connected devices has grown exponentially reaching tens of billions [1][2] and overtaking the global population [3]. There are more connected devices than people. In fact, the IoT (*Internet of Things*) applications [4][5], such as *Smart Cities* and *Smart Homes*, are connecting more devices than ever before (massive IoT) increasing the density and scale of the sensor deployments (large-scale) [6][7][8]. These deployments are composed of things capable to sense the environment, communicate with other things, and make intelligent decisions. Wireless networks are required to connect these things providing robust and energy-efficient operations while covering wider geographical areas. Things are expected to operate for a longer period (five to ten years) without any maintenance as they are typically battery-powered, and also to cover large areas [9]. Traditional technologies such as cellular (2G, 3G, and 4G) and non-cellular (short-range Bluetooth, and Zigbee) are not fully suitable to face this growth rate and the deployment problems involved. On the one hand, cellular technologies offer good throughput and communication range but they consume energy reducing the battery lifetime of the devices. On the other hand, non-cellular Bluetooth, and Zigbee technologies offer good battery lifetime but limited communication range and throughput.

In this context, LPWAN (*Low Power Wide Area Network*) has emerged as an alternative to traditional technologies [5][10] providing low power connectivity and low data rate while covering large areas through a simple network topology [11]. In the literature, several studies have reviewed different LPWAN technologies among standardization activities: IEEE (*Institute of Electrical and Electronics Engineers*), IETF (*Internet Engineering Task Force*), 3GPP (*3rd Generation Partnership Project*), ETSI (*European Telecommunications Standards Institute*) as well as industrial activities: LoRa (*Long Range*) alliance, Weightless-SIG, Dash7 alliance [11]. They can be divided into networks based on cellular infrastructure [9][12], networks with third-party infrastructure [13], and autonomous networks without any third-party infrastructure [14]. The first group, NB-IoT (*Narrow Band Internet of Things*) [12], LTE-M (*Long Term Evolution for Machines*) [15][16], EC-GSM (*Extended Coverage - Global System for Mobile*) [17] raised intensive research to overcome heavy interference problems due to a new massive wave of IoT devices in addition to the already densely populated existing cellular network. The second group includes proprietary networks and service providers such as Ingenu [18], SigFox [13], and Weightless [19]. The last group includes the LoRa technology, which is an open-source technology that enables autonomous network set-up at low cost [9].

LPWAN aims to accommodate the IoT demand [20], more particularly to connect WSN (*Wireless Sensor Networks*). These networks composed of sensor devices and gateways are characterized by the following constraints: critical energy on the side of the sensors, critical communication range, susceptibility to interference, and infrequent transmissions of small data. The principal problems in WSN deployments are coverage and connectivity. Furthermore, WSN deployments need to be autonomously operational without manual instructions to minimize maintenance costs. The network should self-deploy and adapt its configurations according to environment changes, due to interference, for example, to optimize a performance indicator such as power consumption or the packet delivery ratio. In the self-deployment approach, the network can take into account the environment by measuring link quality indicators or metrics. Then, it analyzes these metrics to make a decision. Finally, it applies this decision of re-configuring the network to optimize its performance, e.g., reliability and energy efficiency.

Among the LPWAN technologies we will focus on the LoRa technology because it presents several advantages for adaptive networks to self-deploy WSN. These advantages are the degrees of freedom of its communication parameters, the adaptation flexibility, the maturity of the solution, the openness of the technology, and the robustness to interference thanks to its chirp spread spectrum modulation. LoRa networks have been largely deployed for private networks (like smart buildings [21], smart cities [22], smart agriculture [23], smart meters [24], smart islands [25], smart golf course [26], smart water quality

monitoring [27][28][29][30], and smart air quality monitoring [31][32][33]) thanks to its low-cost and its subscription-less feature, reducing large-scale deployment costs. However, LoRa has presented several challenges [34][35][36][37] in terms of: network scalability and adaptation to use cases with high congestion. Several solutions have been proposed to deal with these problems. They can be divided in two categories: *link adaptation* and *network densification* strategies. Furthermore, none of these studies have evaluated both strategies with all the network parameters such as device configuration heterogeneity, network topology, deployment density and traffic intensity. In this thesis, we evaluate these strategies using an accurate simulator taking into account the quasi-orthogonality of the spreading factors, gateway capture effect, and realistic use of the spectrum considering the time-frequency dependency of the communications.

Scope and Motivation

This thesis has been developed within the Wireless Communications Department at CEA-Leti and the Drakkar Group at Grenoble Informatics Laboratory.

This work is performed in the context of WSN frequently deployed in harsh environments. These networks need to be autonomous with optimized lifetime, reliable connectivity, and robust to interference. In that sense, the objective of this thesis is to ensure the Internet of Things communication with high reliability, energy-efficiency, and robust to interference by exploiting a new generation of transceivers, such as LoRa Semtech transceivers, within a communication protocol stack. Moreover, this thesis aims to make wireless sensor network deployments easier in harsh environments by self-deploying these networks and adapting to the context. In this thesis, we will focus on a static approach in the context of network deployment automation. We will propose a protocol to detect, characterize, and adapt the radio transceiver parameters to optimize the link budget and increase the reliability taking into account the constraints of coverage and connectivity of the WSN, as well as capacities and limitations of the LoRa technology.

To achieve the objectives of the thesis, we decided to follow a simulation approach using the WSNet (*Wireless Sensor Networks Simulator*) that is an event-driven simulator for large scale WSN. We followed this approach rather than real test-beds because it is more practical for implementing and testing the adaptive protocols to self-deploy WSN. The real implementation constraint of large scale deployments is the cost that would involve the deployment of thousands of devices. Note that at the beginning of this thesis there were a limited number of LoRa simulators. We decided to use and improve the WSNet simulator because it implements the required communication protocol layers and simulates the network behavior with a high level of accuracy. In that sense, we integrate new features of transceivers such as LoRa Semtech and reconfiguration functionalities in the WSNet simulator. Thus, we developed additional more realistic models such as the model of the LoRa PHY (*physical*) layer to exploit spatial reuse and the orthogonality of spreading factors. Moreover, a MAC (*Medium Access Control*) layer model in a star topology or a star of star topology was developed to evaluate the impact of the protocol on the network performance.

This work extends the knowledge about LPWAN technologies, more specifically, the LoRa technology in large scale deployments, its performance, limitations, and flexibility for adaptive networks. This thesis aims to answer the self-deployment issues of WSN by adapting the network to improve its performance. It addresses the following research questions:

Question 1: What are the different LPWAN technologies? What are their advantages and limitations?

There are several LPWAN technologies composed of various implementations and protocols. They could be proprietary or open-source that principally share some characteristics such as operation on small inexpensive batteries for years, and operating range typically of kilometers. However, a physical limitation to achieve long-range and low consumption is the small data size and data rate. More specifically, we would like to know about the adaptability of its communication parameters, scalability, and coverage. These questions will be answered in Chapter 1.

Question 2: How flexible is the LoRa technology for adaptive networks? What are the degrees of freedom of the LoRa technology? Is there an interest for energy saving?

Among the existing LPWAN technologies, we are looking for the most suitable one for adaptive networks. It seems that the LoRa technology could be a good candidate to focus on due to the degrees of freedom of its communication parameters. We would like to know how flexible this technology is, by taking into account energy consumption constraints, deployment density of end-devices, and the communication coverage. The LoRa technology is characterized by low power consumption, long communication range, and massive access deployments. In Chapter 2 of this thesis we theoretically analyze the impact on the energy consumption of varying LoRa communication parameters such as the transmission power, the spreading factor of the modulation, the bandwidth, and deployment.

Question 3: What are the performance and limitations of LoRa technology for massive access of end-devices? What is the impact of varying its communication parameters? What are the weaknesses of LoRaWAN and the Adaptive Data Rate?

We analyze performance and limitations of LoRa technology by simulation taking into account more realistic hypothesis such as the constraints of the network implementation and deployment . We would like to know the limitations of the LoRa technology in massive access deployments. They involve interference and packet collision problems that need to be considered. Thus, we analyze performance in terms of reliability and throughput through accurate simulations using the WSNet simulator. Furthermore, we would like to know the limitations of the ADR (*Adaptive Data Rate*) mechanism proposed by LoRaWAN to improve it taking into account: the capacity of each spreading factor, the orthogonality of spreading factors, the traffic intensity, multiple channels, bi-directional communication (uplink and downlink), multiple gateways, different environments, etc. These questions will be answered in Chapter 3.

Question 4: How to improve the performance and reliability of LoRa networks? How to adapt its communication parameters? How to efficiently deploy LoRa networks depending on the context?

We look for improving LoRa performance because the ADR is not appropriate to the context, nor to the massive number of nodes, nor to the access with multiple gateways. Through a simulation approach, we are going to focus on supporting a massive number of end-devices while still providing good packet delivery ratio and communication range by adapting the LoRa communication parameters, more particularly the spreading factor. To deal with these requirements, we propose two types of solutions: link adaptation and network densification. We propose solutions for single-gateway scenarios and multi-gateway scenarios by adapting the spreading factor at the initialization of the network operation when all nodes join the network. These questions will be answered in the first part of Chapter 4.

Question 5: How to self-deploy LoRa networks by adapting its communication parameters over time when end-devices progressively join the network?

The LoRa technology aims to connect a massive number of end-devices sharing the limited spectrum. The massive access problem involves two aspects: link coordination and resource allocation. Massive deployments require link coordination through MAC protocols to avoid collisions. We are going to focus on the resource allocation of the communication parameters. Varying LoRa communication parameters result in different transmission qualities. Thus, efficiently allocating resources to end-devices based on the deployed environment improves massive access, scalability, and reliability. We are going to allocate spreading factors to end-devices following the self-deployment approach: measuring metrics, analyzing to take a decision, and applying the decision to allocate the optimal spreading factor to end-devices. Furthermore, we propose a solution to improve the LoRaWAN adaptive data rate mechanism in a more realistic scenario by adapting the spreading factor over time when nodes progressively join the network. Note that in this approach new nodes joining the network are configured without modifying the nodes that already joined the network. This approach is more realistic because there are several private LoRa networks already deployed and we do not have access to modify the node's configuration of those networks. However, we can measure the current network performance and based on that we can configure a node joining our network. These questions will be answered in the second part of Chapter 4.

Contributions

We present five contributions organized into three axes addressing the above questions. The first axis includes Contribution 1 where we theoretically analyze the LoRa technology flexibility for adaptive networks. We propose adaptation strategies for saving energy. The second axis includes the LoRa simulator based on WSNet that is the Contribution 2: we developed several modules considering the characteristics of the LoRa Semtech transceivers and the LoRaWAN protocol. Finally, the third axis is based on the analysis of the simulation results including Contributions 3, 4, and 5. They are the following: performance and limitation analysis of LoRa networks for massive access devices, an improvement on performance through spreading factor allocation strategies, and adaptation strategy to self deploy LoRa networks in more realistic scenarios. Our principal contributions are listed below:

Contribution 1: Analyzing LoRa technology for adaptive networks. Evaluating the flexibility of its communication parameters. Theoretically showing the interest of LoRa for energy saving. Proposing adaptation strategies of its communication parameters for energy saving.

We analytically investigate the energy efficiency for different network topologies to improve energy consumption by adapting LoRa communication parameters in star and mesh topologies. The impact on energy consumption of the network density and network coverage is also investigated. We implemented an analytical model in Matlab according to the LoRaWAN specification and technical documents.

Contribution 2: Developing and implementing a LoRa simulator based on WSNet.

We use an accurate and realistic WSNet-based simulator [38] written in C / Modern C++ under CeCILL free license. WSNet is a modular event-driven wireless network simulator that implements the required communication protocol layers and simulates the network behavior with a high level of accuracy. We have extended the simulator in several aspects (e.g., spectrum use, interference, capture effect) to take into account flexibility and specificity of the LoRa PHY / MAC layers.

Contribution 3: Analysing performance and limitation of LoRa network deployments for massive access of end-devices. Showing the impact of varying its communication parameters for different network sizes and different traffic intensities.

The first part of this contribution is the investigation of LoRa network deployments of nodes with homogeneous communication parameters. This investigation allows us to obtain the performance of each spreading factor individually to calculate their capacity for each network size assuring a given packet delivery ratio. This individual spreading factor performance allows us to understand advantages and limitations, and also to propose more allocation protocols using different spreading factors. The second part of this contribution is the investigation of LoRa network deployments of nodes with heterogeneous communication parameters. This investigation explores more spreading factor allocation protocols to improve network performance by exploiting LoRa physical layer features such as spreading factor quasi-orthogonality. These spreading factor allocation protocols configure nodes: (i) according to their link budget like the ADR of the LoRaWAN specification, (ii) randomly, and (iii) aiming at an equal number of nodes per spreading factor. The final part of this contribution is the detailed performance analysis of the spreading factor allocation protocol based on the link budget that corresponds to the ADR of the LoRaWAN under steady-state assumptions. This analysis allows us to understand the impact of allocating the spreading factor using ADR on the network performance in several aspects: (i) network deployment, (ii) environment, (iii) multiple channels, and (iv) bidirectional communications. We evaluate all these aspects under the same assumptions. Capabilities and limitations are clarified to investigate more optimal allocation protocols exploiting principally the individual capacity of each spreading factor and their quasi-orthogonality to improve the ratio of received packets.

Contribution 4: Improving the performance of LoRa networks through efficient spreading factor allocations. Proposing network deployment strategies to make LoRa deployments easier depending on the context.

Improvements are proposed because the network deployment should not have a strong impact on network performance. We propose several strategies to deploy LoRa networks by adapting the parameter

spreading factor at the initialization when all nodes join the network. We propose improvements to the classical spreading factor allocation and to the adaptive data rate mechanism that depends on the network deployment impacting the network performance: (i) enhanced link adaptation, and (ii) joint link and topology adaptation strategies. They improve the network capacity and transmission quality in terms of packet delivery ratio.

Contribution 5: Proposing adaptation strategies to self-deploy LoRa networks over time when end-devices progressively join the network.

We propose a strategy to self-deploy LoRa networks by adapting the spreading factor parameter over time when nodes progressively join the network. We propose a progressively joining strategy based on the link, network, and distribution metrics of previous joined end-devices to set up the configuration of joining end-devices to self-deploy LoRa networks according to the context. Note that we have no influence on the configuration of the end-devices that already joined the network because there could be other private LoRa networks deployed on the same geographical area as our LoRa network. However, we can use current network performance metrics to configure an end-device joining the network.

Contributions Beyond the State of the Art

Given the state of the art, several insights and strategies were proposed for link adaptation and topology adaptation. In this thesis, we perform a global evaluation of different communication parameters using the radio LoRa technology. The research challenges in LoRa deployments can be divided into five categories: (i) energy consumption, (ii) communication range, (iii) multiple access, (iv) error correction, and (v) security. Among these categories, this thesis investigates (i), (ii), and (iii).

Error correction is not considered in this thesis. However, it is important to notice that corrupted packets due to channel effects or environmental conditions can be overtaken with two types of solutions [9]: (i) channel coding and (ii) interference cancellation. These solutions could improve performance by decoding even corrupted messages. Security is also a major issue, but this thesis does not consider it. Nevertheless, note that several investigations are been carried out.

Energy consumption:

Energy consumption is a major challenge for LoRa networks. Nodes are expected to have 5 to 10 years of life time with minimal maintenance. Consumption can be due to (i) micro-controller operations and (ii) wireless transmissions. LoRa consumes less energy by directly using the bandwidth for transmitting a signal and employing light MAC protocols. However, nodes consume more power due to unavoidable circumstances like network deployment constraints (nodes located far from the gateway), network topology, and collisions followed by re-transmissions.

From the literature, authors identified that generating carrier signals is the most power consumption operation. They also identified that LoRa is able to receive weak signals but decoding them depends on the signal SNR and the minimum SNR that the receiver can demodulate. They suggest to place more gateways and to allocate dynamically the transmitted power to face energy consumption issues. However, note that no performance analysis (neither theoretical nor by simulation) have been made on energy consumption.

In this thesis, more particularly in Chapter 2, we address the energy consumption problem exploiting the flexibility of several radio LoRa parameters and not only the transmitted power. These parameters are: (i) the transmitted power, (ii) the spreading factor, and (iii) the bandwidth. We analytically investigate energy consumption due to LoRa wireless transmissions and receptions varying these radio parameters for different network topologies (star and mesh). Indeed, we investigate what parameter should be adapted to optimize energy consumption and the different trade-offs when changing a parameter. For example, decreasing the spreading factor and the transmitted power may reduce energy consumption but we need to clarify which variation better optimizes energy consumption. We may gain in energy consumption but

communication range is reduced. Hence, the impact of the network density and network coverage are investigated to propose adaptation strategies to adapt the LoRa radio parameters and network topology.

Communication range:

Estimating the coverage of LoRa networks is also a challenge. LoRa deployments aim to include several scenarios and use cases. We have to take into account diverse deployment conditions and propagation loss to improve the network coverage. Attenuated signals below a given threshold may be detected by the gateways but not decoded. Thus, the communication range could be improved with new techniques for decoding these signals, placing more gateways, or with multi-hop communications.

From the literature, authors performed test-bed measurements [9][39] and proposed solutions to improve the communication range of sparse deployments. They also proposed new hardware to extend coverage and battery lifetime. They gave some insights found from experimental measurements. They suggest to place more gateways to increase network density. However, note that at the moment when we started this thesis, no analysis had been made about network deployment with multiple gateways. Moreover, only the star topology was considered for LoRa deployments, which may be improved using mesh topologies by increasing communication range through relay nodes.

In this thesis, we theoretically investigate the communication range and energy consumption of transmitting and receiving packets through some relay nodes (multi-hop communication) by adapting the radio LoRa parameters. We improve the communication range using a mesh topology and we evaluate energy consumption depending on the network coverage. Moreover, we propose an adaptation strategy to switch from the star topology to the mesh topology depending on the communication range and network density. Passing to the mesh topology allows to reach longer distances. This thesis also investigates the impact of different environments (e.g. factory of the future), network topologies, multiple gateway (adding gateways increases the network coverage and the network performance), the minimum number of gateways required to cover the whole area of deployment, and their positioning. We propose strategies giving the number of required gateways to cover and assure a given reliability for a given network size. These strategies make LoRa deployments easier.

Multiple access:

Connecting a massive number of devices is also a major issue. It is expected that LoRa networks connect thousand of devices sharing the limited spectrum. Multiple access involves several problems and they can be divided into two groups according to the literature: (i) Link coordination and (ii) Resource allocation. The first one aims to coordinate transmissions using MAC protocols to avoid collisions. The second one aims to allocate resources reasonably to devices depending on the deployment constraints to improve scalability and massive access. When we talk about resources, we mean the radio LoRa parameters: TP (transmission power), SF (spreading factor), BW (bandwidth), channel, which affect the transmission quality.

From the literature, authors suggested to take advantage of new LoRa gateways able to receive packets with different SFs in the same channel simultaneously to improve packet delivery [40]. They also recommend further investigation varying transmission parameters according to the deployment environment. They investigated several solutions, but most of them only considered homogeneous communication parameters of devices. There are some solutions [41][42][43][44][45][46][47][48] considering heterogeneous communication parameters allocating SFs with the ADR mechanism for example. However, they did not consider the fact that SFs are not completely orthogonal. In fact, SFs are quasi-orthogonal, there is rejection between signals with different SF on the same channel. Furthermore, the ADR mechanism has drawbacks and does not exploit all the potential of the LoRa technology, more specifically the quasi-orthogonality of SFs. Densifying the network by increasing the gateways may improve network performance but it increases collisions because the number of devices using low SFs increases, saturating these low SFs. Thus, the ADR mechanism needs to be improved through fairer SF allocation depending on the environment and deployment constraints.

In this thesis, we investigate performance of LoRa deployments connecting a massive number of devices and different traffic intensities. To do this, we investigate the capacity of each *SF* depending on the traffic and the number of end-devices. Then, we investigate multiple access of end-devices with heterogeneous parameters taking into account that *SFs* are not fully orthogonal. Co-channel rejection of different *SFs* is considered in our interference model in WSNet allowing more accurate simulation results. Thus, we investigate heterogeneous communication parameters of devices and how they impact performance. Indeed, we explore several *SF* allocation strategies to self-adapt the network. We aim to allocate optimally the *SFs* considering the packet delivery ratio and throughput as performance metrics. Furthermore, we investigate in detail the ADR performance showing the impact of the deployment, and its drawbacks when over-using and under-using *SFs* to improve it.

Outline

This thesis is organized into two parts: (i) state of the art and (ii) contributions. The first part presents the state of the art of the LPWAN technologies in the context of IoT and WSN. It presents the existing solutions and a table comparison. Furthermore, we present the LoRa technology, its characteristics, the LoRaWAN protocol, and the reasons why we have chosen it for adaptive networks. Moreover, we present the related work of LoRa deployments, link and topology adaptation, and a discussion of the general methodology followed in this thesis. The second part presents our contributions divided into three chapters: 2, 3, and 4. This thesis is organized as follows:

Part I, Chapter 1: LPWAN and LoRa. This chapter investigates the LPWAN landscape of the technologies and protocols to understand features, challenges, and flexibility for adaptive networks. There are several LPWAN technologies such as LoRa, SigFox, NB-IoT, Ingenu, 802.11.ah, etc. Among these technologies, LoRa technology and the LoRaWAN specifications are presented in detail. Indeed, we analyze the degrees of freedom of the LoRa technology to adapt the network. We define the methodology for the investigation of network deployment through theoretical studies, simulations, or real measurements. This chapter also presents the related work on two major issues: (i) LoRa network deployments for which we detail work using experimental measurements or simulations, the LoRa evaluation and its limits and the LoRa network deployment strategies. (ii) LoRa adaptation for which we present the link and the topology adaptation.

Part II, Chapter 2: Is LoRa technology a good candidate for adaptive networks? This chapter investigates the degrees of freedom of LoRa communication parameters to understand the trade-offs and challenges when adapting its parameters such as the transmitted power, the spreading factor, the bandwidth, the coding rate, and the topology of the deployment. This chapter focuses on the investigation of energy consumption and the communication range as network performance indicators to decide if LoRa is an appropriate technology for adaptive networks. Thus, we analytically investigate the energy efficiency for different network topologies to improve energy consumption by adapting LoRa communication parameters in star and mesh topologies. The impact on energy consumption of the network density and network coverage is also investigated. We show the flexibility of LoRa parameters to pursue the investigation in adaptive networks.

Part II, Chapter 3: Performance and limitations of large scale LoRa networks. This chapter evaluates the performance and limitations of massive access LoRa networks for different application cases and traffic intensities. We also analyze the impact of varying the communication parameters. These analyses are done in the same simulation and under the same assumptions. Indeed, we analyze: (i) the capacity of each spreading factor in homogeneous deployments, (ii) the impact of the orthogonality of the spreading factors in heterogeneous deployments, (iii) the performance of the ADR, (iv) the impact of different environments, (v) the impact of using multiple channels, (vi) the impact of the downlink communication, and (vii) the network densification, i.e. multiple gateways.

We analyze the performance of LoRa deployment of end-devices with homogeneous and heterogeneous communication parameters to propose and evaluate spreading factor allocation strategies. Moreover, we analyze the impact of the network deployment, i.e., uniform and dense deployment of end-devices. Furthermore, we analyze the limitations of the adaptive data rate of LoRaWAN showing the trade-offs between over-used and under-used spreading factors. Another addressed important issue is the analysis of the impact of the environment, especially in a FoF (*Factory of the Future*) environment. The impact of multiple channels is also analyzed as well as the degradation of the packet delivery ratio due to downlink transmissions. Finally, we analyze the impact of improving the network density by placing multiple gateways in LoRa deployments of end-devices with homogeneous communication parameters. This analysis allows us to improve performance taking advantage of the spectrum spatial reuse and to propose an adaptation strategy giving the number of gateways needed to assure a certain level of reliability for given network size. This adaptation strategy limits the number of covered nodes per gateway serving them with better packet delivery ratio, especially in large scale deployments.

Part II, Chapter 4: Efficient spreading factor allocation in massive access LoRa multiple gateway adaptive networks. In this chapter, we look for improving the performance of LoRa massive access networks allocating efficiently the spreading factor to end-devices and increasing the network density of the infrastructure by placing more gateways in the right way. We propose improvement to the adaptive data rate mechanism of LoRaWAN: (i) the ELA (*Enhanced Link Adaptation*) algorithm and (ii) the MGELA (*Multiple Gateway Enhanced Link and Topology Adaptation*). Moreover, we propose network deployment strategies to make LoRa deployments easier depending on the context, e.g. the network size. Performance evaluation of ELA is also presented: it investigates the impact of the network deployment, the pathloss environment, multiple channels, downlink communications, and multiple gateways. Furthermore, we propose adaptation strategies to self-deploy LoRa networks over time when end-devices progressively join the network. We analyze the impact of these adaptation strategies on network performance, in uniform and dense deployments. Whatever the environment is our strategy will exploit the capacity of each spreading factor and the quasi-orthogonality of them in every gateway taking into account realistic estimated metrics based on network performance measurements. Note that there are imperfections when estimating the metrics to decide the network configuration.

Conclusion and future directions. We started by comparing different LPWANs to focus on the LoRa technology. It offers several degrees of freedom on its communication parameters making it a good candidate for adaptive networks. Then, we theoretically evaluated energy consumption of LoRa networks showing the interest to focus on LoRa for adaptive networks and we also proposed adaptation strategies. Next, we investigated performance and limitations of LoRa networks identifying drawbacks of ADR. This investigation allowed us to propose enhancements by allocating SF optimally to improve reliability and fairness taking into account deployment constraints and exploiting LoRa properties. This thesis is only a first step in LoRa adaptive networks. Future research is necessary in mesh networks, machine learning techniques for parameter allocation, experimental validation of our proposals, optimal placement of the gateways, bandwidth adaptation, and coding rate adaptation, to adapt a network deployment.

Part I

State of the Art

LPWAN and LoRa

Contents

Introduction

This chapter investigates the competitive landscape of LPWAN technologies and protocols to understand features, challenges, and flexibility for adaptive networks. We present the details of the LoRa technology and the LoRaWAN specification. Thus, we look for a technology offering flexibility and degrees of freedom of its communication parameters to focus on.

This chapter also focuses on the state of the art of LoRa technology. Mainly, it presents related work of the LoRa deployments divided in four parts: (i) the real LoRa deployments, (ii) the LoRa network deployments of both experimental measurements and simulations, (iii) the LoRa evaluation and limits, and (iv) the LoRa network deployment strategies. Moreover it presents the related work of the LoRa adaptation: (i) the link and (ii) the topology adaptation. Finally, we present the methodology of the investigation of network deployments in this thesis, i.e., through (i) theoretical studies, (ii) simulations, or (iii) real measurements.

1.1 LPWAN Technologies

LPWAN technologies are promising for the Internet of low power, low cost, and low throughput things [11] offering long range and long battery life time. They achieve a long range and low power at the cost of lower data rate. Several applications for smart cities, smart metering, environmental monitoring, logistics, agriculture, etc. require infrequent and small amount of data and longer battery life time of devices covering large areas. Thus, many LPWAN technologies generated interest for these applications. In this section, we highlight the most important LPWAN technologies.

1.1.1 LoRa

LoRa is a proprietary technology that modulates signals using a spread spectrum technique [49] developed and commercialized by Semtech [50]. It uses unlicensed ISM (*Industrial, Scientific and Medical*) bands: (i) the EU863-870 MHz and the EU433 MHz bands in Europe and some countries in Africa and Middle East, (ii) the US902-928 MHz band in North America and South America, (iii) the AS920-923 MHz band in Japan, South Korea, and some countries in Asia, (iv) the CN470-510 MHz and CN779-787 MHz bands in China, (v) the AU915-928 MHz band in Australia, and (vi) the IN865-867 MHz band in India. The LoRa technology also uses the 2.4 GHz band for smart homes and wearable IoT applications. Its physical layer is based on the CSS (*Chirp Spread Spectrum*) modulation. The CSS spreads a narrow band signal over a wider band resulting in a noise-like signal enabling resilience to interference and noise. LoRa supports multiple SF (*Spreading Factors*) trading off data rate and communication range. High SFs achieve long ranges but low data rates. Low SFs achieve high data rates but short ranges. Typical values of BW (*Bandwidth*) are 125, 250, and 500 kHz but smaller bandwidths like 62.5, 31.25, 15.625, and 7.8125 kHz are also allowed in the LoRa specification. LoRa can use several channels, i.e., frequency diversity. In Europe, ETSI regulations allow 14 dBm as the maximum Tx (*Transmit Power*) with exception of the g3 (869.4–869.65 MHz) band that allows 27 dBm. In North America it allows a Tx up to 30 dBm (typically 20 dBm). The LoRa technology allows a MCL (*Maximum Coupling Loss*) of 150 dB (sensitivity of -136 dBm and Tx of 14 dBm). The LoRa link budget allows communication ranges of tens of kilometers (typically 5-15 km) depending on the surrounding environment, the Tx of nodes, the SF, the BW, etc. The packet size depends on the SF with a maximum size between 59-230 Bytes for high and low SF respectively. In Europe the DC (*Duty Cycle*) is regulated by the ETSI EN300.220 standard [51]. This standard defines the DC of the following sub-bands: (i) 1% in g (863.0–868.0 MHz), (ii) 1% in g1 (868.0–868.6 MHz), (iii) 0.1% in g2 (868.7–869.2 MHz), (iv) 10% in g3 (869.4–869.65 MHz), and (v) 1% in g4 (869.7–870.0 MHz). LoRa allows bidirectional communications where uplink (i.e., from nodes to gateways) transmissions are predominant. The TTN (*The Things Network*) is a public community network. It has a Fair Access Policy that limits the uplink time on air to 30 s per day per node and the downlink messages to 10 messages per day per node. The data rate goes from 290 b/s to 37.5 kb/s depending on the SF, the BW, and the CR (*Coding Rate*). Thus, e.g. the TTN policy approximately allows 23 packets of 50 Bytes per day per node using SF_{12} (2816 packets of 50 Bytes per day per node using SF_6). The power consumption varies according to the output power and the supply current: (i) 0.2-1 μA in

Sleep mode, (ii) 1.5 μA in Idle mode, (iii) 1.6-1.8 mA in Standby mode, (iv) 10.3-12.6 mA in Receive mode, and (v) 20-120 mA in Transmit mode. A LoRa gateway is able to receive simultaneously multiple transmissions using different spreading factors providing a third degree of diversity along with time and frequency. LoRa allows a star of stars topology, a transmitted packet is received by all gateways in the range improving reception diversity (redundancy). Duplicate packets are eliminated in the backend system. However, multiple gateways may increase costs. The access protocol in LoRa is the simple access method ALOHA. Several commercial and industrial partners formed a group called LoRa Alliance proposing LoRaWAN which is an open standard defining upper layers. Note that LoRa denotes the physical layer while LoRaWAN denotes the MAC layer. The adaptability of this technology is based on the degrees of freedom of its parameters: (i) the Tx, (ii) the SF, (iii) the BW, (iv) the CR, (v) and the topology (star, star of stars, and mesh). Note that LoRa at 2.4 GHz allows bandwidths of 203, 406, 812, and 1625 kHz. It increases data rates up to 202 kb/s (with SF_5, 1625 kHz, and 4/5 of CR).

1.1.2 SIGFOX

SIGFOX is a service provider for IoT and offers end-to-end connectivity based on a patented technology. It uses unlicensed ISM bands: (i) the RC1 868-878.6 MHz band in Europe, Middle East and Africa, (ii) the RC2 902.1375-904.6625 MHz band in North America and Brazil, (iii) the RC3 922.3-923.5 MHz band in Japan, (iv) the RC4 920.1375-922.6625 MHz band in Latin America and Asia Pacific, (v) the RC5 922-923.4 MHz band in South Korea, (vi) the RC6 865-867 MHz band in India, and (vii) a draft of the RC7 868.8-869.1 MHz band in Russia. It uses a BPSK (*Binary Phase Shift Keying*) modulation in a UNB (*Ultra Narrow Band*) of 100 Hz. With an ultra narrow band, noise levels are low, receiver sensitivity is high and energy consumption is low. SIGFOX allows 10 μW - 100 mW of Tx. Its typical MCL is 156 dB for receiver sensitivity of -136 dBm and Tx of 20 dBm. The SIGFOX link budget allows communication range of tens of kilometers depending on the environment (e.g., 3-10 km and 30-50 km in urban and rural environments respectively). The packet size is fixed to 12 bytes upstream and 8 bytes downstream. In Europe the DC is 1 % limiting the number of uplink messages per day to 140. SIGFOX is predominantly using uplink communication with limited downlink capability. The data rate is limited to 100 b/s limiting the use cases. At the beginning, SIGFOX only supported uplink communications, but then it evolved to bidirectional asymmetric communication. Downlink communications are limited to few packets per day (4 messages of 8 bytes per day). The power consumption depends on the supply current: (i) < 4 μA in Sleep mode, (ii) < 49 mA in Transmit mode (Tx of 14 dBm), and (iii) 10 mA in Receive mode. The SIGFOX network is based on a star topology and requires an operator to carry the traffic. The access protocol in SIGFOX is an ALOHA-based protocol operating in a range of random frequency and time without having any knowledge of the channel state. Time frequency diversity and redundant transmissions improve reliability even it acknowledgements for uplinks are not supported. The frequency diversity consists of transmitting multiple times over different channels randomly selected, e.g., in Europe, the 868 MHz band is divided into 400 channels of 100 Hz [52]. The adaptability of this technology depends on the degrees of freedom of its parameters: (i) only the Tx.

1.1.3 Ingenu

Ingenu is a proprietary technology. It is known as On Ramp Wireless. Contrarily to other proprietary technologies, it operates in the 2.4 GHz ISM band leaving aside better propagation properties in sub GHz band but benefiting from more relax regulations on spectrum [53]. Ingenu uses a patented RPMA (*Random Phase Multiple Access*) [54]. The RPMA enables multiple transmitters to share a single time slot. However, it first increases time slot duration then scatters the channel by adding a random delay to each transmitter reducing overlapping and increasing SNR (Signal Noise Ratio). Gateways use multiple demodulators to decode the signals arriving at different times in a slot. The BW required is 1 MHz supporting up to 40 channels simultaneously. Ingenu allows up to 20 dBm of Tx. The RPMA offers high receiver sensitivity (-142 dBm) and 168 dB of the link budget [53]. Thus, Ingenu allows communication ranges depending on the environment, e.g., 1-3 km and 25-50 km in urban and rural environments respectively. The packet size is flexible (6 Bytes to 10 kBytes). Ingenu has no DC as it leverages the 2.4 GHz ISM band. This technology provides bidirectional communications, all messages are acknowledged. The data rate is 624 kb/s for uplink and 156 kb/s for downlink per sector assuming 8 channels access point. The current consumption of an access point is

350 mA maximum (290 mA typical). The Ingenu network is based on a star topology but a tree topology is also supported with an RPMA extender. The access protocol used by Ingenu is the LBT (*Listen-Before-Talk*). Ingenu claims high scalability adding more access points without disrupting current capacity. The adaptability of this technology depends on the degrees of freedom of its parameters: (i) TX and the (ii) data rate.

1.1.4 NB-IoT

Narrow Band IoT is a cellular IoT technology standardized by 3GPP. It can coexist with LTE (*Long Term Evolution*) and GSM (*Global System for Mobile*) cellular technologies in licensed frequency bands depending on the region. In Europe, it uses: B3 (1800 MHz), B8 (900 MHz), and B20 (800 MHz) bands. In North America, it uses: B4 (1700 MHz), B12 (700 MHz), B26 (850 MHz), B66 (1700 MHz), and B71 (600 MHz) bands. In Asia Pacific: B1 (2100 MHz), B3 (1800 MHz), B5 (850 MHz), B8 (900 MHz), B18 (850 MHz), B20 (800 MHz), B26 (850 MHz), and B28 (700 MHz) bands. In Middle East and North Africa: B8 (900 MHz) and B20 (800 MHz) bands. In Sub Saharan Africa: B3 (1800 MHz) and B8 (900 MHz) bands. In Latin America: B2 (1900 MHz), B3 (1800 MHz), B5 (850 MHz), and B28 (700 MHz) bands. NB-IOT uses SC-FDMA (*Single Carrier Frequency Division Multiple Access*) in uplink communications and OFDMA (*Orthogonal Frequency Division Multiple Access*) in downlink communications [55]. Similarly to GSM and LTE, NB-IOT uses 200 kHz of BW as a resource block. Only a software upgrade in the existing LTE infrastructure is necessary to support this technology. The maximum TX is 20 dBm. NB-IOT aims at 164 dBm of the link budget for long coverage. The communication range depends on the environment (e.g., 1-5 km and 10-15 km in urban and rural environments respectively). Its packet size is 125 bytes for uplink and 85 bytes for downlink. There is no DC limitations. NB-IOT provides bidirectional communications. The data rate is 250 kb/s with multitone configuration and 20 kb/s with single tone configuration. The power consumption depends on the supply current: (i) 4 μA in Sleep mode, (ii) 5 mA in Idle mode, (iii) 220 mA in Transmit mode, and (iv) 20 mA in Receive mode. The NB-IOT network is based on a star topology. It uses a time slotted synchronous protocol. Improvement of NB-IoT continues with new releases by 3GPP. They plan to extend this technology for localization and multicast services, mobility, and further technical details to enhance applications [56]. NB-IOT claims to serve 50 thousand nodes per gateway with the potential of scaling up by adding more carriers [11]. The adaptability of this technology depends on its degrees of freedom: (i) TX and the (ii) data rate.

1.1.5 IEEE 802.11ah

IEEE 802.11ah is is an extension of the IEEE 802.11 standard to meet IoT application requirements [57]. This standard extends the communication range and improve energy efficiency. It was proposed by the TGAH (*Task Group AH*) and TIG (*Topic Interest Group*) in LRLP (*Long Range Low Power*). It proposes the PHY and MAC layers based on IEEE 802.11ac reducing some control frames and the MAC header length. It also introduces OFDM (*Orthogonal Frequency Division Multiple*) and MIMO (*Multiple Input Multiple Output*) technologies [58]. In the sub 1 GHz ISM band, it specifies the following bands: (i) 863-868 MHZ in Europe, (ii) 902-928 MHz in USA, (iii) 755-787 MHz in China, (iv) 916.5-927.5 MHz in Japan, (v) 917.5-923.5 MHz in Korea, and (vi) 866-869 MHz and 920-925 MHz in Singapore. In the PHY layer, this standard defines different channel widths (1 MHz, 2 MHz, 4 MHz, 8 MHz, and 16 MHz). Channelization depends on the country regulations. There are several MCS (*Modulation & Coding Scheme*) operating with different bandwidths and coding rates. Modulation could be BPSK, QPSK (*Quadrature Phase-Shift Keying*) and QAM (*Quadrature Amplitude Modulation*). The TX depends on the country's regulations: 10 mW-1000 mW. Its typical link budget is 126 dB (e.g., sensitivity of -126 dBm). This link budget allows communication ranges up to 1 km outdoor. The packet size could be up to 7991 bytes without aggregation and up to 65536 bytes with aggregation. In Europe (the g 863-870 MHz band), the DC is limited to 2.8 % but devices can implement LBT and AFA (*Adaptive Frequency Agility*) mechanisms. IEEE 802.11ah provides bidirectional communications. The data rate varies from 150 kb/s up to 346.66 Mb/s in both uplink and downlink. Table 1.1 shows the data rate for different BW and different types of MCS. The typical current consumption is: (i) 300 mA in Transmit mode and (ii) 50 mA in Receive mode. Its typical network topology is star. In the MAC layer, this standard adopts a grouping-based Medium Access Control protocol in order to reduce contention overhead, support

advanced power saving mechanism, and throughput enhancement. Sensors are divided in several groups and the channel access time is divided in beacon intervals, each interval is divided in a number of equal duration RAW (*Restricted Access Window*) slots. Then, each RAW is assigned to a group of sensors, the only group allowed to access RAW, reducing collision probability [59]. The adaptability of this technology depends on its degrees of freedom: (i) TX, (ii) BW, (iii) MCS, and (iv) CR.

Table 1.1: Data rate in Mb/s for the IEEE 802.11ah standard [60].

PHY characteristics		MCS	Bandwidth				
Modulation	Coding Rate		1MHz	2MHz	4MHz	8MHz	16MHz
BPSK	1/2 & 2x repetition	MCS_0	0.30	0.65	1.35	2.93	5.85
BPSK	1/2	MCS_1	0.60	1.30	2.70	5.85	11.70
QPSK	1/2	MCS_2	0.90	1.95	4.05	8.78	17.55
QPSK	3/4	MCS_3	1.20	2.60	5.40	11.70	23.40
16-QAM	1/2	MCS_4	1.80	3.90	8.10	17.55	35.10
16-QAM	3/4	MCS_5	2.40	5.20	10.80	23.40	46.80
64-QAM	2/3	MCS_6	2.70	5.85	12.15	26.33	52.65
64-QAM	3/4	MCS_7	3.00	6.50	13.50	29.25	58.50
64-QAM	5/6	MCS_8	3.60	7.80	16.20	35.10	70.20
256-QAM	3/4	MCS_9	4.00	-	18.00	39.00	78.00
256-QAM	5/6	MCS_{10}	0.15	-	-	-	-

1.1.6 LPWAN Comparison

LoRa, SIGFOX, NB-IoT, Ingenu and IEEE 802.11ah are the leading LPWAN technologies competing for large-scale IoT deployments. Mekki et al. [56] showed that LoRa and SIGFOX are advantageous in terms of battery life time and cost. Meanwhile, NB-IoT is advantageous in terms of no DC restrictions and synchronous protocols. We compare these leading technologies in terms of quality of service, battery life time, scalability, network coverage, the deployment model, and adaptability. Furthermore Table 1.2 shows an overview comparing the LPWAN technologies. UL refers to uplink and DL referes to downlink communications.

- Quality of service: LoRa, SIGFOX, Ingenu and IEEE 802.11ah operate using unlicensed bands. LoRa and SIGFOX use asynchronous communication protocols. However, NB-IoT seems to provide better quality of service due to the use of licensed bands and LTE-based synchronous protocols. This improvement comes with an expensive cost of licensed LTE spectrum for the operators. Ingenu provides good uplink rate but it is relatively high pricing.

- Battery life time: Nodes are in sleep mode most of the time in these technologies, reducing energy consumption. However, NB-IoT (220 mA), Ingenu (290 mA) and IEEE 802.11ah (300 mA) consume more energy than LoRa (20-120 mA) and SIGFOX (49 mA).

- Scalability: All these technologies support a massive number of devices. They exploit the diversity of the channel, time, and space. However, NB-IoT and Ingenu claim high scalability connecting up to 100 thousand and 384 thousand nodes, respectively. LoRa depends on the application use case and SIGFOX is limited to 140 messages per day per node. IEEE 802.11ah connects up to 8191 devices per access point.

- Network coverage: Ingenu and NB-IoT offer the longest Link Budget (168 dB and 164 dB) covering 1-5 km in urban and 10-50 km in rural areas. LoRa and SIGFOX offer 150 dB and 156 dB of Link Budget covering 2-10 km in urban and 15-50 km in rural areas. IEEE 802.11ah offers the lowest Link Budget (126 dB) covering up to 1 km outdoor.

- Deployment model: LoRa, SIGFOX and Ingenu are mature technologies under commercialisation in several cities around the world. However, NB-IoT and IEEE 802.11ah are under standardisation and starting to be deployed. A major advantage of the LoRa technology is its flexibility offering local as well as public network deployments, contrary to SIGFOX and NB-IoT.

- Adaptability: It is the degrees of freedom of the parameters. LoRa offers the highest adaptability (TX, SF, BW, CR, and topology). IEEE 802.11ah also offers high adaptability but it is limited in coverage.

Table 1.2: LPWAN technologies comparison.

Standard	LoRa	SIGFOX	Ingenu	NB-IoT	IEEE 802.11ah
Frequency Band	ISM sub-GHz + 2.4 GHz	ISM sub-GHz	ISM 2.4 GHz	Licensed LTE band	ISM sub-GHz
Modulation	CSS, FSK	DBPSK, GFSK	RPMA-DSSS	OFDMA, SC-FDMA	OFDMA
Channel Width	125, 250, 500 kHz + 7.8, 15.6, 31.25, 62.5 kHz + 200, 400, 800, 1600 kHz @ 2.4 GHz	100 Hz	1 MHz (40 channels)	200 kHz	1,2,4,8,16 MHz
Transmit Power	EU: max. 14 dBm, US: max. 30 dBm	-20 to 20 dBm	up to 20 dBm	up to 20 dBm	0-30 dBm
Link Budget	150 dB	156 dB	168 dB	164 dB	126 dB
Range	2-5 km urban 15 km rural	3-10 km urban 30-50 km rural	1-3 km urban 25-50 km rural	1-5 km urban 10-15 km rural	up to 1 km outdoor
Packet Size	max. 59-230 bytes	12 bytes UL 8 bytes DL	flexible (6 to 10 kbytes)	125 bytes UL 85 bytes DL	up to 7991 bytes without aggregation up to 65535 bytes with aggregation
Bidirectional	yes, UL predominant	no, limited DL	yes	yes	yes
Data Rate	290 b/s to 37.5 b/s	UL: 100 b/s to 140 messages per day DL: max. 4 messages per day	UL: 624 kb/s DL: 156 kb/s (assuming 8 channels AP)	up to 250 kb/s with multitone configuration	150 kb/s - 346.66 Mb/s
Power Consumption	sleep: 0.2-1 μA idle: 1.5 μA standby: 1.6-1.8 mA Rx: 10.3-12.6 mA Tx: 20-120 mA	sleep: 4 μA Rx: 10 mA Tx: 49 mA	typical 290 mA	sleep: 4 μA idle: 5 mA Rx: 20 mA Tx: 220 mA	typical Rx: 50 mA Tx: 300 mA
Devices per Access Point	depends	up to 1 M	up to 384000 per sector	up to 100 k	8191
Topology	star of star	star	star	star	star
Protocol Access	ALOHA	ALOHA	LBT, slotted	LBT, slotted	RAW mechanism
Governing Body	LoRa Alliance	SIGFOX	Ingenu	3GPP	IEEE
Degrees of Freedom	Tx, BW, SF, CR, topology	Tx	Tx, data rate	Tx, data rate	Tx, BW, MCS, CR

At the beginning of this thesis, we explored the IEEE 802.11ah: an improvement of WiFi for IoT communications in the 1 sub-GHz ISM bands improving the range of communication and energy consumption. This technology presents some degrees of freedom, principally we can tune BW, Tx and MCS. Allowed BWs depends on the region, e.g., BW can be 1 MHZ, 2 MHZ, 4 MHz, 8 MHz, and 16 MHz. It also defines eleven MCSs and several data rates are available depending on the modulation, BW and the CR. However, communication range (up to 1km) is still limited. Thus, even though this technology seems to be a good candidate, we explored other technologies: Ingenu, NB-IoT and the popular SIGFOX and LoRa technologies. We discarded SIGFOX technology because it is proprietary technology with less degrees of freedom for adaptive networks. We also discard Ingenu and NB-IoT because of their low degrees of freedom of its parameters. On the other hand, the LoRa technology is an open technology, mature, with several degrees of freedom of its radio communication parameters. It also presents unique properties like long distance, low cost and complexity devices, long lifetime, spreading factors quasi-orthogonality allowing concurrent reception gateways, robustness to interference and Doppler effect. Indeed, a deeper analysis of the LoRa technology for adaptive networks has been required. It is presented in the following sections. Also, the impact of tuning its radio communication parameters for energy efficiency will be presented in Chapter 2.

1.2 LoRa Technology

In this section, we present in detail the physical layer of the LoRa technology. It is based on the OSSS (*Orthogonal Sequence Spread Spectrum*) using the CSS modulation patented by Cycleo [61]. LoRa trades data rate for sensitivity within a fixed channel bandwidth. It implements a variable data rate, utilizing orthogonal spreading factors to trade data rate for range or power, so as to optimize network performance [62]. Note that LoRa refers to the physical layer.

1.2.1 Architecture

The typical architecture of LoRa is composed of: end devices, gateways, a network server, and an application server as shown in Figure 1.1. The end devices, called as well nodes, are sensor devices that send data to the application server. Nodes may also receive data, more particularly, commands from the network server through the gateways to execute instructions of reconfiguration for example. A gateway covers areas where nodes should be deployed. When nodes send a packet, several gateways in the communication range may receive the same packet. In this case, the network server filters duplicate packets. Gateways forwards packets from end-devices to the backend (network and application servers). A single gateway can serve thousands of end-devices. The communication between nodes and gateways are through LoRa radio and LoRaWAN specification, while from the gateway to the network and application server, it is through high bandwidth networks like cellular 3G or 4G, WiFi, or Ethernet. The gateways are installed in fixed locations. They communicate with nodes within their coverage to acknowledge packet reception or to command reconfigurations for example. The network server forwards messages from end-devices to the application server. It is in charge of the data collection, it is able to manage and coordinate the gateways, and it knows with which gateways the nodes are able to communicate. The intelligence of the network is placed at this level allowing for network optimization (link coordination and resource allocation).

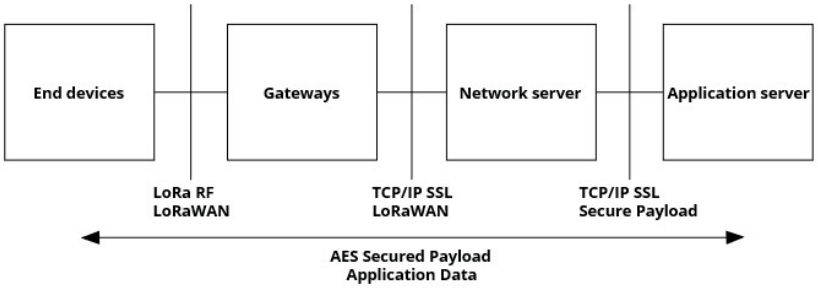

Figure 1.1: LoRa Architecture.

1.2.2 Communication Bands

The LoRa technology can operate in different unlicensed frequency bands. We can divide them into two groups: sub-GHz and GHz ISM bands. The sub-GHz bands are: (i) EU863-870 MHz and EU433 MHz in Europe, Middle East and some countries in Africa, (ii) US902-928 MHz in North America and South America, (iii) AS920-923 MHz in Japan, South Korea, and some countries in Asia, (iv) CN470-510 MHz and CN779-787 MHz in China, (v) AU915-928 MHz in Australia, and (vi) IN865-867 MHz in India. The LoRa technology also uses the 2.4 GHz band. In this thesis we assume that LoRa deployments operate in the EU863-870 MHz band (868 MHz) due to favorable propagation conditions compared to higher bands such as in the 2.4 GHz band. Another reason is that DC is regulated in the EU863-870 MHz band.

$$P_L = (\frac{4\pi df}{c})^2 \tag{1.1}$$

The free space pathloss (P_L) is shown in the equation 1.1, where c is the speed of light, f the operation frequency, and d is the communication range. Comparing the range (d) for the same budget link (difference between the transmitted power and the receiver sensitivity), the sub-GHz bands reaches longer distances than the GHz bands. Moreover, longer wavelengths penetrate thicker obstacles.

Regulations and DC restrictions are different depending on the communication band and region. In Europe, the 868 MHz band is limited in terms on DC and Tx depending on the sub-bands: (i) 1% and 14 dBm in the 863.0–868.0 MHz band, (ii) 1% and 14 dBm in the 868.0–868.6 MHz band, (iii) 0.1% and 14 dBm in the 868.7–869.2 MHz band, (iv) 10% and 27 dBm in the 869.4–869.65 MHz band, and (v) 1% and 14 dBm in the 869.7–870.0 MHz band. Note that DC restrictions do not apply if devices use LBT or CSMA (*Carrier Sense Multiple Access*). Note also that the 868.0–868.6 MHz band encompasses the three default LoRa channels of 125 kHz of BW: (i) 868.1 MHz , (ii) 868.3 MHz, and (iii) 868.5 MHz. They are spaced by 200 kHz. The default Tx is 14 dBm and the DC is < 1 %. The 2.4 GHz band allows 100 % DC, which is one of the reasons why WiFi and Bluetooth deployments are at this band. However, no DC restrictions leads to more collisions, interference, and mainly to high energy consumption. In the context of IoT and WSN at the sub GHz bands, the data packets should be small and they should be transmitted infrequently, e.g., one packet every hour.

1.2.3 Chirp Spread Spectrum Modulation

Here we focus on the CSS modulation that is used in the LoRa system. A CSS transmission occupies much larger bandwidth than is needed for the considered data rate. It is a subcategory of DSSS (*Direct-Sequence Spread Spectrum*), which takes advantage of the controlled frequency diversity to recover data from weak signals. The DSSS permits to alleviate the constraint on the receiver's sensitivity and increase the communication range at the cost of a reduced data rate. This reason makes the DSSS compliant with the IoT network requirements. In the CSS modulation, the spreading effect is obtained through a continuous variation of the carrier frequency. The spreading factor characterizes the increase in the band occupation. Each symbol is 2^{SF} chips long. The chip-rate is equal to the modulation bandwidth. Therefore, the time duration of a symbol T_{symbol} is:

$$T_{symbol} = \frac{2^{SF}}{BW} \tag{1.2}$$

where SF is the spreading factor of the modulation used in the LoRa system and BW is the bandwidth over which the signal is spread.

The LoRa waveform is given by the basic element of the CSS, i.e. the CHIRP (*Compressed High Intensity Radar Pulse*) which is defined by:

$$c(t) = \begin{cases} e^{j\Phi(t)} & ,if -\frac{T_{Symbol}}{2} \leq t \leq \frac{T_{Symbol}}{2} \\ 0 & ,otherwise. \end{cases} \tag{1.3}$$

where $\Phi(t)$ is the chirp phase. Thus, the resulting instantaneous frequency is:

$$f(t) = \frac{1}{2\pi}\frac{d\Phi(t)}{dt} \tag{1.4}$$

A linear chirp is a 1 bit coded chirp using an up-chirp (α=1) or down-chirp (α=-1) with an instantaneous frequency given by:

$$f_c(t) = F_c + \alpha\frac{BW}{T_{Symbol}}t \tag{1.5}$$

where F_c is the central frequency.

In LoRa technology, a single chirp may code up to SF=12 bits. To do so, a specific frequency trajectory is defined for each of the 2^{SF} symbols during one chirp period. This is done by shifting the frequency ramp based on the symbol value, as illustrated in Figure 1.2 [63]. Thus, each coded chirp is obtained by a cyclic shift of the reference chirp. This introduces a sharp edge in the instantaneous frequency trajectory. The instantaneous frequency of the coded chirp becomes:

$$f_{c2}(t) = \begin{cases} F_c + \alpha\frac{BW}{T_{Symbol}}(t - \frac{k}{BW}) + BW & ,if -\frac{T_{Symbol}}{2} \leq t \leq \frac{k}{BW} \\ F_c + \alpha\frac{BW}{T_{Symbol}}(t - \frac{k}{BW}) & ,if \frac{k}{BW} \leq t \leq \frac{T_{Symbol}}{2}. \end{cases} \tag{1.6}$$

where k is the number of shifted chips.

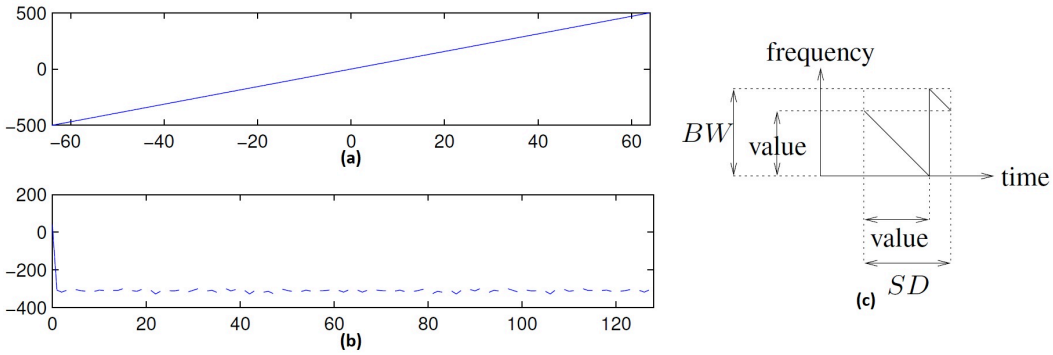

Figure 1.2: (a) Instantaneous frequency of an up-chirp. (b) Multiplication of the up-chirp by complex conjugate (down-chirp). (c) Coding a down-chirp, it encodes 1 symbol (SD is the Symbol Duration and BW the bandwidth).

Note that larger SFs means longer chirps as shown in Figure 1.3. Note also that during one SD (*Symbol Duration*) (i.e. the T_{symbol}), each of the 2^{SF} symbols codes SF bits. Thus, the symbol rate is: $R_s = \frac{BW}{2^{SF}}$. Moreover, the bit rate is: $R_b = SF\frac{BW}{2^{SF}}$.

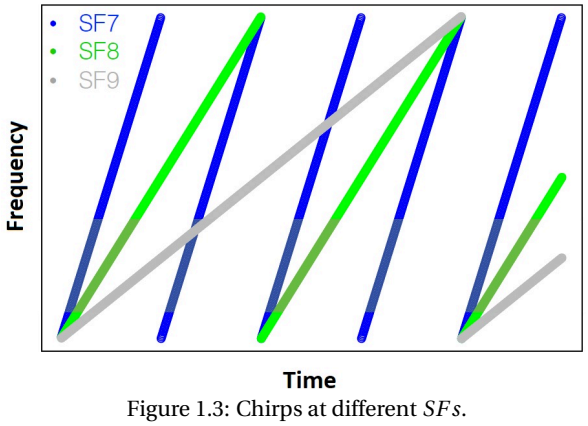

Figure 1.3: Chirps at different SFs.

The demodulation of an up-chirp consists in multiplying the received signal with a frequency shift value by a complex conjugate chirp (down-chirp), then sample with the bandwidth frequency and compute the FFT of the sampled signal. The result is a peak at the shift value. Thus, multiplying the received LoRa signal by the inverse chirp we obtain the decoded symbols as shown in Figure 1.4 as example.

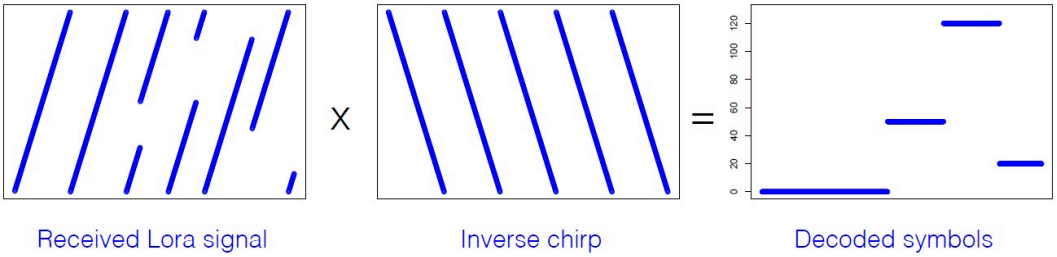

Figure 1.4: Decoded symbols of a LoRa received signal.

1.2.4 LoRa Frame Structure

A LoRa frame begins with a preamble of constant upchirps covering the whole BW. The last two upchirps encode the synchronisation word to differentiate LoRa networks using the same frequency band. The synchronisation word is followed by 2.25 downchirps. After the preamble, we have the header that specifies payload length in bytes, Forward Error Correction (FEC), Code Rate (CR), and whether the 2 bytes payload CRC (Cyclic Redundancy Check) field is used or not. The header field is transmitted with a CR of 1/2. The header may also include CRC to discard packets with invalid headers. Then, we have the payload limited to 255 bytes and its optional CRC to protect the integrity of the payload. Figure 1.5 shows the LoRa PHY frame format. The LoRaWAN specification utilizes explicit frame formats (i.e. a frame has a header including information of payload length, CR, and whether the payload CRC is used or not). Furthermore, Figure 1.6 illustrates the structure of the preamble [63]. Note that BW and SF are constant for the frame.

Preamble	Header	Header CRC	Payload	Payload CRC
min. 4.25 symbols	2 bytes	2 bytes	max. 255 bytes	2 bytes

Figure 1.5: LoRa PHY frame format.

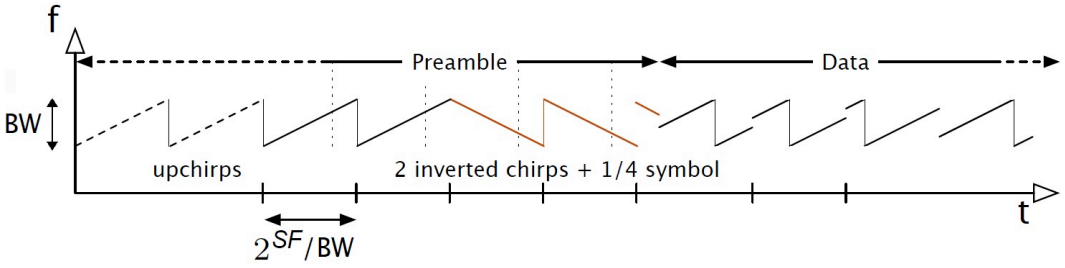

Figure 1.6: LoRa Preamble.

The frame air time is defined for a given SF, CR, and BW. It is the sum of the transmission time of the preamble and the payload as shown below:

$$T_{frame} = T_{preamble} + T_{payload} \tag{1.7}$$

$$T_{preamble} = (n_{preamble} + 4.25)\,T_{symbol} \tag{1.8}$$

where T_{symbol} is the time symbol and $n_{preamble}$ is the programmable length of the preamble. The number of symbols to transmit the payload is $n_{payload}$. Thus, the duration of the payload $T_{payload}$ is calculated as:

$$T_{payload} = n_{payload}.T_{symbol} \tag{1.9}$$

The $n_{payload}$ is defined by the following equation:

$$n_{payload} = 8 + max(ceil[\frac{8PL - 4SF + 28 + 16CRC - 20IH}{4(SF - 2DE)}](CR + 4), 0) \tag{1.10}$$

where PL is the payload size in bytes, SF is the spreading factor, CRC is 1 if it is enabled or 0 otherwise, IH is 1 if the header is enabled or 0 otherwise, and DE is 1 if low data rate optimisation is enabled or 0 otherwise. The low data rate optimization aims to reduce the number of symbols of the payload ($n_{payload}$) when the symbol time is larger than 16 ms (e.g., for SF_{11} and SF_{12} with 125 kHz of BW). Note that the minimum packet size is 8 symbols. From the previous equations, we can conclude that the transmission time of the LoRa frame (T_{frame}) is highly dependant on the SF. It also depends on the BW, the payload size, and the frame format. Note that high SF values imply long air time.

1.2.5 LoRa Transceiver

The Semtech LoRa transceiver claims to be long range with high interference immunity while minimizing power consumption. The CSS modulation allows transceivers to achieve high sensitivities, e.g. -136 dBm with SF=12 and BW=125 kHz. The LoRa modulation also adds error correction in data transmission. The coding rate (CR) configuration adds between 0 to 4 redundancy error correction bits allowing the LoRa signal to endure short interference. Equation 1.11 shows CR:

$$CR = \frac{4}{4 + N_p} \tag{1.11}$$

where N_p is the number of parity bits. In this thesis, we use the value of $CR = \frac{4}{5}$. Furthermore, it is recommended to increase N_p if there is interference in the channel. However, this also rises the duration of the transmission impacting the data rate. Indeed, the effective data rate (R_b) is defined in the following equation:

$$R_b = CR\frac{SF}{2^{SF}}BW \tag{1.12}$$

The data rate depends on the spreading factor, coding rate, and used bandwidth. LoRa allows to use channels with several values of BW: 7.8125 KHz, 15.625 KHz, 31.25 KHz, 62.5 KHz, 125 KHz, 250 KHz, and 500 KHz depending on the frequency plan. SF impacts the transmission time of the packet. R_b goes from 290 bps to 9380 bps for different values of SF with CR=$\frac{4}{5}$ and BW= 125 KHz. Table 1.3 shows the bit rate and sensitivity values for typical values of BW (125, 250, and 500 KHz) and a CR of $\frac{4}{5}$ for different SFs. Note that higher data rates are obtained with higher BWs at the cost of lower sensitivities (i.e. shorter ranges). Note also that lower data rates are obtained with higher SFs (i.e. higher sensitivities and larger ranges).

Table 1.3: LoRa bit rate and sensitivity.

	BW=125 KHz		BW=250 KHz		BW=500 KHz	
	sensitivity [dBm]	R_b [kb/s]	sensitivity [dBm]	R_b [kb/s]	sensitivity [dBm]	R_b [kb/s]
SF_6	-118	9.38	-115	18.75	-111	37.50
SF_7	-123	5.47	-120	10.94	-116	21.88
SF_8	-126	3.13	-123	6.25	-119	12.50
SF_9	-129	1.76	-125	3.52	-122	7.03
SF_{10}	-132	0.98	-128	1.95	-125	3.91
SF_{11}	-133	0.54	-130	1.07	-128	2.15
SF_{12}	-136	0.29	-133	0.59	-130	1.17

Sensitivity ρ_{dBm} is defined according to the Semtech designer guide [64] as:

$$\rho_{\text{dBm}} = -174 + 10log_{10}(BW) + NF + SNR, \tag{1.13}$$

where -174 accounts for the thermal noise effect, BW is the receiver bandwidth, NF is the receiver noise factor for a given hardware implementation, and SNR is the minimum ratio of the desired signal power to noise that can be demodulated. In our system model, we used the AWGN channel model. NF depends on the hardware implementation. We consider a NF of 6 dB in this thesis. Note that there are several sensitivity values depending on SF. Varying SF trades-off data rate and the communication range. The minimum SNR depends on SF as well.

LoRa performance can be evaluated through the analytical BER (*Bit Error Rate*) of CSS. BER is function of SF and the energy per bit to noise ratio $\frac{E_b}{N_0}$ [34], shown in Equation 1.14.

$$BER_{\text{CSS}} = Q(\frac{log_{12}(SF)}{\sqrt{2}} \frac{E_b}{N_0}) \tag{1.14}$$

where $Q(x)$ is the Q-function. The general expression that relates SNR and $\frac{E_b}{N_0}$ is given by:

$$SNR_{dB} = \frac{E_b}{N_0} + 10.log_{10}(R_s) + 10.log_{10}(SF) + 10.log_{10}(CR) - 10.log_{10}(BW) \tag{1.15}$$

From Equations 1.14 and 1.15, we can calculate LoRa performance in terms of BER for different values of SNR and SF as shown in Figure 1.7. High $SNRs$ are required to obtain low $BERs$. We observe that for each SF increase, SNR decreases by about 3 dB. When channel noise conditions increases, we need to increase the SF to keep the same BER. This increases the available link budget, but reduces the data rate. Moreover, we can decrease SF to keep the same BER when there are favorable channel noise conditions, which permits to optimize energy consumption.

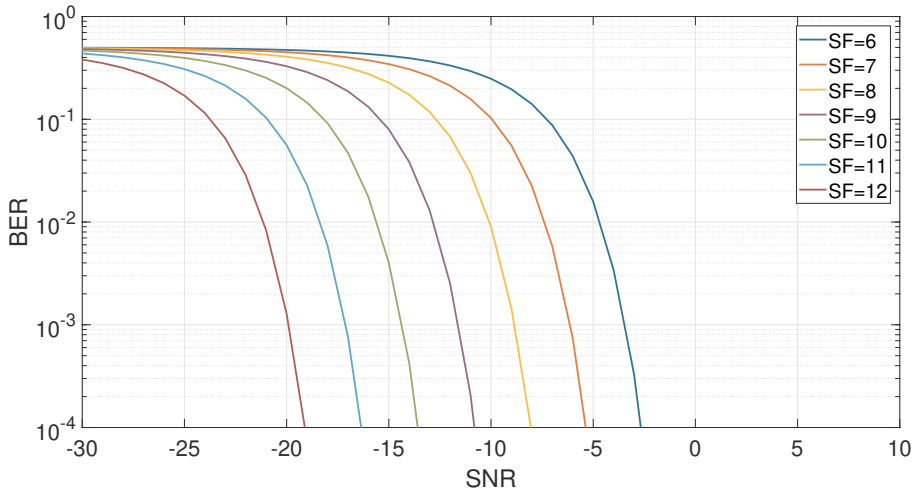

Figure 1.7: Bit error rate for LoRa. CR=$\frac{4}{5}$.

In this thesis, end-devices are based on the Semtech SX1276 trasceivers that provide high sensitivity trading-off communication range, interference immunity and energy consumption [65]. The LoRa demodulator SNR requirements for different SFs are shown in Table 1.4. Gateways are based on Semtech SX1301 that offers gateway capabilities with a multi-channel high performance transmitter / receiver designed to simultaneously receive several LoRa packets with different SFs and up to 8 channels [40]. It claims robust communications for a large number of nodes spread over a wide range. We also consider the gateway capture effect: if the gateway receives two packets overlapped with the same SF, the gateway will receive the first detected packet if it is stronger by 6 dB. Moreover, the gateway may receive, depending on the reception power, several packets with different SFs configurations thanks to the quasi-orthogonality with respect to each other.

Table 1.4: LoRa demodulator SNR.

SF	Symbols	Demodulator SNR
6	64	-5 dB
7	128	-7.5 dB
8	256	-10 dB
9	512	-12.5 dB
10	1024	-15 dB
11	2048	-17.5 dB
12	4096	-20 dB

1.2.6 Reliability, Interference, and Collision

The PDR (*Packet Delivery Ratio*) is defined as the ratio of successfully received packets to the total number of packets sent. Packets can be lost due to different causes such as high path loss (due to long distances or obstacles affecting the received signal power), and packet collision.

The use of unlicensed ISM bands allows to create private LoRa networks. However, when the number of LoRa devices grows significantly, the capacity of the network will saturate, leading to performance degradation. This problem is intensified by the fact that all gateways in the vicinity, regardless of their network provider, will receive packets from any LoRa device, causing inter-network interference. This interference leads to collisions and packet loss. In LoRa, collision occurs when packets overlap in time and use the same parameters: BW, SF, and carrier frequency. Thanks to the capture effect, a packet received with at least 6 dB higher can be decoded during collision. If packets are set at different SF configuration ($SF_6, SF_7, SF_8, SF_9, SF_{10}, SF_{11}, SF_{12}$), they may be received without collision but with low co-channel rejection depending on SF. Table 1.5 presents co-channel rejection for all combinations of the desired signal SF_d and the interferer signal SF_i [66]. These values define the interference model.

Table 1.5: Co-channel rejection [dB] for all combinations of SFs.

$SF_d \backslash SF_i$	6	7	8	9	10	11	12
6	-6	12	14	16	16	26	18
7	21	-6	16	18	19	19	20
8	24	24	-6	20	22	22	22
9	27	27	27	-6	23	25	25
10	30	30	30	30	-6	26	28
11	33	33	33	33	33	-6	29
12	36	36	36	36	36	36	-6

The probability of collisions depends on the selection of LoRa parameters used to transmit a packet. When several devices use the same configuration, the probability of occurring collisions is high. Furthermore, the selection of Tx and SF influences the coverage, some packets do not collide due to the signal attenuation over distance. The probability of collision is also affected by traffic, the periodicity of transmission and the packet size. More frequent transmissions and larger packet sizes lead to higher time on air and channel occupancy.

In this thesis, we aimed to adapt and optimize the different layers to channel and interference conditions varying in time. We take advantage of the quasi-orthogonality of SFs to receive several packets per channel at the same time. As shown in Table 1.5, a signal with the same SF and BW configurations presents high co-channel rejection. There exists also rejection between different SFs and the same BW but it is low. In fact, high SFs are more robust compared to low SFs. Furthermore, another insight is to exploit the quasi-orthogonality of signals with different SFs and different BWs. However, these signals can also be non orthogonal. For example, all these three signals: (BW=125kHz, SF_7), (BW=250kHz, SF_9), and (BW=500kHz, SF_{11})

are not orthogonal. Note that in this thesis, we only evaluate interference due to LoRa signals. However, our LoRa simulator can take into account interference due to non LoRa signals.

1.2.7 Properties of LoRa

LoRa presents some key properties, overviewed by Sundaram et al. [9], and experimentally verified by Liando et al. [67]. They are listed below:

- Long distance: Thanks to the high link budget (e.g., 150 dB) it achieves up to tens of kilometers (e.g., with SF_{12}) in line-of-sight, assuring a PDR of 70% [37]. In non-line-of-sight, it achieves around 2 km [68]. Note that communication distance is impacted by BW, SF, Tx, and CR.

- Low cost and complexity: LoRa devices are cheap and not complex to fabricate. When a node transmits, it wakes up, transmits and goes to sleep. There is no complex signaling overhead. Only preambles are verified.

- Long lifetime: Power consumption is around 120-150 mW during transmissions and around 10-15 mW for MCU operations [9]. This can be about 2-5 years of lifetime on a 2000 mAh battery [67].

- Concurrent reception gateways: A LoRa gateway is able to receive on several channels simultaneously (e.g., 8 channels in the Semtech SX1301). Thanks to the quasi-orthogonality of SFs, different SFs can be received on the same channel. So, considering 7 SFs, between SF_6 to SF_{12}, a total of 56 LoRa signals can be received concurrently by a single gateway.

- Robustness to Doppler effect: The LoRa CSS modulation resists to Doppler effect. Mobile devices at constant speed (50-80 km/h) in line-of-sight can achieve PDR higher than 85% (transmissions of 50 bytes with SF_{12} and packet duration of 2.35 s)[67].

- Bandwidth scalable: The LoRa modulation is bandwidth and frequency scalable according to Semtech [62]. It can be used for narrow-band frequency hopping and wide-band direct sequence applications. LoRa can also be adapted for either mode of operation with simple configuration changes.

- Ranging and localization: Thanks to the property of LoRa to linearly discriminate between frequency and time errors, Semtech [62] claims that it is the ideal modulation for radar applications and suited for ranging and localization applications.

1.3 LoRaWAN

It defines the MAC protocol for LoRa and it is specified by the LoRa Alliance [69]. A typical topology is star of stars where gateways forward packets between nodes and the network server in the backend. Gateways communicate with the network server via IP connections while end-devices use a single hop LoRa communication to one or several gateways. Thus, packets transmitted by end-devices are received by all the gateways in the range, exploiting the reception diversity and increasing the ratio of delivered packets. Duplicates are filtered by the network server. Communications are bidirectional, but uplink communication is the expected predominant traffic.

Communication between end-devices and gateways uses different frequency channels and data rates. The selection of the data rate is a trade-off between range and packet duration. Communications with different data rates do not interfere with each other (the co-channel rejection is negligible). However, in a context of large scale deployments, this interference needs to be taken into account. The LoRa network can manage the data rate and power output for each end-device to maximize its battery lifetime and network capacity. This mechanism is called: ADR (Adaptive Data Rate).

End-devices may transmit on any available channel at any time using any data rate as long as they respect the following rules: (i) a pseudo-random channel changing for every transmission to exploit frequency diversity. (ii) respect of the DC relative to the sub-band used and local regulations. Furthermore, LoRaWAN uses two modes to handle multiple access: (i) ALOHA allowing transmissions as soon as nodes wake up. (ii) a TDMA scheduler allowing time slots for each node.

1.3.1 MAC Layer

This layer provides the Adaptive Data Rate (ADR), ACK scheduling, channel access, energy saving, security and GPS geolocalization functionalities [70]. LoRaWAN uses ALOHA channel access with ACK mechanisms. The MAC protocol defines three device classes , one compulsory and the others optional, to address various applications: class A, B, and C channel access strategies as shown in Table 1.6.

Table 1.6: LoRa device classes.

<table>
<tr><td colspan="7">Application</td></tr>
<tr><td colspan="7">MAC layer</td></tr>
<tr><td colspan="2">Class A</td><td colspan="2">Class B</td><td colspan="3">Class C</td></tr>
<tr><td colspan="7">LoRa modulation</td></tr>
<tr><td>EU 863-870 MHz
EU 433 MHz</td><td>US 902-928 MHz</td><td>AS 920-923 MHz</td><td>CN 470-510 MHz
CN 779-787 MHz</td><td>AU 915-928 MHz</td><td>IN 865-867 MHz</td><td>LoRa @ 2.4 GHz</td></tr>
</table>

Class A end-devices can schedule an uplink transmission based on ALOHA protocol. Each uplink transmission is followed by two downlink receive windows. Class B end-devices uses scheduling methods in addition to random receive time windows. They receive a beacon from the gateway for the time synchronization. Class C end-devices have almost continuously open receive time windows. They are only close while transmitting. Thus, this class is the more energy consuming compared with the others. Note that the Class A is the most energy efficient and it is considered more appropriate for energy constraint devices.

1.3.1.1 Class A

LoRaWAN adopts the ALOHA random access method to keep simple network complexity. Class A is mandatory and end-devices have to implement the specification [69]. End-devices have two active receive window for downlink communication, they are activated after an uplink transmission is performed.

There are two types of frame formats detailed below:

- Uplink frames: They are transmitted from end-devices to the network server and received by all gateways in the communication range. Uplink frames use LoRa radio packet explicit mode (e.g., the PHDR and PHDR_CRC are included). The PHDR, PHDR_CRC, and payload CRC fields are inserted by the radio transceiver. Figure 1.8 shows the uplink frame format:

Figure 1.8: Uplink frame format.

where:

  - Preamble is at least 4.25 symbols.
  - PHDR is the Physical Header.
  - PHDR_CRC is the the Cyclic Redundancy Check of the Physical Header.
  - PHYPayload is the payload.
  - CRC is the Cyclic Redundancy Check of the payload.

- Downlink frames: They are transmitted from the network server to end-devices through the gateway. Each downlink frame is sent to a specific node relayed by a single gateway. Downlink frames also use the radio packet explicit mode (e.g., the PHDR and PHDR_CRC are included). Note that the CRC of the payload is not included to keep frames as short as possible. Figure 1.9 shows the downlink frame format.

Preamble	PHDR	PHDR_CRC	PHYPayload

Figure 1.9: Downlink frame format.

An uplink transmission triggers two downlink receive windows. The downlink receive windows are shown in Figure 1.10. $RX1$ is the first downlink receive window, it is opened after $Receive\_Delay\_1$ (1 sec +/- 20 μs) the end of the uplink transmission. By default, frequency channel and data rate are the same as the uplink transmission parameters. The second receive window $RX2$ opens $Receive\_Delay\_2$ (2 sec +/- 20 μs) after the end of the uplink transmission. It uses fixed configurable data rate and frequency channel using MAC commands to improve robustness of transmissions.

Note that the length of a receive window must be at least the time required to detect a downlink preamble by the end-device. If a preamble is detected, the radio receiver stays active until the downlink frame is demodulated. If a frame is detected and demodulated during $RX1$, and the frame is designated for the correct end-device, $RX2$ is not open. When the network server sends a frame to an end-device, it must initiate the downlink transmission at the beginning of one of the receive windows. Note also that end-devices during receive windows shall not transmit uplink frames.

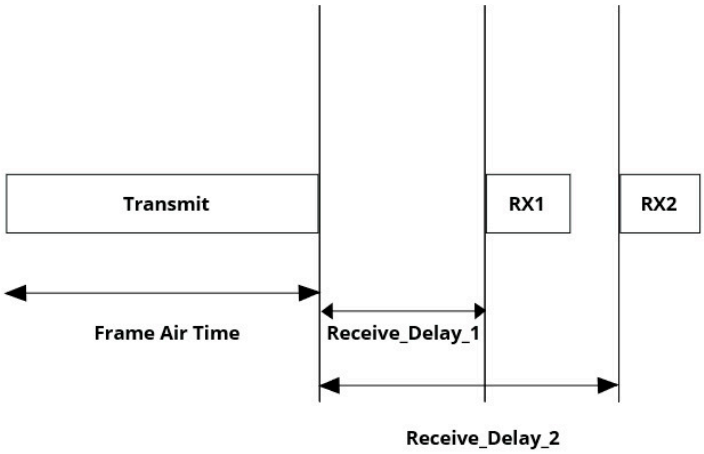

Figure 1.10: Downlink receive windows.

1.3.1.2 Class B

Class B devices aim to enable the transmission of downlink packets in Class A devices by using synchronized reception windows. Gateways transmit a broadcast packet with timing references to end-devices. Then, end-devices use these references to open receive windows with pre-determined time slots only in scheduled times. End-device timers are controlled by beacon frames. We have to notice that all nodes have to implement Class A starting the network with the same joining process. Then, devices are able to operate Class B following these steps: the node has to request to operate as Class B through a beacon, the node selects appropriate ping slot data rate and slot period depending on the signal strength and battery level. Figure 1.11 shows the beacon periods and timing for Class B devices.

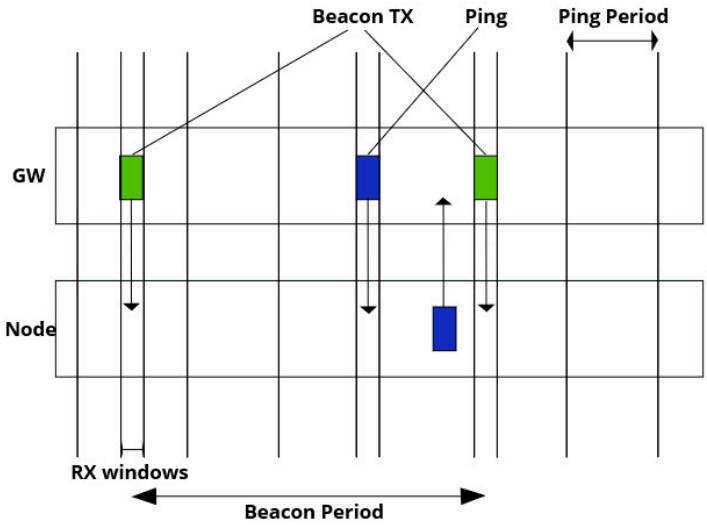

Figure 1.11: Class B reception window.

1.3.1.3 Class C

CLass C devices have always the downlink receive windows active (e.g., always on). Class C is the least energy efficient device since the downlink receive windows are always on. Class C devices implement Class A reception windows with an extended receive windows after the $Receive\_Delay\_2$ as shown in Figure 1.12.

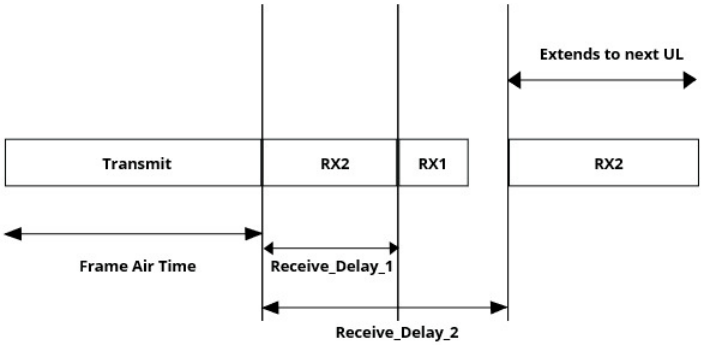

Figure 1.12: Class C reception window.

1.3.2 MAC Frame Format

The MAC layer handles transmission and reception of MAC commands and application data from the application layer. LoRaWAN specification defines the frame format at each protocol stack as shown in Figure 1.13.

Radio PHY layer:

Preamble	PHDR	PHDR_CRC	PHYPayload	CRC

PHYPayload:

		MHDR	MACPayload	MIC

MACPayload:

		FHDR	FPort	FRMPayload

FHDR Frame header format:

	DevAddr	FCtrl	FCnt	FOpts

Figure 1.13: MAC frame format.

All LoRa uplink and downlink frames carry a payload (PHYPayload) with a single-octet MAC Header (MHDR) followed by a MAC payload (MACPayload) with a maximum length depending on the region, and ending with a 4-octet Message Integrity Code (MIC). The MAC header field (MHDR) includes a 3-bit field for different types of MAC frames (MType) according to which major version (2-bit field Major). The remaining 3 bits are reserved for future usage. All the LoRaWAN MAC frames are identified based on MAC frame types. LoRaWAN MAC frame types are shown in Table 1.7.

Table 1.7: LoRaWAN MAC frame types.

MType	Description
000	Join Request
001	Join Accept
010	Unconfirmed Data Up
011	Unconfirmed Data Down
100	Confirmed Data Up
101	Confirmed Data Down
110	RFU
111	Proprietary

where:

- Join Request and Join Accept: are used to join the network between LoRa end-devices and the gateway.
- Confirmed Data frames: require to be acknowledged by its receiver.
- Unconfirmed Data frames: do not require any acknowledgement.
- RFU means Reserved for Future Usage (e.g., Rejoin-request).
- Proprietary is used to incorporate non standard frame format functionalities.

The MAC payload contains a frame header (FHDR) of 7-22 bytes followed by a field (FPort) and an optional frame payload field (FRMPayload). The frame header (FHDR) contains the short device address of the end-device (4-byte DevAddr), a frame control (1-byte FCtrl), a frame counter (FCnt 2-byte), and a frame option (0-15 bytes FOpts) used to transport MAC commands. The FCtrl content for downlink and uplink frames are shown in Figure 1.14 and Figure 1.15, respectively.

bit# 7	6	5	4	[3...0]
ADR	RFU	ACK	FPending	FOptsLen

Figure 1.14: Downlink FCtrl fields.

bit# 7	6	5	4	[3...0]
ADR	ADRACKReq	ACK	ClassB	FOptsLen

Figure 1.15: Uplink FCtrl fields.

Note that the field ADR refers to the Adaptive Data Rate mechanism of LoRaWAN that is presented in the following subsection.

1.3.3 Adaptive Data Rate (ADR)

It is part of the LoRaWAN specification and it aims to provide reliable and energy efficient connectivity by adapting the spreading factor (SF) and the transmission power (TP) to link condition changes. When a node observes an absence of downlink response from the network server after several consecutive uplink transmissions, it assumes loss of connectivity and gradually increases its transmission power to the maximum allowed before increasing the spreading factor. Figure 1.16 [71] shows the ADR mechanism on the node side according to LoRaWAN specification v1.1. ADR_ACK_LIMIT and ADR_ACK_DELAY control the number of uplink messages. ADR_ACK_CNT counts the number of expected ACKs when sending uplink (UL) packets. If a downlink (DL) packet is received, the counter and the $ADRACKReq$ are reset to 0. Otherwise, without any downlink response, the counter increases until it reaches the ADR_ACK_LIMIT. Then, if TP and SF are not already operating at the maximum values, the ADR ACK request bit is set to 1. It requires the

network to reply with a DL frame within the next delay (*ADR_ACK_DELAY*). If no reply is received within this delay, the node must try to reconnect first by increasing step by step the TP, and then by increasing the SF. This process is repeated as long as the TP and SF do not reach the maximum and there is no DL packet received after an UL transmission. When a DL packet is received the counter and the ADR ACK request are reset to 0.

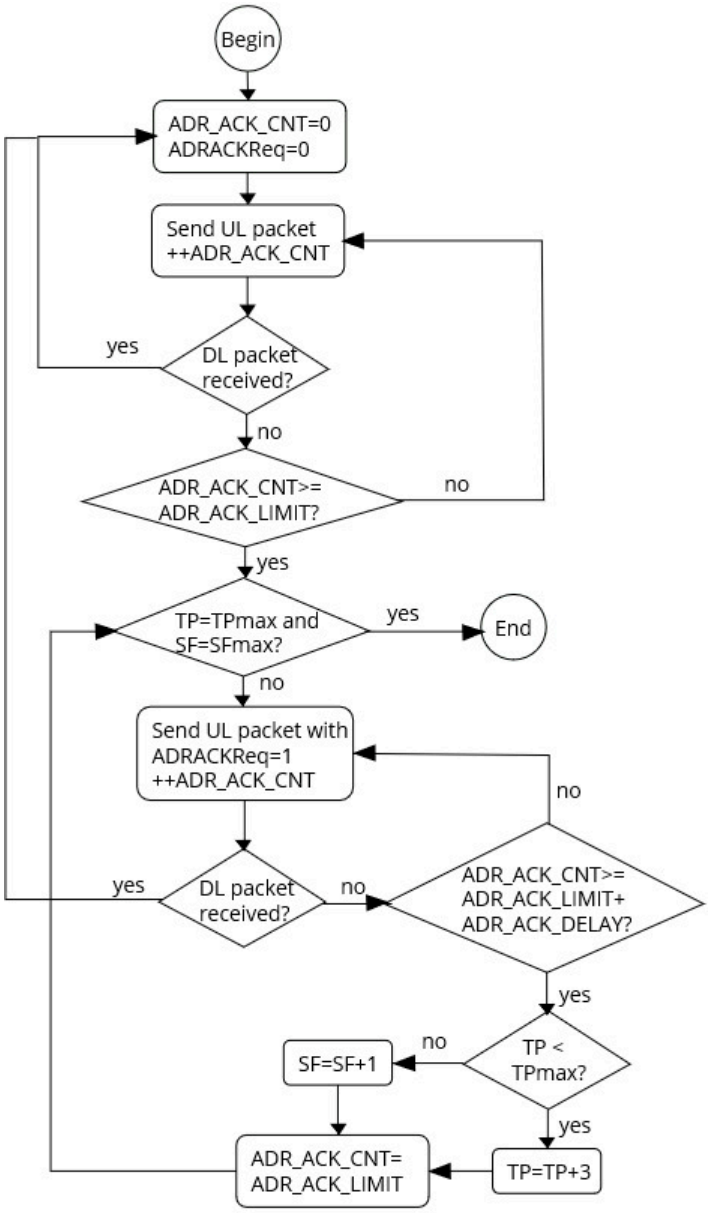

Figure 1.16: ADR mechanism at the end-device.

The network can monitor the quality of the uplink receptions. The link quality can be calculated over a set of last packets (N). If there is a high margin above the minimum receiver sensitivity threshold, the network reduces SF or TP. Reducing SF will increase data rate consuming less energy. There is a recommendation to implement the ADR algorithm at the network proposed by Semtech and adopted by different operators such as The Things Network (TTN). In this recommended algorithm, we need the 20 last received frames ($N = 20$) with their respective maximum signal to noise ratios (SNR_{max}). Figure 1.17 [71] shows the ADR mechanism at the network.

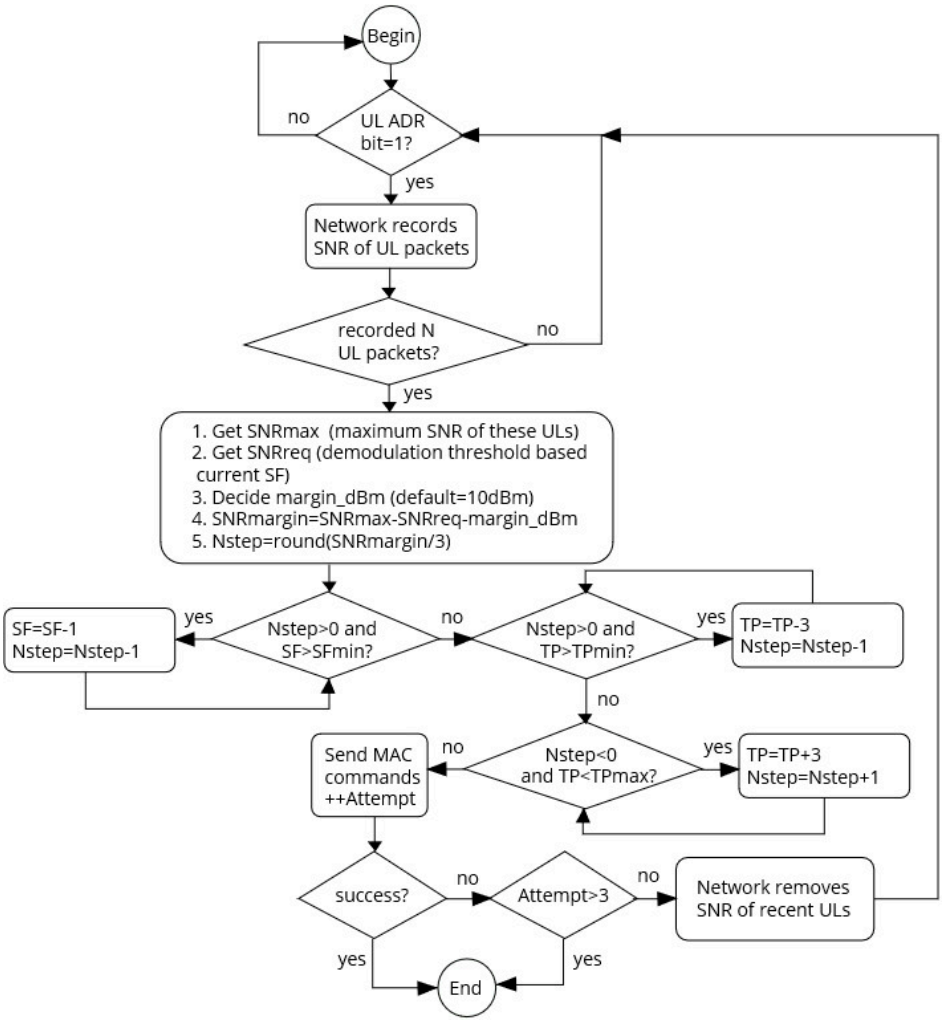

Figure 1.17: ADR mechanism at the network.

1.4 LoRa Deployment Discussion

This section presents and discusses real LoRa deployments in field, experimental measurements studies, performance evaluation, and limits. Moreover, LoRa network deployment and spreading factor allocation strategies are discussed.

1.4.1 Real LoRa Deployments

There are many real LoRa networks implemented in field for many use cases such as smart buildings [21], smart cities [22], smart agriculture [23], smart meters [24], smart islands [25], smart golf course [26], smart water quality monitoring [27], smart air quality monitoring [31], smart parking [72], and smart lighting [73]. We discuss and overview the most popular real deployments coming up next:

- Smart cities: Semtech white paper [22] explains how to make cities smart providing efficient usage and governance. IoT applications aim to improve and ease people's daily life. A waste management LoRa system is deployed in Seoul, Korea to periodically collect the capacity of waste bins to clear them when they are filled. It reduces costs by 83%, collection activity by 66% and increases recycling by 46%. An integrated sensing platform of solar power plants is deployed in Carson city, USA to monitor the current environment state of the solar plants. It reduced by 15% operational expenses. Power consumption monitoring in houses were deployed in Grenoble and Lyon, France to monitor power usage and turn-off unwanted devices, reducing 16% of power consumption.
- Smart meters: Semtech white paper [24] evaluates the capacity of LoRa smart metering applications deployed in Gehrden, Germany. It reduces the human intervention for monitoring power usage by transmitting readings periodically from meters to a gateway.
- Smart islands: Semtech technical report [25] presents LoRaWAN sensor deployments to aid water management systems by reporting periodically water quality and water levels in Mallorca, the largest island of Spain. It increased water savings by 25%.

We can conclude that there is a large scope of applications, real networks deployed. However, they are not easy to reproduce. Thus, we need simulation approaches.

1.4.2 From Experimental Measurements to Simulations

Some authors deployed LoRa networks and experimentally studied their performance [74] [75] [76] [77] [78] [79]. Measurements were done in city centers, campus of universities, tactical troop tracking and sailing monitoring systems. Nevertheless, experimental results in real life networks are not reproducible and MAC layer optimization is difficult. Blenn et al. [80] performed simulations based on traces from experiments and analyzed results based on real life and large scale measurements from The Things Network. However, their simulations are limited to the deployed scenario making optimization difficult. To and Duda [81] presented LoRa simulations in NS-3 and validated test-bed experiments. They considered the capture effect and showed the reduction of the packet drop rate due to collisions with a CSMA approach. Haxhibeqiri et al. [37] studied the scalability for LoRaWAN deployments in terms of the number of nodes per gateway in system level simulator. Simulations were performed for 1% duty cycle. However, the network size of deployments are limited to 1000 nodes.

Note that at the beginning of this thesis there were not several accurate simulators available. That is why we used the WSNET simulator that implements the required communication protocol layer and simulates the network behavior with high level of accuracy. It takes into account the flexibility and specificity of the LoRa PHY and MAC layers.

1.4.3 LoRa Evaluation and Limits

Several authors evaluated performance and limits of LoRa networks. Reynders et al. [34] evaluated Chirp Spread Spectrum (CSS) and ultra-narrow-band (UNB) networks. They proposed a heuristic equation that

gives BER for a CSS modulation as a function of SF and Signal to Noise Ratio (SNR). Cattani et al. [82] evaluated the impact of the LoRa physical layer settings on the data rate and energy efficiency. They evaluated the impact of environmental factors such as temperature on LoRa network performance and showed that high temperatures degrade the Received Signal Strength (RSS) and the Packet Delivery Ratio (PDR). Goursaud et al. [66] studied performance of the CSS modulation. They showed the possibility of interference between different SFs and evaluated co-channel rejection for all combinations of SFs. Feltrin et al. [83] discussed the role of LoRaWAN for IoT and showed its application to many use cases. They considered the effect of non perfect orthogonality of SFs for a link level analysis. Waret et al. [84] provided a theoretical analysis of the achievable LoRa throughput in uplink, where the capture conditions specific to LoRa are included. Results show the throughput losses from imperfect SF orthogonality, under different SF allocations. Petajajarvi et al. [36] analyzed the scalability of a LoRa wide area network and showed its good coverage (e.g., up to 30 km on water for SF12, BW of 125kHz and 14 dBm transmit power with more than 60% of PDR). They also showed the maximum throughput for different duty cycles per node per channel. Mikhaylov et al. [85] discussed LoRa performance under European frequency regulations. They studied performance metrics of a single end-device, and the spatial distribution of several end-devices. They showed LoRa strengths (large coverage and good scalability for low uplink traffic) and weaknesses (low reliability, and poor scalability of downlink traffic). Bor et al. [86] presented and analyzed the capability of the LoRa transceiver. They also proposed LoRaBlink protocol for link-level parameter adaptation. We analytically showed [87] the potential gain of adaptive LoRa solutions choosing suitable radio parameters (i.e., spreading factor, bandwidth, and transmit power) to different deployment topologies (i.e., star and mesh).

These studies provide the first view of LoRa performance and its limitations. In conclusion, we need to take into account the capture effect and the imperfect orthogonality of SFs. We contribute with an accurate LoRa simulation model considering the co-channel SF interference and the gateway capture effect, allowing accurate performance analysis in large scale simulations for different deployment scenarios. We extend previous evaluations of LoRa limits analyzing reliability, and network throughput from sparse to massive network deployment scenarios for single and multiple gateway scenarios.

In the simulation evaluation, we use the WSNet simulator to automatize LoRa deployments in static scenarios. We integrated the characteristics of new transceivers (Semtech SX1276 for end-devices and SX1301 for gateways) and reconfiguration options in the simulator. Then, we defined a decision module cross-layer (TX-PHY-MAC) to self-deploy the network (i.e., the network takes into account the environment by measuring metrics to analyze them, to make a decision, and to apply it to reconfigure the network to optimize its performance). These metrics are the packet delivery ratio (PDR) and the Throughput defined below:

$$PDR = \frac{number\ of\ received\ packets}{number\ of\ transmitted\ packets} \tag{1.16}$$

$$Throughput = \frac{number\ of\ received\ packets}{duration}\ [packets/s] \tag{1.17}$$

1.4.4 LoRa Network Deployment Strategies

Some authors studied LoRa network deployments and SF allocation strategies. Bor et al. [88] studied LoRa transceiver capabilities and its limitations. They showed that LoRa networks can scale if they use dynamic selection of transmission parameters. Georgiou et al. [89] investigated the effects of interference in a network with a single gateway. They studied two link-outage conditions, one based on SNR and the other one based on collision of concurrent transmissions of the same SF. They showed, as expected, that performance decreases when the number of nodes increases and highlighted the interest of studying spatially heterogeneous deployments, i.e., deployment of nodes with heterogeneous radio communication parameters (TP, BW, SF, CR, frequency channel). Croce et al. [90] showed the effect of the quasi-orthogonality of SFs and found that overlapped packet transmissions with different SFs may suffer from losses. They validated the findings by experiments and proposed SIR (*Signal to Interference Ratio*) thresholds for all combinations of SFs. They remarked that LoRa networks cannot be studied as a superposition of independent networks

because of the imperfect SF orthogonality. Abeele et al. [91] studied the capacity and scalability of LoRaWAN for thousands of nodes per gateway. They showed the importance of considering the capture effect and interference models. They proposed an error model from BER simulations to determine communication ranges and interference. They also analyzed three strategies of network deployments (random SF allocation, fixed, and according to PDR), the last one presenting the best performance. Lim et al. [92] analyzed the LoRa technology to increase packet success probability and proposed three SF allocation schemes (equal interval based, equal area based, and random based). They found that the equal area scheme results in better performance compared with other schemes because of the reduced influence of SFs.

In conclusion, the literature indicates the interest in heterogeneous deployments and SF allocation strategies. Thus, in Chapter 3 we analyze homogeneous and heterogeneous deployments with different SF allocations as a function of the number of nodes and traffic intensity to show network performance and the benefits of radio parameters heterogeneity for large scale networks. Moreover, there are more strategies, like the ADR mechanism, that can be improved by exploiting the radio heterogeneity of LoRa.

1.5 Link and Topology Adaptation Discussion

This section discusses two LoRa adaptation approaches: (i) link and (ii) topology adaptation to improve network performance. Link adaptation aims to adapt the link depending on the link budget and capacities of the technology while topology adaptation aims to densify the network infrastructure increasing the number of gateways.

1.5.1 Link Adaptation

Several authors studied SF allocation strategies in the literature. Hauser et al. [41] analyzed the ADR algorithm defined in LoRaWAN and proposed improved variants of the algorithm. They showed the need of better simulation models to support more complex networks to evaluate their proposed algorithms performance in quantitative terms. Slabicki et al. [42] evaluated the impact of the channel variability on ADR and showed that link-based adaptation is not sufficient in dense network deployments. Hence, as future work, they proposed to improve ADR by balancing the link budget for every link and the packet delivery ratio PDR for the entire network. Reynders et al. [43] proposed a scheme for transmitted power and SF allocation in long range networks, and an algorithm controlling transmission power, spreading factor and channel index. They analyzed the optimal distribution of the spreading factors to optimize PDR and make the network more fair. Amichi et al. [44] considered the problem of SF allocation optimization under co-SF and inter-SF interferences, for uplink transmissions from end-devices to the gateway. To provide fairness, they formulated the problem as maximizing the minimum achievable average rate in LoRa, and proposed an SF allocation algorithm based on matching theory. Cuomo et al. ([45][46]) presented several adaptive strategies allocating spreading factors to end-devices. EXPLORA-SF allocates equitably each SF only taking into account the link budget. EXPLORA-AT equalizes the devices time on air with different SFs to not overload the usage of a SF. EXPLORA-KM reallocates SF of devices located in overcrowded areas. However, these strategies are only analyzed in single-gateway network scenarios considering a single channel. We studied similar enhanced strategies, considering multiple channels, bi-directional communications, different environments, and multi-gateway (MG) deployment scenarios. Furthermore, we take into account the quasi-orthogonality of SFs.

Another interesting approach is replacing ADR with Multi-Arm Bandit (MAB) algorithms to select transmit power and SF. Kerkouche et al. [47] presented a MAB optimization of LoRaWAN and made a trade-off between reliability and energy consumption. Similarly, Azari et al. [48] proposed a self-organized distributed approach based on MAB learning. In this approach, each node evaluates a reward (i.e., based on the reception of ACK packets) and finds iteratively the best action (i.e., the selection of a transmission power, a sub-channel and a SF). However, these approaches are complex, only adapted to single-gateway scenarios, need time to converge, and need to consider the imperfect orthogonality of SFs. Finally, we analytically

investigated other radio parameters (e.g., BW) and network topology (e.g., mesh) [87]. We will show the potential gain of adaptive LoRa solutions in Chapter 2.

The state of the art recommends several strategies for link adaptation and resource allocation. Nodes should be configured according to their radio environment (e.g., link budget) but also according to the scenario criteria (e.g., energy efficiency, network load).

Similarly to other approaches [42] [43], and [45], our first approach will adapt the link according to its link budget and the GW capacity. Thus, whatever the type and the complexity of the deployment, the adaptation algorithm will consider a fairer distribution of the configuration than the ones only based on the link budget (e.g., ADR). We took ADR in steady state as reference approach to compare our proposals.

1.5.2 Topology Adaptation

Some authors expressed the idea of network densification with multiple gateways as future work [45], [46] and [47]. Bor et al. [88] showed that LoRa networks can scale using dynamic transmission parameters selection and/or densifying the network with multiple-gateways. However, this approach was evaluated only when nodes select the same SF configuration. Abboud et al. [93] investigated the gateway selection for downlink communications in LoRaWAN in order to improve the throughput of the network. They aim to evaluate several algorithms for selecting the best gateway for downlink while increasing LoRaWAN throughput for different types of gateway deployment. They show that the system throughput depends on the deployment and that balancing the number of end-devices per gateway improves the performance compared to choosing the gateway with the highest signal quality. Voigt et al. [94] evaluated the impact of inter-network interference on LoRa networks and showed that interference can dramatically reduce the performance. Thus, directional antennas and multiple gateways can improve performance under interference. Caillouet et al. [95] proposed a theoretical framework for maximizing the LoRaWAN capacity in terms of the number of end nodes, when they all have the same traffic generation process. The model optimally allocates the spreading factor to the nodes so that attenuation and collisions are optimized. They considered physical capture and imperfect SF orthogonality while guaranteeing a given transmission success probability to each served node in the network. Numerical results show the effectiveness of the SF allocation policy. The framework also quantifies the maximum capacity of single cell networks and the gain induced by multiplying the gateways on the covered area. In [96], Cuomo et al. proposed AD-MAIORA to balance the Air-Time of different SF modulations in a multi-gateway scenario interconnected to the same network server. It adaptively allocates SF with the objective to reduce the pressure of using SF on a GW (i.e., to balance a per-SF-pressure load at each GW). The strategy was first to choose the best node, then to find the best SF. However, their evaluations are based on the network with thousand nodes and they assume high traffic intensity (packet transmission every 10 s) with respect to the regulation. Thus, we need new evaluations with more accurate results for new deployment scenarios to validate their results (e.g., throughput). We also need to evaluate if an end-device should be adapted towards a single gateway, multiple gateways, or the whole network.

Our second approach will improve network performance by densifying the network infrastructure without link adaptation, i.e., by increasing the number of GWs. We will extend the star topology to star of stars topology (or multi-gateway infrastructure). The multi-gateway approach will exploit the spatial reuse and provide a certain level of redundancy. It maximizes the overall capacity of the global network for different SF configurations.

Then, our third approach (joint link and topology adaptation) will improve the network transmission quality by exploiting the quasi-orthogonality of various SFs, the spatial reuse of the communication and the capacity of the gateway according to each SF capacity.

Finally, in our last approach we proposed nodes progressively joining the network algorithms based on several metrics to improve the third approach in more realistic deployments (e.g., denser in the center). We aim to exploit a combination of several metrics based on link quality, network quality, and network

distribution of SFs. However, the accuracy of these metrics depends on the accuracy of the base metrics. We look for maximizing PDR by configuring nodes joining the network without modifying the nodes that already joined the network. Note that we do not have access to the configuration of nodes belonging to other private networks.

1.6 Methodology

In this section, we present the methodology of this thesis to face the research problems and objectives taking into account the existing work at the beginning of this thesis. Note that this thesis was developed while several other LoRa investigations were also developed.

- First, we characterize LoRa deployments and the state of the network performance by measuring different metrics: PDR, throughput, energy consumption, and metrics based on link quality, network quality, and network distribution of SFs.
- Second, we evaluate these metrics like link quality estimators (LQE) or link quality indicators (LQI) as well as interference level estimation.
- Third, we define a decision module to self-adapt the LoRa deployment to network performance and interference conditions for a given application profile like defined traffic load of sending packets every minute deployed over a defined geographical area.
- Fourth, we select and apply the more appropriate configurations to the transceivers according to the adopted strategy. Figure 1.18 depicts these four stages.

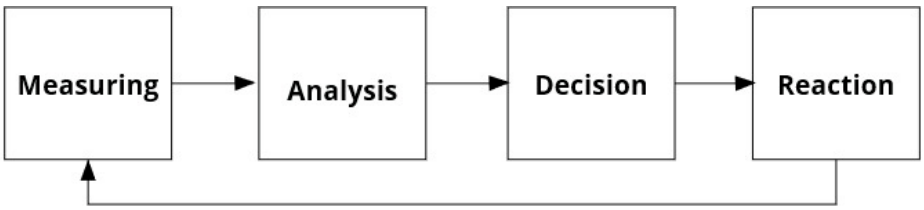

Figure 1.18: Methodology to adapt the network.

We decided to divide our work in two study-parts. The first one is a theoretical study of the communication link. The second one is the simulation evaluation using the WSNet simulator.

In the theoretical study, we analyzed the link budget and the different parameters we can tune. We have to notice that a communication link is established when the link budget is respected. Equation 1.18 shows the link budget, where P_{Tx} is the transmitted power, L represents the channel losses, P_{Rx} is the received power, and ρ is the sensitivity power of the receiver.

$$P_{Tx} - L = P_{Rx} > \rho_{\text{dBm}} = SNR_{min} - 174\text{dBm/Hz} + 10log_{10}(BW) + NF \tag{1.18}$$

Regarding this equation, we observe several trade-offs to adapt the link budget. Thus, from the last equation we can adapt the following parameters:

- P_{Tx}: Emitted power control.
- SNR_{min}: Modulation and coding rate adaptation.
- BW: Data rate adaptation.
- NF: Noise factor control.

Note that, these adaptations are for a single link. For several links in a network deployment, we add the topology adaptation.

When tuning these parameters in an optimal way, power consumption and reliability may be improved. In fact, we look for optimizing the communication link taking into account the deployment to increase battery life-time of sensors an to improve the reliability of the communication.

Then, we define a technology to focus on. This technology should present degrees of freedom on its communication parameters in order to enable adaptation and control (power control, modulation adaptation, data rate adaptation, noise factor control, etc.).

Conclusion

In this chapter, we presented a short overview of different LPWAN technologies for IoT, particularly for WSN deployments. We also presented a comparative table of the principal LPWAN technologies: LoRa, SIGFOX, Ingenu, NB-IoT, and IEEE 802.11ah. Among these technologies, we are looking for the one that is suitable for adaptive networks to self-deploy WSNs. We consider the LoRa technology as a good candidate for several reasons such as the degrees of freedom of its communication parameters, the robustness to interference, the openness and the maturity of the technology. Thus, we presented more in detail the LoRa technology (PHY layer) and the LoRaWAN specification (MAC layer). We also presented the Adaptive Data Rate mechanism of LoRaWAN on the node and at the network side. However, a deep analysis of the flexibility of LoRa communication parameters is required to understand the trade-offs when changing one parameter. An analytical investigation of energy consumption by adapting LoRa communication parameters in different network topologies will be presented in Chapter 2 to evaluate if LoRa is suitable for adaptive networks.

This chapter also discussed current real LoRa deployments for many applications in smart cities and smart meters reducing operation costs and improving people's life. However, the MAC layer optimization is difficult since experimental measurements in real life networks are not reproducible. Several studies provide insights on LoRa performance and limitations. We conclude that we need to take into account the capture effect and imperfect orthogonality of spreading factors as well as performance analysis at massive network deployments. The reviewed literature indicates the interest of heterogeneous deployments and optimal spreading factor allocation strategies to improve network performance.

Finally, we discussed link and topology adaptation approaches. Several studies agree that nodes should be configured according to their radio environment, but also to the scenario criteria taking into account the network load and energy efficiency. We identified some insights to adapt link considering fairer distribution of the spreading factors. We are going to exploit the spatial reuse of the communication by densifying the network infrastructure increasing the redundancy by placing more gateways. Also, we are going to exploit the quasi-orthogonality of different spreading factors and the capacity of gateways and each spreading factor. Furthermore, we propose an algorithm to self-adapt nodes progressively joining a network based on several metrics.

Part II

Contributions

Is LoRa a Good Candidate for Adaptive Networks?

This chapter is adapted from:

- *M. Nunez, A. Guizar, M. Maman, A. Duda.* Evaluating LoRa Energy Efficiency for Adaptive Networks: From Star to Mesh Topologies. *In IEEE 13th International Conference on Wireless and Mobile Computing, Networking and Communications (WiMob). IEEE, 2017.* [87]

Contents

Introduction

In this chapter, we investigate the degrees of freedom of LoRa communication parameters to understand the trade-offs and challenges when adapting its parameters. These parameters can be: (i) the transmitted power (P_{tx}), (ii) the spreading factor (SF), (iii) the bandwidth (BW), (iv) the coding rate (CR), and (v) the topology of the deployment. The objective is to investigate if LoRa is an appropriate candidate for adaptive networks. This chapter focuses on the investigation of energy consumption and the communication range as performance network indicators.

This chapter analytically investigates the energy efficiency for different network topologies to improve energy consumption by adapting LoRa communication parameters in star and mesh topologies. The impact on the energy consumption of the network density and the network coverage is also investigated. We implemented an analytical model in Matlab according to the LoRaWAN specification and technical documents.

This chapter is structured as follows. After the introduction, Section 2.2 details the methodology and the system model. Then, we investigate LoRa parameters adaptation in star topology in Section 2.3 detailing the energy consumption dependency on the spreading factor, transmitted power, and bandwidth and proposing adaptation strategies. Section 2.4 investigates LoRa adaptation in mesh topologies showing the energy consumption dependency on the network density and the network coverage and proposing an adaptation strategy. The impact of the network topology: star versus mesh topology is investigated in Section 2.5 proposing an hybrid adaptation strategy. Finally, Section 2.6 concludes this chapter showing the flexibility of LoRa parameters to pursue investigation in adaptive networks.

2.1 Methodology and System Model

Here, we describe the methodology to analyze energy consumption for sending a 50 Bytes packet using a LoRa radio with multiple degrees of freedom: transmitted power (i.e., 2 dBm, 5 dBm, 8 dBm, 11 dBm, and 14 dBm according to the LoRaWAN specification [69] for the EU863-870MHz band), modulation schemes (i.e., spreading factors), bandwidth, and the network topology (i.e., star and mesh). In our analysis, we do not consider MAC protocols.

2.1.1 Radio Propagation Model

We consider the Okumura Hata propagation model for an open rural environment operating at 868 MHz frequency. Thus, pathloss (PL) is given by the following expression:

$$PL_{\text{Hata}} = A + Blog(d) + C \tag{2.19}$$

where A, B, and C depend on the frequency and antenna height.

$$A = 69.55 + 26.16log(f_c) - 13.82log(h_b) - a(h_m) \tag{2.20}$$

$$B = 44.9 - 6.55log(h_b) \tag{2.21}$$

where f_c is in MHz and d in km. For rural environments, $a(h_m)$ and C are given by the following expressions:

$$a(h_m) = (1.1log(f_c) - 0.7)h_m - (1.56log(f_c) - 0.8) \tag{2.22}$$

$$C = -4.78(log(f_c))^2 + 18.33log(f_c) - 40.98 \tag{2.23}$$

We consider antenna heights h_m and h_b of 1 m and 2 m, respectively.

2.1.2 Energy Consumption Model

We consider two main sources of energy dissipation:

- Energy dissipated in the transmitter E_{tx}. In this case, we consider the supply current for each transmitted power, as shown in Table 2.8, under the following conditions: 3,3 V supply voltage, 25 °C temperature, and 868 MHz band.

Table 2.8: Supply current for transmitter [65]

P_{tx}	2 dBm	5 dBm	8 dBm	11 dBm	14 dBm
I_{tx}	24 mA	25 mA	25 mA	32 mA	44 mA

- Energy dissipated in the receiver E_{rx}. In this case, the supply current depends on the bandwidth. Table 2.9 shows supply current for each bandwidth under the same conditions as transmission. Note that the gateway is powered, but this energy consumption in reception can be for a multi-hop communication scenario (e.g. at the relay node).

Table 2.9: Supply current for receiver w.r.t. the bandwidth [65]

BW	125 kHz	250 kHz	500 kHz
I_{rx}	10,3 mA	11,1 mA	12,6 mA

We took all supply current values from the datasheet Semtech SX1276 [69].

2.2 LoRa Adaptation in Star Topology

We study energy consumption to transmit a packet using various possible configurations of the spreading factor, transmission power, and bandwidth for a transceiver operating according to the LoRaWAN technology. In a star topology, we consider one single hop to reach the sink node. As shown in Figure 2.1, D represents the distance between a node and the sink node (e.g., gateway).

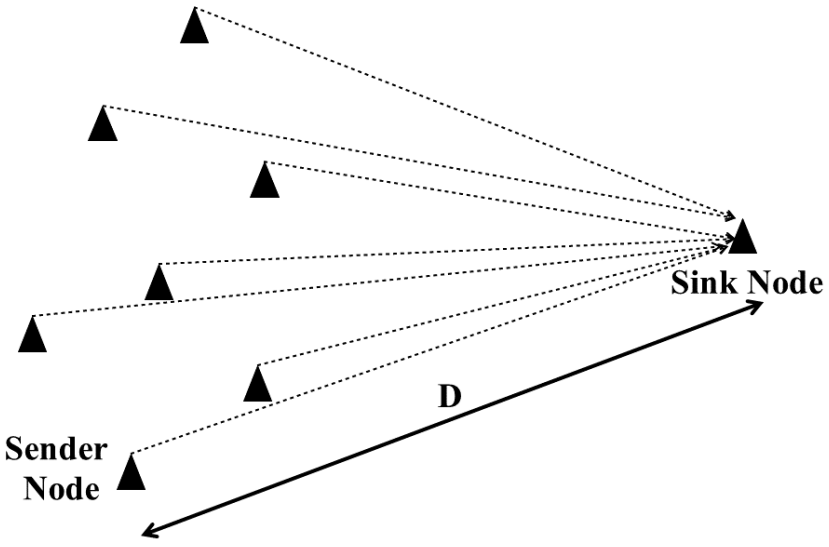

Figure 2.1: Star topology.

2.2.1 Energy Consumption Depending on SF and P_{tx}

Here, we analyze energy consumption and the maximal reachable distance D_{max} as a function of SF and P_{tx}. In this scenario, the bandwidth is set to 125 kHz.

To do so, we have first analyzed the Maximum Coupling Loss (MCL) permitted for the link communication in Table 2.10, i.e., the maximum link budget permitted for each value of SF and P_{tx}. MCL is determined according to the receiver sensitivity and transmitted power. PL_{Hata} has to be smaller than MCL to guarantee correct signal demodulation. Thus, PL_{Hata} gives the maximal distance permitted for transmission (D_{max}). In Table 2.10, we can observe that MCL increases when SF and P_{tx} increase. However, combinations of SF and P_{tx} give different values of energy consumption. Therefore, there is a trade-off between the range and energy consumption.

Table 2.10: Maximum coupling loss of LoRa with a 125 kHz bandwidth.

SF/P_{tx}	2dBm	5dBm	8dBm	11dBm	14dBm
6	120	123	126	129	132
7	125	128	131	134	137
8	128	131	134	137	140
9	131	134	137	140	143
10	134	137	140	143	146
11	135	138	141	144	147
12	138	141	144	147	150

For the star topology network, we evaluate the energy consumption of a single hop as:

$$E_{star(SF,P_{tx})} = E_{tx} + E_{rx} \tag{2.24}$$

where E_{tx} is the energy consumption caused by the transmission and E_{rx} caused by the reception. For this calculation, we only consider the time spend in transmission and reception, respectively. Time on air of a packet (t_{packet}) depends on SF, BW, and CR. Accordingly, energy consumption for the star topology can be expressed as follows:

$$\begin{aligned} E_{star(SF,P_{tx})} &= t_{packet}.(P_{tx} + P_{rx}) \\ &= \frac{L_{packet}}{R_b}.(P_{tx} + P_{rx}) \end{aligned} \tag{2.25}$$

where L_{packet} is the size of the transmitted packet in bits. P_{tx} and P_{rx} are the consumed power according to the supply current and supply voltage for transmitter and receiver, respectively as specified in Tables 2.8 and 2.9.

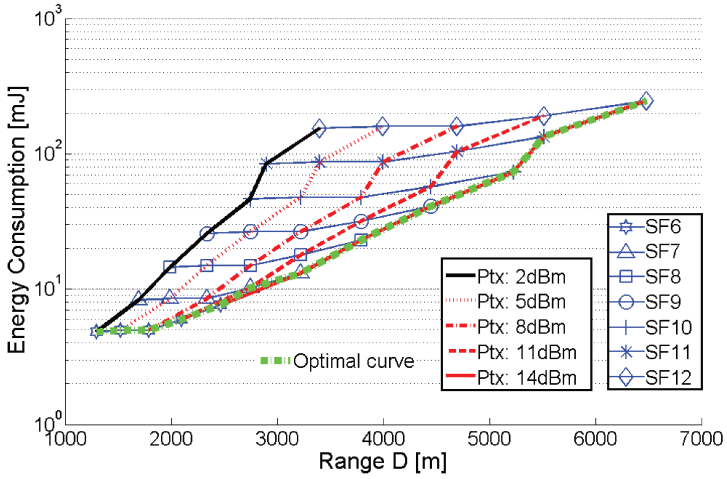

Figure 2.2: Energy consumption for various configurations of SF and P_{tx} in star topology. BW is set to 125 kHz and CR to $\frac{4}{5}$.

Figure 2.2 shows energy consumption as a function of range D for different values of (SF, P_{tx}). When increasing P_{tx} (blue curves), a smooth energy consumption increase is observed for fixed SF. When switching

SF ascendantly with fixed P_{tx} (red curves), energy consumption increases faster. Thus, it is preferable for increasing the range, to first increase P_{tx} and then to increment the spreading factor. For a (SF6, P_{tx} = 2 dBm) configuration, Figure 2.2 shows that the maximum reachable range is D_{max} = 1,3 km and energy consumption is E = 4,8 mJ. Note that the maximum range (D_{max} = 6,5 km) is reached using SF12 and P_{tx} = 14 dBm. Beyond 6,5 km, it is not possible to establish a communication in a star topology (i.e., with a single hop).

What are the best SF and P_{tx} configurations to improve the battery lifetime?

Proposed strategy: From these results, the optimal configuration strategy to achieve lower energy consumption over distance D is shown in Figure 2.3.

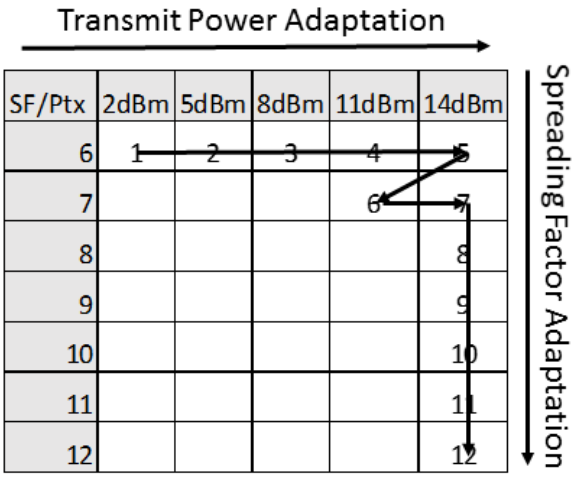

Figure 2.3: Spreading factor and transmitted power adaptation strategy. Bandwidth is fixed to 125 kHz.

Thus, starting from the lowest energy consumption configuration (SF6, P_{tx} = 2 dBm), the strategy is firstly to adapt the transmitted power until we reach (SF6, P_{tx} = 14 dBm), then, adapt the spreading factor until reaching (SF12, P_{tx} = 14 dBm). This strategy defines the optimal energy consumption curve (as shown with the green curve in Figure 2.2).

2.2.2 Energy Consumption Depending on SF, P_{tx}, and BW

We extend our energy consumption analysis to three values of bandwidth: 125 kHz, 250 kHz, and 500 kHz. We follow the same approach as in Section 2.2.1 to analyze energy consumption for 250 kHz and 500 kHz bandwidth. The optimal energy consumption curve for each BW is shown in Figure 2.4.

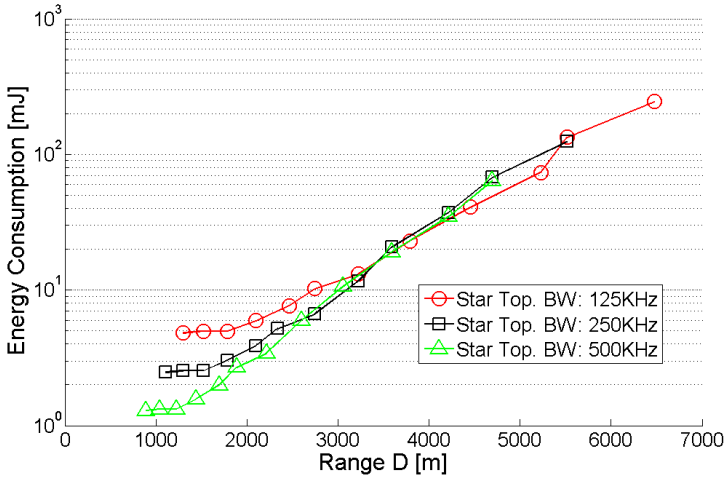

Figure 2.4: Optimal energy consumption for various values of bandwidth: 125 kHz, 250 kHz, and 500 kHz in the star topology.

We observe that the maximum range increases when BW decreases. This is because MCL is higher with lower BW. However, low BW comes with lower throughput and therefore, a longer time on the air, leading to higher energy consumption. Accordingly, for a range of D < 2,6 km, using BW = 500 kHz permits lower

energy consumption. Beyond $D = 2{,}6\,\text{km}$, energy consumption is similar for the three values of bandwidth. Then, BW adaptation does not have significant impact on energy consumption. However, it is important for the coverage: smaller BW results in longer communication ranges.

How to exploit the multiple "degrees of freedom" (concerning SF, P_{tx}, and BW) of LoRa radio to improve the battery lifetime in a star topology?

Proposed strategy: For adapting SF, P_{tx}, and BW, Figure 2.5 presents the optimal strategy.

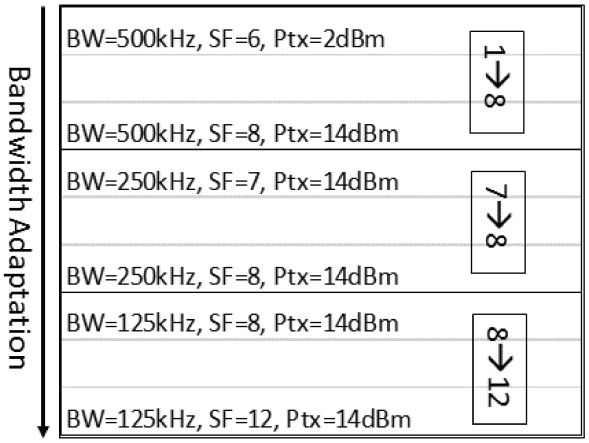

Figure 2.5: (SF, P_{tx}, BW) adaptation strategy.

The lowest energy consumption configuration is ($BW = 500\,\text{kHz}$, SF6, $P_{tx} = 2\,\text{dBm}$). For $BW = 500\,\text{kHz}$, the box at the right side (1–>8) refers to the adaptation strategy as shown in Figure 2.3. Thus, the best strategy is still first to adapt the transmitted power (up to $P_{tx} = 14\,\text{dBm}$) and then, adapt the spreading factor (up to SF8). Afterward, the adaptive strategies are applied to bandwidth of 250 kHz and 125 kHz according to the boxes.

For the sake of simplicity in the hardware implementation, we recommend to directly switch from $BW = 500\,\text{kHz}$ to $BW = 125\,\text{kHz}$.

2.3 LoRa Adaptation in Mesh Topology

In this section, we analyze energy consumption to transmit a packet from a sender node to the sink node through some relay nodes. To do so, we consider a line multi-hop topology as shown in Figure 2.6. We define D, the end-to-end distance (i.e., between the sender and sink node) and d, the distance between each relay.

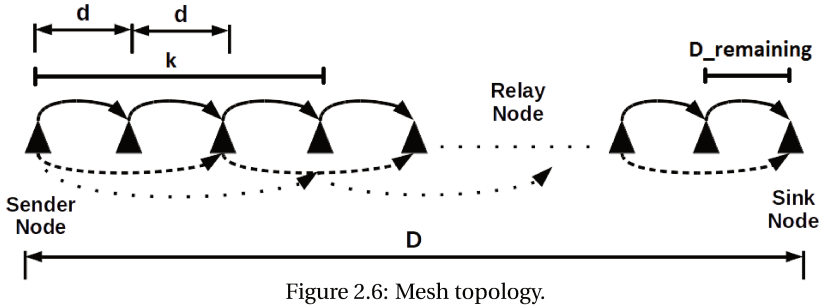

Figure 2.6: Mesh topology.

We assume that one hop takes advantage of the maximal distance reachable for a given SF and P_{tx} according to the inter-relay distance granularity d. In other words, depending on the maximal range of the selected configuration, the furthest relay at distance k is reached. It is computed as follows:

$$k = \left\lfloor \frac{D_{\max}}{d} \right\rfloor .d, \tag{2.26}$$

where $D_{\max}$ is the maximal transmission distance for given (SF, P_{tx}). Then, n is defined as the total number of hops to reach the sink node. We denote $D_{\text{remaining}}$ as the distance between the sink node and the last relay to reach it defined as:

$$D_{\text{remaining}} = D - k.\left\lceil \frac{D}{k} \right\rceil \tag{2.27}$$

If $D_{\text{remaining}}$ is zero, n is computed as:

$$n = \left\lceil \frac{D}{k} \right\rceil \tag{2.28}$$

else, we verify if it is possible to reach the sink node from the penultimate relay by a single hop. Then, n is computed as:

$$n = \left\lceil \frac{D}{k} \right\rceil - \left\lfloor \frac{D_{\max}}{k + D_{\text{remaining}}} \right\rfloor \tag{2.29}$$

In Figure 2.6, the maximal transmission range k of chosen (SF, P_{tx}) reaches the third relay, then the packet goes over 3 hops. In this case, it is important to evaluate what is the best relaying strategy in terms of energy consumption: one direct hop with the third node using an appropriate configuration or three hops with a more energy-efficient strategy.

Energy consumption assuming n hops to reach the sink node is:

$$E_{\text{mesh}} = \sum_{i=1}^{n} (E_{\text{tx},i} + E_{\text{rx},i}), \tag{2.30}$$

where $E_{\text{tx},i}$ and $E_{\text{rx},i}$ are the energy consumption of the transmitter and receiver, respectively with the current configuration of transmitted power, spreading factor, and bandwidth of hop i.

In the following simulations, the bandwidth is set to 125 kHz. The mesh topology using different spreading factors and transmitted power is analyzed as a function of the network density and the network coverage. The network density can be modeled with the inter-relay distance d and the network coverage with the end-to-end distance D. Thus, we evaluate the energy efficiency of the LoRa mesh for various distances d between relay nodes, when D is fixed, and for various distances D from the sender node to the sink node, when d is fixed.

2.3.1 Energy Consumption Depending on Network Density

Here we evaluate the impact of the inter-relay distance d, i.e., indirectly the network density in the mesh LoRa network. Figure 2.7 shows the energy consumption depending on the inter-relay distance d, when the end-to-end distance is fixed to 10 km. For this distance, direct communications are impossible.

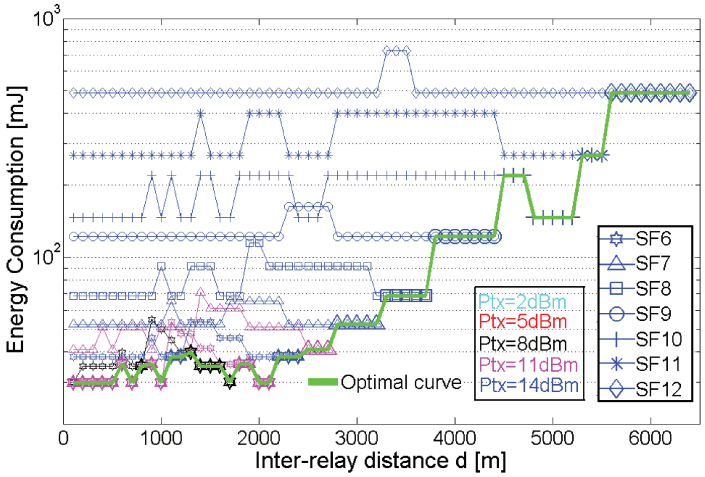

Figure 2.7: Energy consumption of the mesh topology depending on inter-relay distance d when distance D between the sender node and the sink is set to 10 km.

For inter-relay distance d higher than 6,4 km, the link communication cannot be established: this is the limit of the LoRa range in an open rural environment. For inter-relay distance d up to 2,2 km, we observe that the optimal configuration is SF6 (represented by a hexagon) whereas various colors show the optimal P_{tx}. For inter-relay distances larger than 2,2 km, we observe that the optimal configuration to reach fixed

distance D of 10 km is SF7, then SF8, then SF9, and so on until SF12 (for $D > 6{,}4$ km) and for all of them, P_{tx} must be set to 14 dBm (blue).

The green curve represents the optimal strategy for the mesh topology according to the inter-relay distance d, i.e., representing the network density. In other words, in dense networks (i.e., small d), it is better to use the lowest SF (e.g., SF6) with low power and increase progressively the transmission power when d increases. Then, when we reach the maximum permitted power (i.e., 14 dBm), it is better to increment the spreading factor to compensate for the sparsity of the network.

Figure 2.8 extends the analysis to four distances D: 5 km, 10 km, 15 km, and 20 km. Only the optimal strategy curves are displayed.

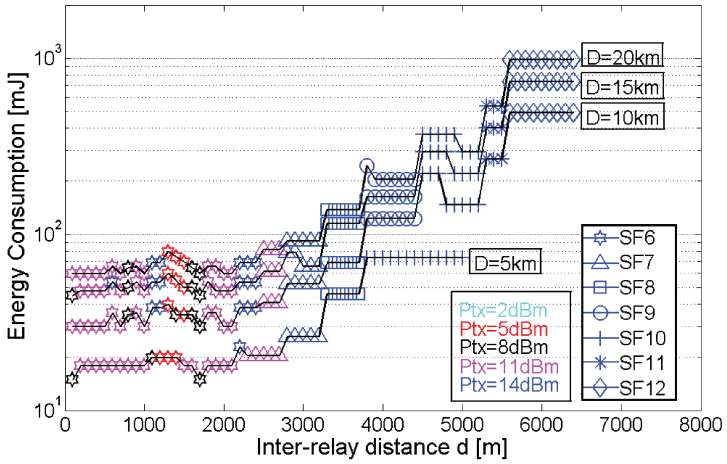

Figure 2.8: Energy consumption depending on d for various ranges D.

We observe that all the curves for end-to-end distance D larger than 10 km follow a similar strategy with multi-hop transmissions to reach the sink. When D is 5 km, multi-hop is useful only when the inter-relay distance is lower than 3,8 km. Otherwise, it is better to communicate directly with (SF10, $P_{tx} = 14$ dBm) configuration. Moreover, we observe that the minimum available power (i.e., 2 dBm) is never optimal because the transmitted power is not the dominating factor of energy consumption with respect to the spreading factor adaptation and the multi-hop strategy. Moreover, our strategy always looks for the optimal number of hops reducing energy consumption. This optimization depends on the maximal transmission distance for a given (SF, P_{tx}) configuration. For instance, in the case of dense networks, where the inter-relay distance is smaller than 1 km, it is preferable to use P_{tx} of 11 dBm rather than 2 dBm because the larger D_{max}, the smaller the number of hops, thus reducing energy consumption. We conclude that depending on the inter-relay distance in dense networks, the best strategy consists in using the lowest SF and the transmission power that optimize the number of hops to reach the sink. However, when the network becomes sparser, we use a scaling up strategy on SF with the maximum permitted power (e.g., 14 dBm).

2.3.2 Energy Consumption Depending on Network Coverage

We evaluate the impact of end-to-end distance D, i.e., indirectly the cell coverage on energy consumption. For this purpose, we have extended the analysis to the case when d is fixed and D varies. In this scenario, we aim to evaluate the total energy consumption needed to transmit a packet to reach the sink node located at D meters from the sender node. To do so, we consider transmissions through the optimal relay nodes with the optimal (SF, P_{tx}) configurations.

In Figure 2.9, we present the energy consumption as a function of end-to-end distance D for various inter-relay distances d (i.e., 0,1 km, 0,5 km, 1 km, 2 km, 3 km, 4 km, 5 km, and 6 km).

For an inter-relay distance smaller than $d < 2$ km, we observe similar energy consumption as using the optimal SF configuration (i.e., SF6, variable P_{tx}). For $d > 2$ km, we observe that the optimal SF configurations are SF7, SF9, SF10, SF12 for $d = 3$ km, 4 km, 5 km, 6 km, respectively. Moreover, we observe that for sparse networks (i.e., $d > 2$ km), the number of hops proportionally increases when the cell coverage increases in a multiple of the inter-relay distance. In these intervals, the radio configuration is the same and energy consumption remains constant. For instance, when $d = 6$ km, the sink is directly reached when D is

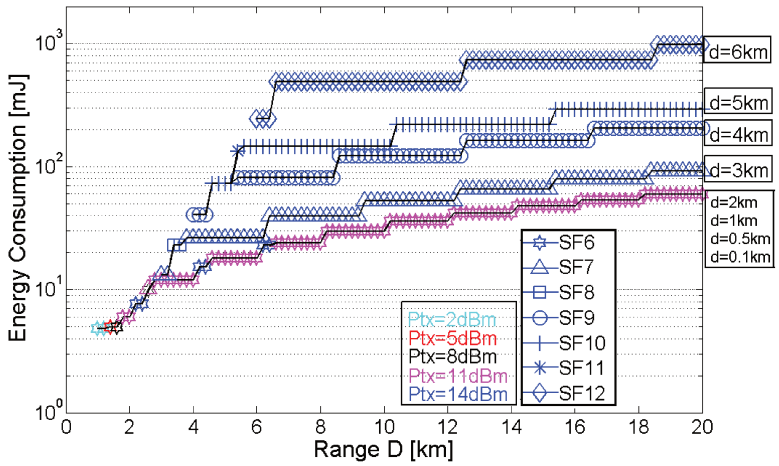

Figure 2.9: Energy consumption depending on range D for various inter-relay distances d.

smaller that 6,4 km, with 2-hops when D is between 6.4 and 12,4 km, with 3-hops when D is between 12.4 and 18,4 km and so on.

How to take advantage of the network architecture by boosting the use of high data rate configurations?

Proposed strategy: The optimal strategy to achieve the lowest energy consumption as a function of inter-relay distance d is shown in Figure 2.10.

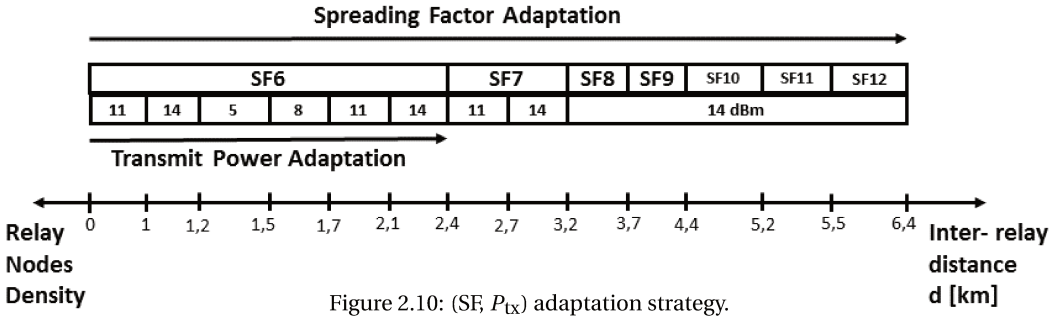

Figure 2.10: (SF, P_{tx}) adaptation strategy.

For small inter-relay distances (i.e. $d < 1{,}2$ km), as the number of relay nodes is large, the best strategy is to maximize the reachable distance of each hop with a configuration using the highest transmitted power (i.e., 11 or 14 dBm) and the smallest spreading factor (i.e., SF6). From $d = 1{,}2$ km to $d = 2{,}4$ km, the strategy is to adapt the transmitted power from 5 dBm up to 14 dBm. Finally, from $d = 2{,}4$ km to $d = 6{,}4$ km, the strategy is to adapt SF: from (SF7, $P_{tx} = 14$ dBm) to (SF12, $P_{tx} = 14$ dBm) configurations.

2.4 Network Topology Impact: Star vs Mesh

We compare the energy consumption of star and mesh topologies. In the star topology, we consider the optimal configuration to achieve low energy consumption and the maximum range, that results in a fair comparison between both topologies. In Figure 2.11, we observe the energy consumption of a LoRa mesh network using a BW of 125 kHz for various network densities (i.e., inter-relay distances d) and the optimal energy consumption curves for the star topology for BW of 125 kHz, 250 kHz, and 500 kHz.

We observe that up to 3 km, the energy consumption of the star topology is the lowest. Beyond $D = 3$ km, the mesh topology becomes interesting.

How to jointly exploit the multiple "degrees of freedom" (concerning SF, P_{tx}, and BW) of LoRa radio and the network topology to improve the battery lifetime?

Proposed strategy: The optimal strategy exploiting both topologies is shown in Figure 2.12. Depending on inter-relay distance d, we propose an adaptive strategy over distance D passing from the star to the mesh topology. In the case of a dense network (i.e., $d < 2{,}4$ km), we propose a star strategy as described in Section

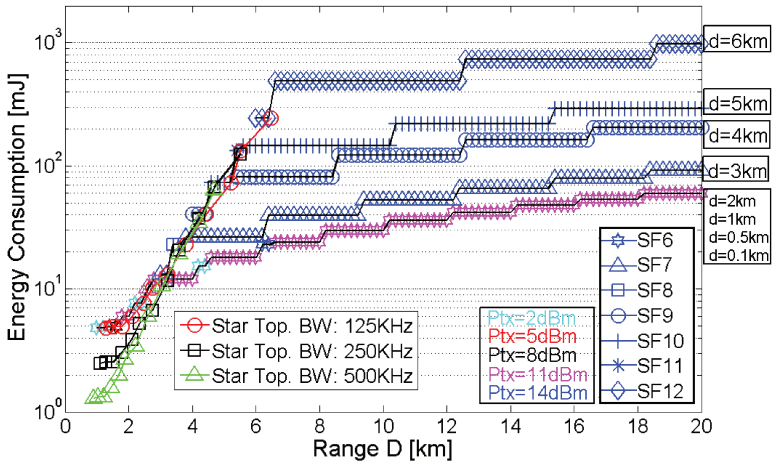

Figure 2.11: Energy consumption in star and mesh topologies.

2.2.2 when $D < 3{,}0\,\text{km}$. Beyond 3,0 km, a mesh strategy with (SF6, $P_{tx} = 11\,\text{dBm}$) configuration becomes more efficient to reach the sink node. For $2{,}4\,\text{km} < d < 3{,}2\,\text{km}$, the best configuration consists in following the star strategy up to $D = 3{,}2\,\text{km}$. Then, we recommend to pass to a mesh strategy. A similar behavior is observed when increasing d up to 6,4 km.

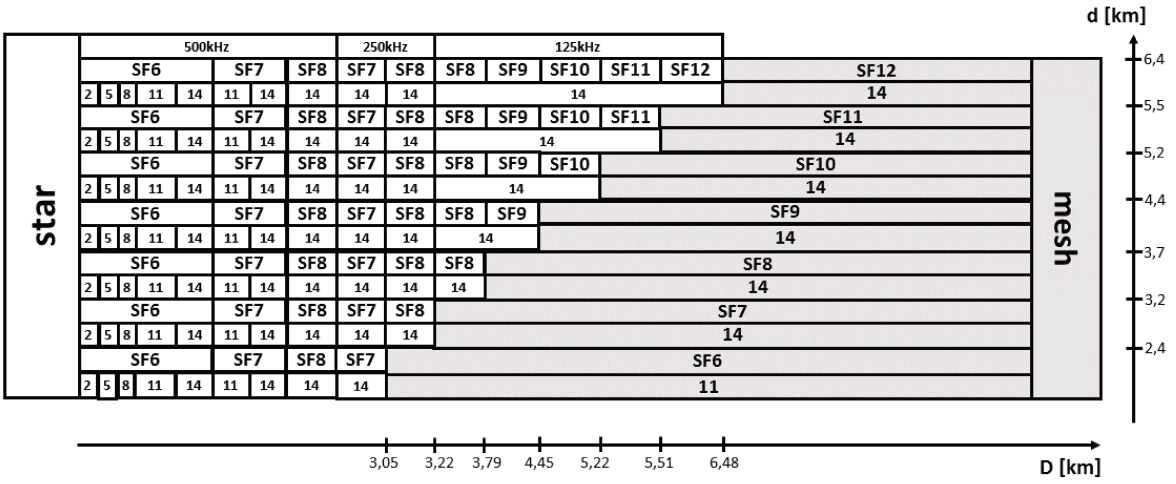

Figure 2.12: Topology adaptation strategy.

Conclusion

In this chapter, we investigated energy consumption for sending a 50 byte packet with various LoRa configurations for star and mesh topologies. The goal was to exploit the LoRa technology by adapting its parameters (i.e., spreading factor, bandwidth, and transmitted power). We compute energy consumption based on the transceiver data sheet Semtech SX1276.

For the star topology, we observe that increasing SF has a more significant impact on energy consumption than increasing P_{tx}, that also makes the communication range longer. The best strategy is firstly to adapt the transmission power and then to increment the spreading factor to obtain the optimal energy consumption. When the bandwidth is considered, our results show that the optimal energy consumption is for $BW =$ 500 kHz up to a range of 3 km. Beyond 3 km, we adapt BW according to the data rate and range constraints.

For the mesh topology, the energy consumption is optimized by exploiting different radio configurations and the network topology (e.g., the number of hops, the network density, the cell coverage). In dense net-

works, the proposed strategy consists of setting the spreading factor to SF6 and progressively increasing the transmitted power with the inter-relay distance. In the case of sparse networks, we recommend to adapt SF until we reach the (SF=12, P_{tx} = 14 dBm) configuration.

According to the topology comparison, we show that a global strategy exploiting both topologies exists and the trade-off between the star and mesh strategies depends on end-to-end distance D (i.e., the network coverage) and inter-relay distance d (i.e. the network density). Adapting the topology and the LoRa radio parameters permits to maintain low energy consumption and to extend the range of communication.

Thanks to the flexibility of its parameters, the openness of the system, the maturity of the technology and low energy consumption, LoRa is a good candidate for Adaptive Networks. However, we need to evaluate performance and limitations, specially for large scale networks, which is the goal of next chapter. Note that, we look for trading-off the LoRa communication parameters regarding the access and not the most energy consumption solution. Star of stars topology will be considered due to simple infrastructure, anyway LoRaWAN uses this topology. Mesh topology will not be evaluated due to the complexity of implementing protocols to adapt the network.

Performance and Limitations of Large Scale LoRa Networks

This chapter is partially adapted from:

- *M. Nunez, L. Suraty, M. Maman, A. Duda.* Large Scale LoRa Networks: From Homogeneous to Heterogeneous Deployments. *In IEEE 14th International Conference on Wireless and Mobile Computing, Networking and Communications (WiMob). IEEE, 2018.* [97]
- *M. Nunez, A. Guizar, M. Maman, A. Duda.* Toward a Self-Deployment of LoRa Networks: Link and Topology Adaptation. *In IEEE 15th International Conference on Wireless and Mobile Computing, Networking and Communications (WiMob). IEEE, 2019.* [98]

Contents

Introduction

In the previous chapter, we showed the flexibility of LoRa parameters investigating energy consumption and coverage. Deeper investigation is required analysing more key network performance metrics and taking into account application, MAC, and physical layers. In this chapter, we present packet delivery ratio and throughput analysis of the LoRa technology for several network sizes and application traffic intensities.

The first contribution of this chapter is the investigation of LoRa network deployments of nodes with homogeneous communication parameters. It allows to obtain the performance of each spreading factor individually to calculate their capacity for each network size assuring a packet delivery ratio. This individual spreading factor performance allows to understand advantages and limitations, and also to propose improved allocation protocols using different spreading factors. From this analysis, we can conclude that low spreading factors achieve high performance but their coverage is limited. Indeed, the capacity of a SF_i approximately is twice the capacity of SF_{i+1}.

The second contribution is the investigation of LoRa network deployments of nodes with heterogeneous communication parameters. We explore spreading factor allocation protocols to improve network performance exploiting LoRa physical layer features as spreading factor quasi-orthogonality. These spreading factor allocation protocols configure nodes: (i) according to their link budget like the Adaptive Data Rate (ADR) of LoRaWAN specification, (ii) randomly, and (iii) with an equal number of nodes per SF. From this analysis, we can conclude that deployments configured with heterogeneous parameters improve network performance thanks to the quasi-orthogonality of spreading factors but it could be even more enhanced. Indeed, deeper investigation is necessary to define the optimal allocation of spreading factors.

The next contribution is the detailed performance analysis of the spreading factor allocation protocol based on the link budget that we will call hereafter ADR. It allows to understand the impact on the network performance in several aspects: (i) network deployment, (ii) environment, (iii) multiple channels, and (iv) bidirectional communications. Capabilities and limitations are clarified to investigate more optimal allocation protocols exploiting principally the individual capacity of each spreading factor and their quasi-orthogonality to improve the ratio of received packets. From this analysis, we can conclude that network performance depends on the usage of the spreading factors, i.e., there should be a trade-off between over-used and under-used spreading factors to achieve a fair allocation.

The final contribution of this chapter is the analysis of the network densification by placing multiple gateways in LoRa networks of nodes with homogeneous parameters. It allows to improve performance taking advantage of the spectrum spatial reuse and to propose the first adaptation strategy giving the number of gateways needed to assure a certain level of reliability for a network size. This adaptation strategy limits the number of covered nodes per gateway serving them with better packet delivery ratio especially for large scale deployments. We also analysed the ADR in multi gateway scenarios. From this analysis, we can conclude that over-sizing the number of gateways saturates the use of low spreading factors by not exploiting the others.

This chapter is structured as follows. After the introduction, we present the system model and the methodology (Section 3.2) explaining the simulation environment and assumptions for the node configuration, network deployment, and application parameters. Then, we present the investigation of LoRa network deployments of nodes with homogeneous and heterogeneous parameters in Section 3.3 and Section 3.4, respectively. After Section 3.5 that analyzes performance of ADR and the impact of several aspects on it, Section 3.6 analyses and discusses the network densification for network deployments of nodes with homogeneous parameters and also for ADR. Finally, Section 3.7 concludes this chapter.

3.1 System Model and Methodology

All simulations have been performed with the WSNet simulator. It integrates several modules modeling the LoRa technology. The LoRa modules are configurable, they can be used to exploit different parameters to enhance network performance. The flexibility of the architecture allows the integration of new protocols.

The system model used to investigate LoRa deployments is defined in Table 3.11. The frequency band is the 868 MHz ISM limited by ETSI regulations to maximum duty cycle of 0.1% or 1%, depending on the selected sub-band, limiting the network capacity and throughput. We decided to focus on this band because of favorable propagation conditions. Sub-GHz band allows penetrating thicker objects compared to GHz bands being the first band preferred for LPWAN. We consider a 125 kHz typical bandwidth in the EU868 MHz band, coding rate of $\frac{4}{5}$, and the transmitted power of 14 dBm, constant parameters in simulations. We consider seven values of available spreading factor, from SF_6 to SF_{12}. Nodes in a network deployment can be configured with only a single SF_i or with many spreading factors depending on the protocol for spreading factor allocation. We call them network deployments with nodes configured with homogeneous and heterogeneous parameters, respectively. Indeed, these values (spreading factor, bandwidth, and coding rate) define the bit rate, e.g., 9375 b/s and 293 b/s for SF_6 and SF_{12}, respectively.

Table 3.11: System Model.

Configuration		Network Deployment	
$FrequencyBand$	868 MHz	$AreaofInterest$	circular area $R = D_{max}(SFi)$, room 100mx100m
$Bandwidth$	125 KHz	$Deployment$	uniform, dense, concentric
$CodingRate$	4/5	$Multi-GW$	MG_1, MG_3, MG_7, MG_9
$TransmissionPower$	14 dBm	$GWposition$	centered, circles covering circle geometry
$SpreadingFactor$	SFi only, or SF_6 to SF_{12}	$PathlossModel$	Okumura Hata, Tanghe
Application			
$ApplicationPeriod$	50Byte packet every 1 min to every 1 day	$Protocol$	Homogeneous, Heterogeneous, ADR
$Multi-Channel$	1CH, or 8CH	$Bidirectional$	UL only, or UL / DL

A scenario is defined by (i) the configuration of the node, both end-devices and gateways, (ii) the network deployment, and (iii) the application, as shown in Table 3.11.

The configuration of the node is defined by: frequency band, BW, CR, TP, and SF. Note that we consider these parameters constant except the SF. All nodes can be configured with the same SF_i (i.e. homogeneous configuration of parameters) or with different SF (SF_6 to SF_{12}, i.e., heterogeneous configuration of parameters).

The network deployment is defined by: the area of interest, the type of deployment (e.g., uniform, dense, and concentric), the multiplicity of the gateways (MG_i means i gateways), their positions, and the environment (pathloss model).

The application is defined by: the application period (e.g., packets transmitted every 1 hour), the number of channels, the SF allocation protocol (e.g., ADR), and the bidirectionality of the communication.

We define several scenarios varying spreading factor, network deployment, and the application. Note that we will reuse Table 3.11 setting up parameters for every analyzed scenario. Following subsections show in detail parameters of the network deployment and the application.

3.1.1 Area of Interest

The area of interest is the geographical zone where nodes are placed. We define two areas: (i) a circular area for open environment and (ii) a square room for a factory of the future environment. The amount of deployed nodes N varies between 1 and 10000 nodes.

3.1.1.1 Circular Area

Nodes are deployed in circular areas of radius R. This radius is the maximum distance of coverage using a SF_i for 14 dBm of transmitted power and a path loss model between the gateway and the nodes. Maximum coverage is denoted by $D_{max}(SF_i)$. Figure 3.1 shows these circular areas of $R = D_{max}(SF_i)$ for each SF_i.

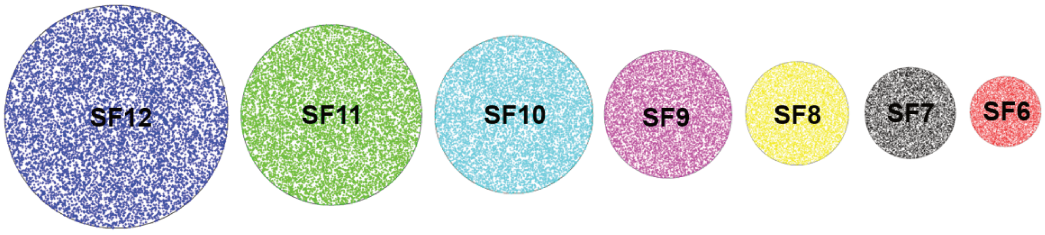

Figure 3.1: Deployment in circular area of $R = D_{max}(SF_i)$.

3.1.1.2 Factory of the Future Room

Nodes are deployed in a room of 100 m x 100 m. This area allows to investigate deployments in a Factory of the Future (FoF) scenarios. These industrial scenarios are characterized by more severe models of path loss, shadowing, and fading. Figure 3.2 illustrates the FoF room.

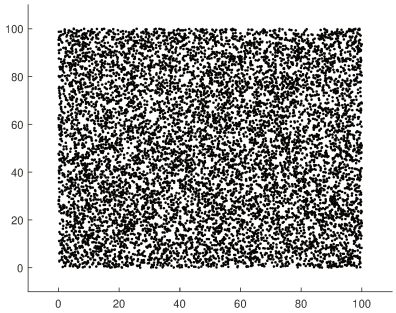

Figure 3.2: Deployment in a room of 100 m x 100 m (FoF scenario).

3.1.2 Deployment

The network deployment of nodes in the area of interest defined previously can be: (i) uniform, (ii) concentric, and (iii) dense. In general, we investigate LoRa networks in uniform deployments. Concentric deployment is investigated for specific spreading factor allocation protocol only in this chapter. Dense deployments are as well investigated for a specific protocol in this chapter, and for several protocols in Chapter 4. We detail these deployments below.

3.1.2.1 Uniform Deployment

Nodes are placed in the area of interest in a random way. So, in uniform random deployments each of the N deployed nodes has equal probability of being placed at any point of the area of interest.

In the case of circular area with radius R, the distance between the node and the center is random variable $r = \sqrt{rand(0,R)}$. Figure 3.3 illustrates this deployment. It is taken into account because it is simple and practical.

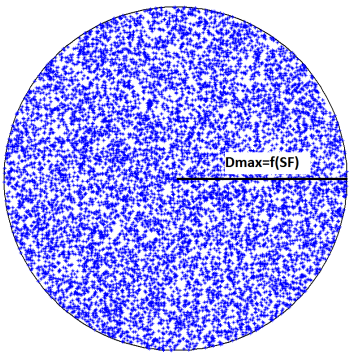

Figure 3.3: Uniform deployment in circular area of $R = D_{max}(SF_i)$.

3.1.2.2 Concentric Deployment

The concentric deployment is the superposition of uniform deployments in circular areas, i.e. the seven disks of radius $R = D_{max}(SF_i)$ superposed concentrically with the same quantity on nodes uniformly deployed in each disk. Figure 3.4(a) shows this deployment. So, we observe that the deployment is denser close to the center of the area of interest which is a circular area of $R = D_{max}(SF_{12})$. The density for the ring i starting from the center is given by $\sigma_i = \frac{N}{7}\sum_{j=i}^{7}\frac{1}{A_j}$, where N is the total number of nodes and A_j is the area of the disk of radius $R = D_{max}(SF_{i+5})$. For example, in a deployment of 7000 nodes the density distributions are 174 nodes/km^2 for the disk in the center; 123, 85, 57, 36, 20 and 8 nodes/km^2 for the farther rings, respectively.

3.1.2.3 Dense Deployment

In this deployment, the distance between the node and the center of the area of interest is a random variable following $r = rand(0, R)^3$. Figure 3.4(b) shows this deployment. Note that we investigate ADR protocol using this deployment in this chapter and several protocols in the next chapter. This deployment is adopted because it is more realistic resembling to a deployment in a city.

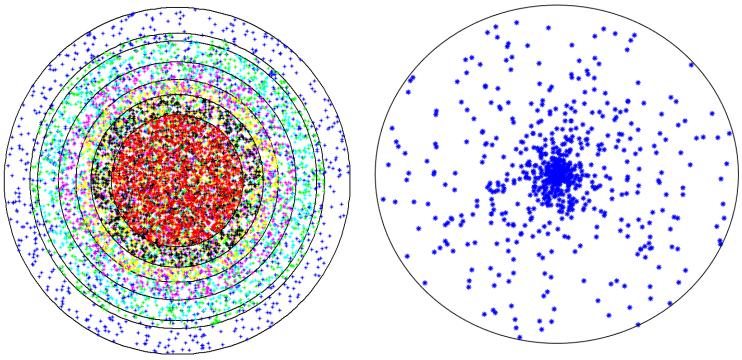

(a) Concentric deployment. (b) Dense deployment.

Figure 3.4: Non uniform deployments in circular areas.

3.1.3 Multiple Gateways and Positions

Several network deployment scenarios were simulated for single and multiple gateways. These simulations were performed for 1, 3, 7, or 9 gateways. MG_i denotes a multi-gateway scenario with i gateways.

For a single gateway, it is placed at the center of the area of interest whereas for multiple gateways, their positions are defined following the circles covering circle geometry [99] to have full coverage of the area of interest (e.g., a disk of radius $R = D_{max}(SF_{12})$). So, gateways are placed at the center of the circles of radius r covering the circle of radius R. Figure 3.5 illustrates the placement of the gateways and the relationship between these two radius.

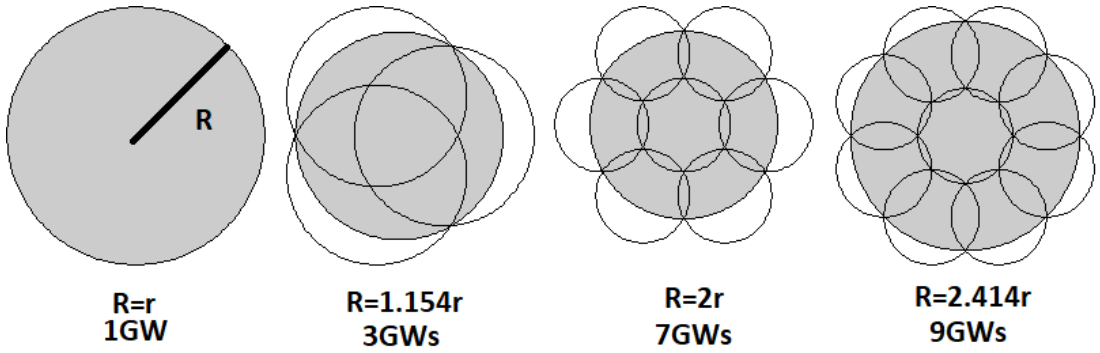

Figure 3.5: Placement of 1, 3, 7, and 9 GWs.

3.1.4 Path-loss Propagation Models

The path-loss between nodes and the gateway is defined by: (i) the Okumura Hata model for open areas or (ii) the Tanghe model for factory of the future (FoF) scenarios. We detail them below.

3.1.4.1 Okumura Hata

The first one is the Okumura Hata propagation model for an open rural environment operating at 868 MHz frequency band. The path-loss (PL) is given by Equation 2.19 previously defined in the radio propagation model of Chapter 2.

The transmitted power, the spreading factor, and this propagation model allow to define the maximal communication distance for each SF_i. Indeed, Table 3.12 shows $D_{max}(SF_i)$ to assure a maximum packet error rate of 1%.

Table 3.12: Maximal distance coverage per SF_i.

SF_i	6	7	8	9	10	11	12
$D_{max}(SF_i)$ [km]	2.508	2.899	3.354	3.885	4.503	5.225	6.068

3.1.4.2 Tanghe

LPWAN and advanced wireless connectivity increased interest for Factory of the Future (FoF). In the literature, there are several propagation models for industry. We considered the pathloss, shadowing, and fading model by Tanghe et al. [100] [101]. This model characterises the industrial environment based on measurements. The pathloss (PL) is given in Equation 3.31.

$$PL(d) = PL_0 + n.10.log_{10}\frac{d}{d_0} + X_\sigma \tag{3.31}$$

where PL_0 is the pathloss attenuation at $d_0 = 15m$ and exponent n. X_σ is the shadowing following a Gaussian distribution with zero mean and standard deviation σ. These parameters depend on the link condition showed in Table 3.13 for the 868MHz band. Tanghe et al. [100] proposed a lognormal distribution with 12.4 mean and 5.4 dB standard deviation for multi-path fading.

Table 3.13: Tangue pathloss model parameters for the 868MHz band.

	LoS	$NLoS$	$NLOS_2$
PL_0	57.67	64.4	69.7
n	2.25	1.94	2.16
σ	5.65	4.97	5.16

3.1.5 Application

On nodes, the application sends a packet every interval called application period (AP). These intervals are configurable as well as the packet length. At every AP occurrence, a node randomly selects a time instant inside the interval and generates one packet. For simulations, we consider a fixed packet length of 50 Bytes. So, nodes transmit a 50 Bytes packet every AP that can be configured between 1 min and 1 day.

The gateway collects received packets and sends them to the network server over IP. LoRa provides a standard to forward packets to the network backend but we did not implement it in our model. We assume the network server is the brain of the network that controls the communications between nodes and gateways. It also determines how many nodes are communicating to a gateway and the statistics of the spreading factor usage of the nodes. In multi gateways scenarios, a packet can be received at different gateways. The network server discards these copies. Algorithms and protocols are implemented at the network server (e.g., the ADR mechanism and our proposals). These algorithms can do spreading factor allocation, power control, and so on. In our simulations, we assume nodes transmit unconfirmed packets. We assume they do not wait for acknowledgements. So, the overhead due to downlink communication is not taken into account unless we specify otherwise.

3.1.6 Metrics

In addition to the metrics defined to analyze network performance: (i) the reliability (the packet delivery ratio (PDR)) and (ii) the total network throughput (the number of received packet per unit time), we define network-wide metrics to evaluate deployment scenarios:

i) Ratio of Covered Nodes: the percentage of nodes within the gateway range according to the path-loss model (e.g., Okumura-Hata).

ii) Redundancy: the number of gateways in the communication range of a node.

iii) Network PDR: the ratio between the number of delivered packets and the number of transmitted packets for all nodes deployed in the area of interest.

iv) Connected PDR: the Network PDR of covered nodes.

Evaluating these metrics we identify three types of deployments:

- *Under-coverage:* the whole zone is not completely covered. Ratio of covered nodes is $< 100\%$ and redundancy is in general < 1.
- *Optimal-coverage:* the whole geographical area of interest is covered by the GWs. Ratio of covered nodes is 100% and redundancy is close to 1.
- *Over-coverage:* the whole zone is totally covered and nodes can detect several GWs. Ratio of covered nodes is 100% and redundancy is > 1.

3.2 Deployments of Nodes with Homogeneous Communication Parameters

The goal of this section is to analyze the performance and limitations of each spreading factor individually. We analyze them in deployments of nodes with homogeneous communication parameters. Note that we defined homogeneous deployments as the deployments where all nodes are configured with the same LoRa parameters (i.e., SF, BW, CR, and TP). Homogeneous deployments aid to characterize the capacity of each SF. This is the first basic SF allocation to evaluate and understand performance and limitations of each SF individually.

We present simulation results for homogeneous deployments with different SFs as a function of: (i) the number of nodes (up to 10000) and (ii) the application period (packet transmissions period). We evaluate transmission quality in terms of packet delivery ratio and throughput for several deployments. We have to emphasize that nodes are deployed in a disk of radius equal to the maximum transmission range of SF_i for each scenario, i.e., the homogeneous SF6 is deployed in a disk of $R = D_{max}(SF_6)$ and so on ensuring communication range of all nodes to the gateway.

3.2.1 Impact of Network Size

Table 3.14: System Model to analyze the impact of network size.

Configuration		Network Deployment	
$FrequencyBand$	868 MHz	$AreaofInterest$	circular area $R = D_{max}(SFi)$
$Bandwidth$	125 KHz	$Deployment$	uniform
$CodingRate$	4/5	$Multi-GW$	MG_1
$TransmissionPower$	14 dBm	$GWposition$	centered
$SpreadingFactor$	SFi only	$PathlossModel$	Okumura Hata
Application			
$ApplicationPeriod$	50Bytes packet every 1 min	$Protocol$	Homogeneous
$Multi-Channel$	1CH	$Bidirectional$	UL only

Simulation parameters are defined in Table 3.14. The frequency band is the 868 MHz, the bandwidth is 125 kHz, the coding rate is 4/5, the transmit power is 14 dBm, and the spreading factor is SF_i for all the nodes. The area of deployment is a circular area with radius $R = D_{max}(SF_i)$, it is an uniform deployment, MG_1 means that there is a single gateway positioned at the center of the area of deployment, and the pathloss model is Okumura Hata. The application (AP) transmits 50-Byte packets every 1 min to stress the single channel, nodes are configured with equal parameters (deployment of nodes with homogeneous parameters), and only the uplink communication is considered.

What is the impact on the PDR when increasing the number of nodes configured with homogeneous parameters (TP, SF, BW, CR)?

Firstly, we evaluate performance varying the number of nodes when each node transmits a packet every minute (1 min AP). Figure 3.6 shows PDR for homogeneous deployments with different SFs from SF_6 to SF_{12}.

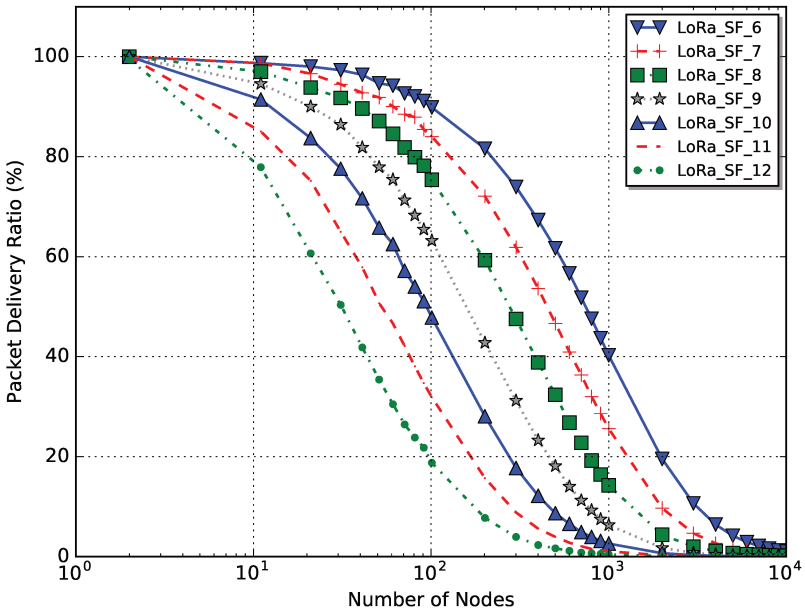

Figure 3.6: PDR for homogeneous deployments as a function of the number of devices generating a 50-Byte packet each 60 s.

We observe that PDR decreases when the number of nodes increases because all nodes are configured with same SF increasing packet collisions. For one single node, all the SF_i homogeneous deployments achieve 100% of delivered packets because the node was deployed in an area with full coverage. As we increase the number of nodes in the network, the number of delivered packets decreases due to collisions and pathloss. This decrease depends on the packet air time. The SF_6 homogeneous deployment has better PDR compared with the others due to its short air time or high data rate. However, its coverage is reduced. Increasing SF, the data rate decreases and the packet air time increases (increasing collision probability). We observe that PDR of SF_{12} homogeneous deployment decreases faster due to its long duration of air time and high collision probability. However, its coverage is larger reaching more end-devices in a uniform deployment. Thus, the packet air time and coverage may significantly impact packet losses.

In conclusion, when increasing the number of nodes and analyzing each SF individually: low SFs present high PDRs limited to smaller coverage and high SFs present low PDRs with larger coverage. Hence, there is a trade-off between data rate and coverage when choosing the SF configuration of end-devices.

What is the impact on the throughput when increasing the number of nodes configured with homogeneous parameters (TP, SF, BW, CR)?

Investigating the throughput, Figure 3.7 shows it in packets per second for homogeneous deployments with different SFs.

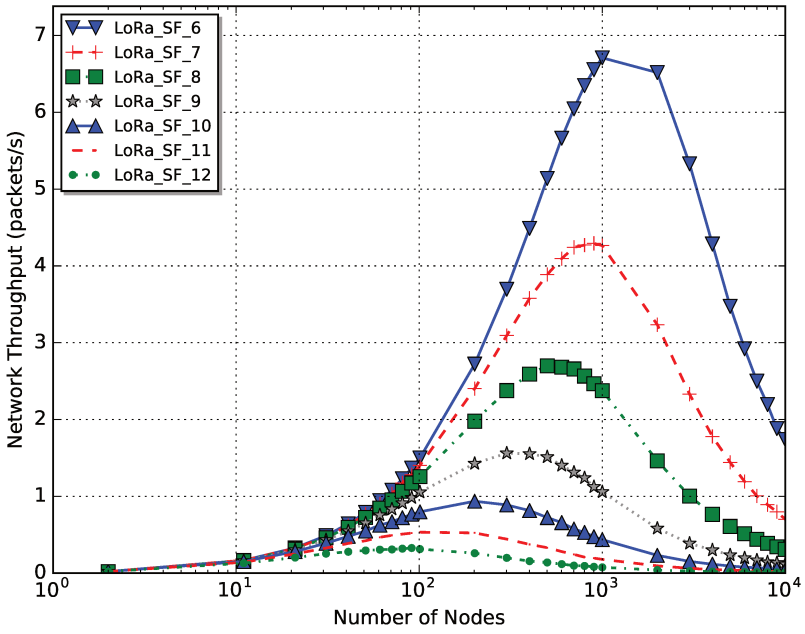

Figure 3.7: Network Throughput for homogeneous deployments as a function of the number of devices generating a 50-Byte packet each 60 s.

We observe that when increasing the number of nodes, throughput increases, then it saturates reaching a maximum and then it decreases. This is because the impact of collisions are more important than the gain, so it starts to decrease. The SF_{12} homogeneous deployment reaches the maximum faster (at 100 nodes approximately) and presents the lowest throughput due to its low data rate or long packet duration. Maximum throughput is achieved for different network sizes (i.e., depending of the number of nodes). For SF_{12}, it is achieved for 100 nodes while for SF_6 it is achieved for more than 1000 nodes.

To conclude, low SFs present higher throughput due to the higher spectral efficiency. Indeed, the capacity of each SF_i is almost twice the capacity of SF_{i+1} depending on the load. Load increases by increasing the number of nodes generating a packet every AP. However, low SFs are coverage limited.

3.2.2 Impact of Traffic Intensity

Table 3.15: System Model to analyze the impact of traffic intensity.

Configuration		Network Deployment	
$FrequencyBand$	868 MHz	$AreaofInterest$	circular area $R = D_{max}(SFi)$
$Bandwidth$	125 KHz	$Deployment$	uniform
$CodingRate$	4/5	$Multi-GW$	MG_1
$TransmissionPower$	14 dBm	$GWposition$	centered
$SpreadingFactor$	SFi only	$PathlossModel$	Okumura Hata
Application			
$ApplicationPeriod$	**50Bytes packet every 1 min to 1 day**	$Protocol$	Homogeneous
$Multi-Channel$	1CH	$Bidirectional$	UL only

Simulation parameters are defined in Table 3.15. Note that all parameters are the same of previous analysis except the application period. Indeed, the application (AP) will transmit 50-Byte packets every 1 min to every 1 day setting up the network size to 10000 nodes. We have to remark that the packet size is also fixed to 50 Bytes.

What is the impact on the PDR when varying the traffic intensity (i.e., application period) in a deployment of nodes configured with homogeneous parameters (TP, SF, BW, CR)?

Secondly, we have extended the previous analysis varying AP from 1 min up to 1 day. We analyse performance and limitations for large-scale deployments (i.e., 10000 nodes). Figure 3.8 shows PDR for homogeneous deployments of each SF_i. Evaluated APs go from 1 to 10 min with steps of 1 min, from 10 to 100 min with steps of 10 min, 10 h, and 1 day.

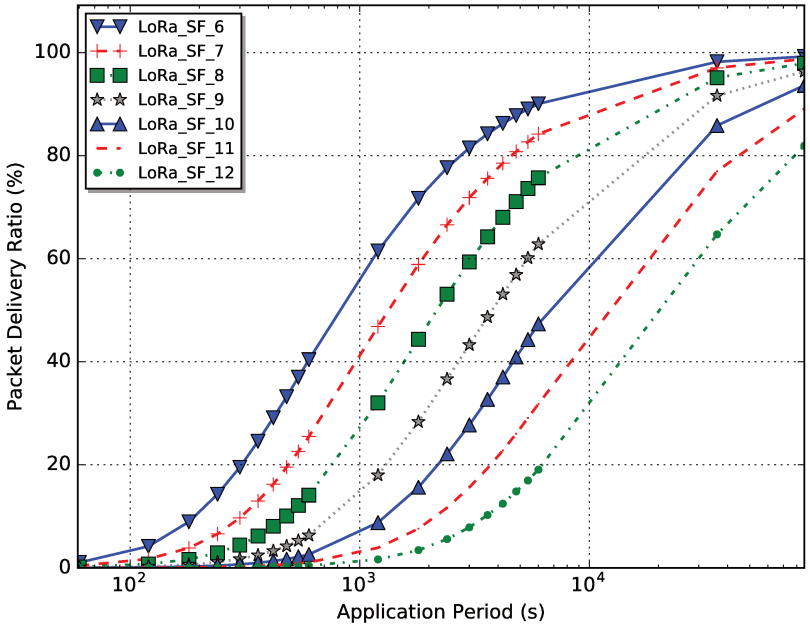

Figure 3.8: PDR for homogeneous deployments of 10000 nodes.

Increasing AP reduces the probability of collision, then PDR increases depending on the packet duration and the load. PDR of homogeneous SF_6 deployment increases faster by increasing AP or decreasing the traffic intensity due to its short packet duration. In fact, end-devices have to generate a packet every 50 min in order to assure at least 80% PDR for homogeneous SF_6. The number of delivered packets increases for shorter packets because collisions are reduced. Moreover, PDR increases when evaluating smaller network deployments (i.e., hundreds or thousands end-devices). In this study, we stressed the network with high traffic intensity (e.g., AP of 1 min) to evaluate limitations of each SF_i.

In conclusion, we need application periods of 50 min until 1 day to assure 80% of delivered packets (for SF_6 and SF_{12}, respectively) for large-scale network deployments of 10000 nodes. Furthermore, increasing

the application period and increasing the number of deployed end-devices shows exactly the opposite tendency on PDR.

What is the impact on the throughput when varying the traffic intensity (i.e., application period) in a deployment of nodes configured with homogeneous parameters (TP, SF, BW, CR)?

The impact on the throughput of varying AP for large-scale network deployment of 10000 nodes has been also evaluated. Figure 3.9 shows the throughput as a function of AP for each homogeneous SF_i deployment.

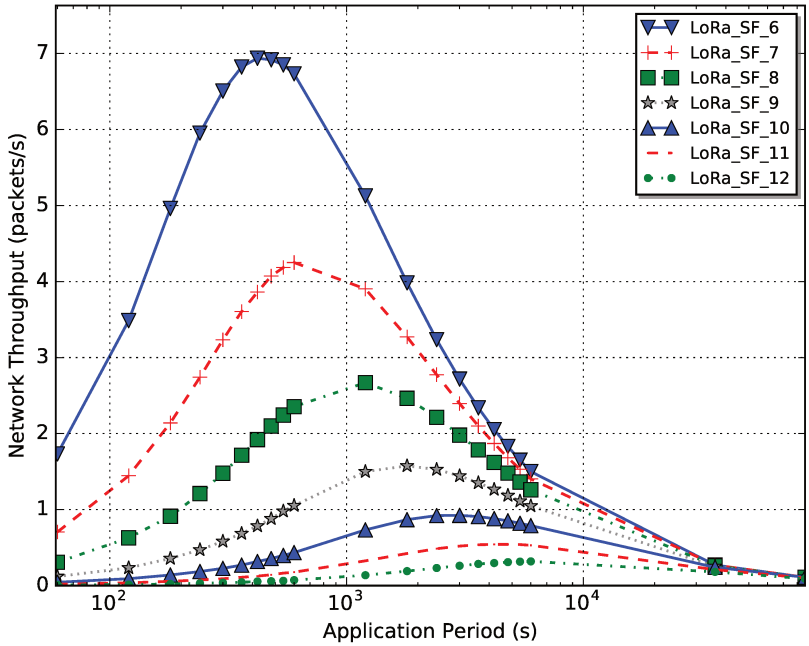

Figure 3.9: Network Throughput for homogeneous deployment of 10000 nodes.

We observe that maximal achieved throughput is higher for end-devices configured with low SFs. In fact, throughput increases achieving the maximum when increasing AP (i.e., decreasing the traffic intensity) because of the reduction of packet collisions. Then, it begins to decrease for higher APs due to the low traffic intensity (i.e., few packets transmitted per AP). We observe that the maximum throughput for different SFs depends on AP. Maximums are 7 packets/sec and less than 1 packet/sec for 8 min AP in homogeneous SF_6 and 100 min AP in homogeneous SF_{12}, respectively.

In conclusion, in large-scale networks with high intensity traffic (low AP), we have to prioritize the use of the SF_6 configuration. Nevertheless, it reduces the range and therefore, multi-hop communications or network densification with several gateways may be necessary to cover the same area of interest. We observe, again, that the capacity of each SF_i is almost twice the capacity of SF_{i+1} depending on the load.

3.3 Deployments of Nodes with Heterogeneous Communication Parameters

In this section, we compare simulation results of the homogeneous SF_{12} deployment with the heterogeneous strategies, i.e., $f(D_{max})$, *random* and *multi-homogeneous* deployments. Each deployment strategy covers the same area of interest (disk of $R = D_{max}(SF_{12})$). We simulated several deployments varying the number of end-devices generating a 50-Byte packet every 60 sec and varying the traffic intensity from 1 min AP to 1 day AP. We only take homogeneous SF_{12} for comparisons to keep the same coverage on the area of interest. Simulations were performed for network deployments up to 10000 nodes. We analyze the impact of heterogeneous networks uniformly deployed and how the multi-homogeneous, that is a dense deployment, impacts the packet delivery ratio.

3.3.1 Protocols

In this section, we introduce four centralized spreading factor allocation strategies. We assume that these strategies have complete knowledge of the network to make the decision to allocate SF for example, i.e., we do not consider the impact of the overhead due to exchanges between nodes and the gateway. We evaluate performance in steady state to better understand the impact of heterogeneous deployments as well as the impact of the network density using the WSNet simulator.

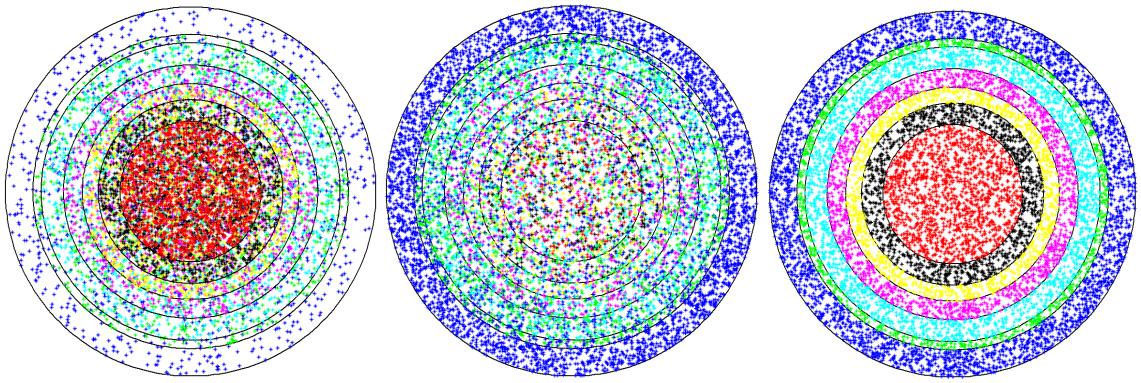

(a) Multi-Homogeneous. (b) Heterogeneous Random. (c) Heterogeneous f(Dmax): ADR-like.

Figure 3.10: Deployment of nodes with heterogeneous parameters.

3.3.1.1 Multi-Homogeneous

First, we define multi-homogeneous deployment as the concentric superposition of independent SF_i homogeneous deployments (i.e., *dense deployment*) resulting in an heterogeneous deployment. That is a concentric deployment as defined in Section 3.1.2.2, a homogeneous deployment of $\frac{N}{7}$ end-devices configured with SF_6 in a disk of $R = D_{max}(SF_6)$, overlapped with a homogeneous deployment of the same amount of end-devices ($\frac{N}{7}$) with SF_7 in a concentric disk of $R = D_{max}(SF_7)$, and so on until SF_{12} with a single gateway at the center. The number of nodes are equally distributed between the homogeneous networks (i.e., $\%SF_i$=14.28%, $i \in \{6,...,12\}$). As each homogeneous deployment with SF_i is independent and uniform, we observed in Figure 3.10(a) higher end-devices density close to the gateway. The objective is to investigate the impact of the quasi-orthogonality when deploying nodes with different SFs. We determine if each homogeneous network can be considered as independent.

3.3.1.2 Heterogeneous Random

Second, we define heterogeneous random deployment like an uniform deployment of end-devices in a disk of radius $R = D_{max}(SF_{12})$ where each end-device randomly selects its configuration among the available ones according to its link budget. Hence, each node randomly selects its LoRa configuration according to its link budget and its needs. Note that nodes deployed in the annulus between $R = D_{max}(SF_{12})$ and $R = D_{max}(SF_{11})$ do not have choice of other SF configuration to communicate with the gateway, so they choose SF_{12}. Note also that nodes deployed in the circular area of $R = D_{max}(SF_6)$ do have all SFs available to choose to communicate with the gateway, so they choose $SF = rand(SF_6, SF_7, SF_8, SF_9, SF_{10}, SF_{11}, SF_{12})$. For example, nodes in the annulus, between $R = D_{max}(SF_9)$ and $R = D_{max}(SF_{10})$, can randomly select their SF among SF_{10}, SF_{11} and SF_{12} depending on their optimization criteria (e.g., energy consumption, data rate, reliability). Figure 3.10(b) shows this deployment.

3.3.1.3 Heterogeneous $f(D_{max})$: ADR-like

Finally, we define heterogeneous $f(D_{max})$ as a uniform deployment of end-devices in a disk of $R = D_{max}(SF_{12})$. The SF allocation strategy is the classical Adaptive Data Rate (ADR) mechanism of LoRaWAN in a steady state (ADR-like). In this approach, each end-device selects its configuration according to its link

budget (i.e., with the maximum data rate or the minimum SF). Figure 3.10(c) shows the deployment when considering only pathloss model. We observe some annuluses naturally appear whose radius are related to the sensitivity of each SF configuration. End-devices in the farthest annulus from the gateway are configured with SF_{12}, in the next annulus with SF_{11}, and so on until the closest disk with SF_6. Note that to communicate with the gateway placed at the center of the deployment, nodes in the farthest annulus configured with SF_{12} do not have choice of other SF configurations. On the other hand, nodes in the closest disk do have all SFs available to choose, so they choose SF_6.

3.3.2 Impact of Network Size

Table 3.16: System Model to analyze the impact of network size in deployment of nodes with heterogeneous parameters.

Configuration		Network Deployment	
$FrequencyBand$	868 MHz	$AreaofInterest$	circular area $R = D_{max}(SF_{12})$
$Bandwidth$	125 KHz	$Deployment$	uniform, concentric
$CodingRate$	4/5	$Multi-GW$	MG_1
$TransmissionPower$	14 dBm	$GWposition$	centered
$SpreadingFactor$	SF_6 to SF_{12}	$PathlossModel$	Okumura Hata
Application			
$ApplicationPeriod$	**50-Byte packet every 1 min**	$Protocol$	Heterogeneous
$Multi-Channel$	1CH	$Bidirectional$	UL only

Simulation parameters are defined in Table 3.16. Note that: nodes can be configured with $SF = (SF_6, ..., SF_{12})$, the area of interest is a circular area of $R = D_{max}(SF_{12})$, deployments can be uniform (e.g., the Heterogeneous Random and $f(D_{max})$ ADR-like protocols) or concentric that is dense in the center (e.g., the Multi-Homogeneous protocol), AP is fixed to 1 packet every 1 min, and the protocol is heterogeneous (Multi-Homogeneous, Heterogeneous Random, or Heterogeneous $f(D_{max})$ ADR-like).

What is the impact on the PDR when increasing the number of nodes configured with heterogeneous parameters (SF_6 to SF_{12})? What is the impact of the quasi-orthogonality? Which allocation protocol is the most appropriate to configure the network?

Firstly, we evaluate the impact of increasing the number of end-devices on the number of delivered packets. Figure 3.11 compares homogeneous and heterogeneous deployments in terms of PDR.

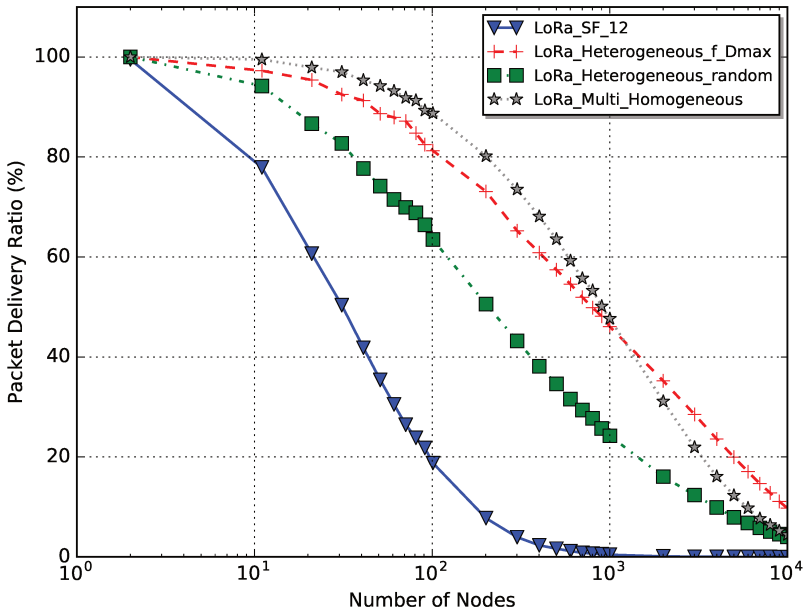

Figure 3.11: PDR of homogeneous and heterogeneous deployments as a function of the number of devices generating a 50-Byte packet each 60 s.

We evaluate the impact of the defined SF allocation strategies in uniform (i.e., the Heterogeneous Random and $f(D_{max})$ ADR-like protocols) and dense (i.e., the Multi-Homogeneous protocol) deployments. Re-

garding the uniform deployments, the Heterogeneous $f(D_{max})$ (ADR-like) strategy presents the best PDR performance compared to the *Random* and Homogeneous SF_{12} strategies because it allocates SF depending on link budget exploiting all the SFs. The SF distribution is shown in Figure 3.12. We observe that the percentage of node distribution for $f(D_{max})$ is proportional to the areas of deployments. The use of high SF is moderate, and the use of SF_6 is high because the area close to the gateway is a disk and not only an annulus.

Moreover, the *Random* strategy presents important enhancement on PDR compared with the SF_{12} strategy because it also exploits other SFs. We also observe in Figure 3.12 that increasing SF, the usage of them increases considerably. In fact, high SFs are over-used and low SFs are under-used. However, it is not as effective as the $f(D_{max})$ strategy. This is due to the fact that heterogeneous deployments reduce packet collision taking advantage of the quasi-orthogonality of SFs and the deployment strategy. In other words, $f(D_{max})$ and *Random* strategies exploit all available SFs, contrarily to SF_{12} strategy that only exploits one SF. We observe that $f(D_{max})$ better exploits SF, which is reflected in better PDR. For 100 end-devices, the gain in terms of PDR for $f(D_{max})$ and *Random* is 400% and 300%, respectively compared to SF_{12} strategy. In fact, PDRs are 20%, 60%, and 80% for SF_{12}, *Random*, and $f(D_{max})$ strategies, respectively.

In dense deployment scenario, the *Multi-Homogeneous* strategy achieves good PDR performance for small to medium size networks (up to 1000 end-devices). It presents even better PDR compared to $f(D_{max})$ which means it is still possible to improve the SF allocation strategy. However, for large-scale networks (e.g., more than 1000 end-devices) it starts to decrease faster due to the saturation of the capacity of SFs and the gateway, e.g., nodes configured with high SFs placed close to the gateway can highly interfere nodes using low SFs despite the quasi-orthogonality. This is because high SFs are more robust compared to low SFs and also because of the impact of non-perfect orthogonality of SFs in larger and denser deployments of nodes being higher.

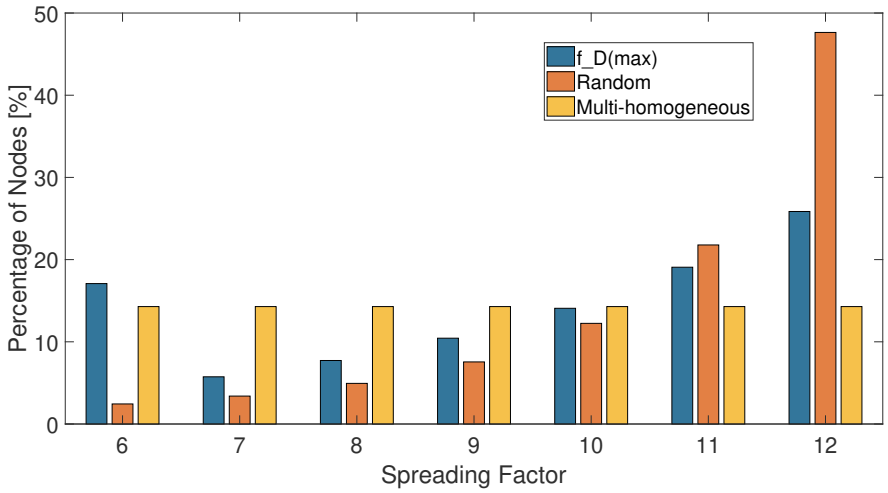

Figure 3.12: Spreading Factor distribution for heterogeneous deployments.

In conclusion, heterogeneous deployments exploit all available SFs and their quasi-orthogonality improving PDR, the $f(D_{max})$ is better than *Random* because of the appropriate use of low and high SFs, in uniform deployments. We have to remark that $f(D_{max})$ is based on the well known ADR mechanism of LoRaWAN in steady state. Furthermore, PDR improvement is possible as it is shown in the *Multi-Homogeneous* strategy for dense deployments depending on the network size.

What is the impact on the throughput when increasing the number of nodes configured with heterogeneous parameters (SF_6 to SF_{12})?

We also evaluated throughput of the heterogeneous strategies. Figure 3.13 compares the network throughput for the homogeneous and heterogeneous deployments in terms of the number of received packets per second.

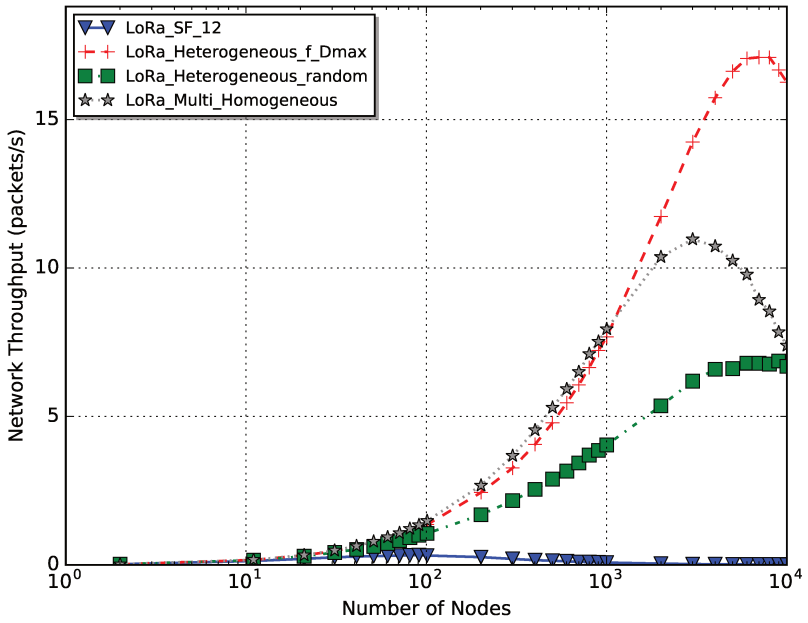

Figure 3.13: Network throughput for homogeneous and heterogeneous deployments as a function of the number of devices generating a 50-Byte packet each 60 s.

Increasing the number of end-devices, the throughput increases achieving the maximum. Then, it begins to decrease for large-scale networks. The heterogeneous $f(D_{max})$ deployment presents better throughput performance compared with others deployments for more than 1000 end-devices up to 10000 end-devices because it is based on the link budget exploiting properly all SFs, i.e., an appropriate use of low and high SFs contrarily to the use in the random strategy where low SFs are little used and high SFs are too much used. For less than 1000 end-devices, the *Multi-Homogeneous* dense deployment presents slight improvement on PDR compared to $f(D_{max})$ showing the possibility of improvement in dense networks and the need of smarter allocation strategies.

In conclusion, heterogeneous strategies improve throughput compared to the homogeneous strategy because of the better use of all SFs exploiting the quasi-orthogonality between them. Indeed, throughput depends on the SF configuration distribution of the network. We observed a more appropriate distribution for the $f(D_{max})$ strategy compared with the *Random* one. Heterogeneous strategies achieve the maximum throughput for larger networks (beyond 1000 nodes) whereas the homogeneous strategy for smaller networks like 100 nodes. In fact, the $f(D_{max})$ strategy achieves the maximum throughput of 17 packets/sec for almost 8 thousand end-devices whereas the *Multi-Homogeneous* one and the *Random* one achieve the maximum throughput of 11 and 7 packets/sec, respectively.

3.3.3 Impact of Traffic Intensity

Table 3.17: System Model to analyze the impact of the traffic intensity in deployment with heterogeneous parameters.

Configuration		Network Deployment	
$FrequencyBand$	868 MHz	$AreaofInterest$	**circular area** $R = D_{max}(SF_{12})$
$Bandwidth$	125 KHz	$Deployment$	**uniform, concentric**
$CodingRate$	4/5	$Multi-GW$	MG_1
$TransmissionPower$	14 dBm	$GWposition$	centered
$SpreadingFactor$	SF_6 **to** SF_{12}	$PathlossModel$	Okumura Hata
Application			
$ApplicationPeriod$	**50Bytes packet every 1 min to 1 day**	$Protocol$	**Heterogeneous**
$Multi-Channel$	1CH	$Bidirectional$	UL only

Simulation parameters are defined in Table 3.17. Note that all parameters are the same of previous analysis except the application period. Here, AP transmits 50-Byte packets every 1 min to every 1 day setting up the network size to 10000 nodes.

What is the impact on the PDR when varying the traffic intensity (i.e., the application period) in a deployment of nodes configured with heterogeneous parameters (SF_6 to SF_{12})? What is the impact of the quasi-orthogonality? Which allocation protocol is the most appropriate to configure the network?

Secondly, we evaluated the impact of varying the traffic intensity. Figure 3.14 compares PDR as a function of traffic intensity (i.e., with AP from 1 min up to 1 day).

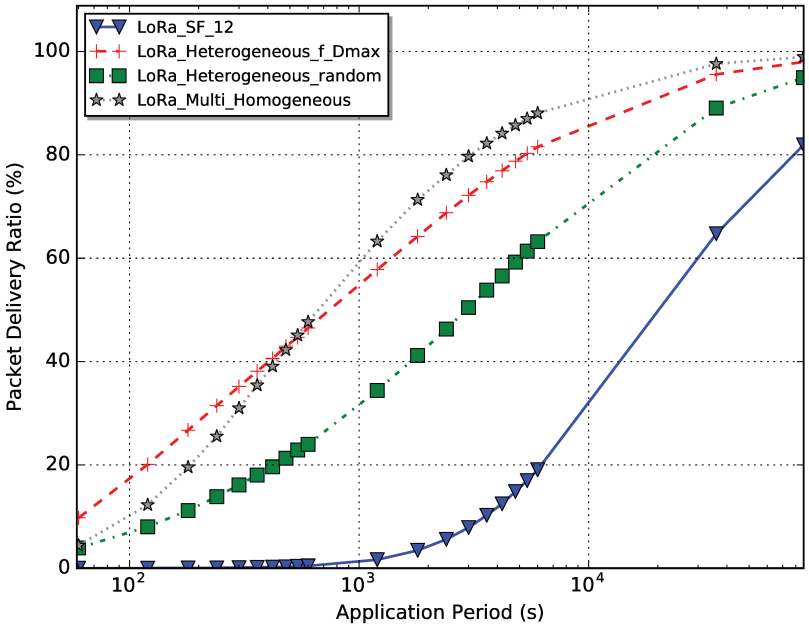

Figure 3.14: PDR for homogeneous and heterogeneous deployments for 10000 nodes.

Decreasing traffic intensity reduces the packet loss, then PDR increases. Regarding the uniform deployments, the heterogeneous $f(D_{max})$ deployment presents better PDR compared to $Random$ and SF_{12} because it takes advantage of the quasi-orthogonality of the SFs reducing the interference and gaining in capacity. All nodes set up to SF_{12} are far from the gateway, then interference to nodes close to the gateway set up to SF_6 is reduced. The Homogeneous SF_{12} deployment presents lower PDR due to its long packet duration and the low spectral efficiency. To assure 80% PDR, the application period of the end-devices has to be 1h40, 5h33 and 1 day for $f(D_{max})$, $Random$, and SF_{12}, respectively. Regarding the *Multi-Homogeneous* dense deployment, it outperforms $f(D_{max})$ in terms of PDR for long application periods (beyond 10 min AP). However, it is strongly impacted for short APs (1 min up to 10 min) because low SFs are over-used increasing collisions, more than $f(D_{max})$ strategy.

What is the impact on the throughput when varying the traffic intensity (i.e., the application period) in a deployment of nodes configured with heterogeneous parameters (SF_6 to SF_{12})?

Furthermore, we evaluated the throughput varying the traffic intensity. Figure 3.15 compares the throughput for homogeneous and heterogeneous deployments of 10000 end-devices.

When traffic intensity decreases, the throughput increases achieving the maximum and then begins to decrease. For high traffic intensity (e.g., 1 min AP), the heterogeneous $f(D_{max})$ deployment presents a throughput of 16 packets per second whereas *Multi-Homogeneous*, $Random$ and the Homogeneous SF_{12} strategies have throughput of 7, 6 and <1 packets per second. Maximum throughput is achieved at 2 min, 3 min, 2 min and 1h40 of AP for $f(D_{max})$, *multi-homogeneous*, $Random$ and SF_{12}, respectively. Regarding the uniform deployment of end-devices, $f(D_{max})$ strategy outperforms $Random$ for high traffic intensities (up to 100 min AP) due to better exploitation of the SF orthogonality and the appropriate distribution of SFs contrarily to the $Random$ strategy that over-uses high SFs and under-uses low SFs.

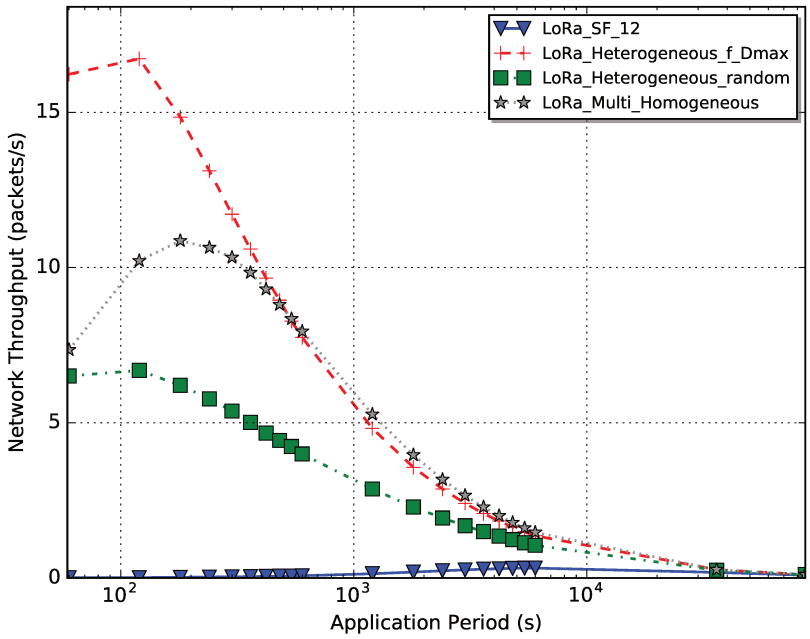

Figure 3.15: Network throughput for homogeneous and heterogeneous deployments of 10000 nodes.

Regarding the *Multi-Homogeneous* dense deployment strategy, it slightly improves network throughput compared to $f(D_{max})$ for low traffic intensities (beyond 8 min AP) showing the possibility of improvement and the need of more general SF allocations strategies.

In this section we conclude that heterogeneous deployments exploit all available SFs improving PDR thanks to their quasi-orthogonality. This improvement depends on the SF configuration distribution of the network. In uniform deployments, the ADR-like $f(D_{max})$ appropriately uses low and high SFs improving PDR compared to the $Random$ one. In dense deployment, the *Multi-Homogeneous* strategy shows the possibility of further improving PDR depending on the network size.

The heterogeneous strategies also improve the throughput because of the better use of all SFs exploiting their quasi-orthogonality. Furthermore, increasing the number of nodes (i.e., increase in traffic load) and increasing the application period (i.e., decrease in traffic load) shows exactly the opposite tendency on PDR and throughput.

However, is the SF allocation based on the link budget as ADR or $f(Dmax)$ optimal? Is it better to allocate equal amount of nodes with each SF as in the *Multi-Homogeneous* dense deployment? Are we over-using or under-using the different SFs regarding the capacity of a gateway? How to improve SF allocation strategy? Regarding multiple gateways scenarios, do we need better allocation strategies? How to still improve the allocation strategy in more general scenarios? These questions will be investigated in Chapter 4.

3.4 ADR Performance Evaluation

In this section, we studied the impact of the network deployment on ADR in uniform and dense deployments, and different environments as Factory of the Future (FoF). Furthermore, we studied the impact of using multiple channels instead of using a single channel. Finally, we evaluated the impact of adding downlink communications instead of only considering uplink communications. Note that the adaptive data rate (ADR) mechanism of LoRaWAN is in steady state for these investigations, i.e., the ADR-like $f(D_{max})$ of the previous section that we call it hereafter ADR. Note also that the link budget is based on the assumption that the network server has the full network knowledge of node positions and the distance to the gateway.

3.4.1 Impact of Network Deployment on ADR

We investigate the impact of the network deployment on the ADR performance, i.e., the ADR flexibility in terms of reliability and throughput for uniform and dense deployments.

Table 3.18: System Model to analyze the impact of network deployment of nodes configured with the ADR.

Configuration		Network Deployment	
$FrequencyBand$	868 MHz	$AreaofInterest$	circular area $R = D_{max}(SF_{12})$
$Bandwidth$	125 KHz	$Deployment$	uniform, dense
$CodingRate$	4/5	$Multi-GW$	MG_1
$TransmissionPower$	14 dBm	$GWposition$	centered
$SpreadingFactor$	SF_6 to SF_{12}	$PathlossModel$	Okumura Hata
Application			
$ApplicationPeriod$	50-Byte packet every 1 min	$Protocol$	ADR
$Multi-Channel$	1CH	$Bidirectional$	UL only

Simulation parameters are defined in Table 3.18. End-devices are deployed over a circular area of $R = D_{max}(SF_{12})$. We analyse the impact of a denser deployment of end-devices in the center (i.e., closer to the gateway) on the performance and compare it with the uniform deployment performance. Note that the dense deployment was defined in Section 3.1.2.3. $MG_i\,ADR$ defines a network deployment with i gateways and end-devices configured with the ADR protocol. We studied single and multiple GW deployments. We performed several simulations for several numbers of end-devices (up to 10000) generating a packet every 60 sec.

What is the impact of the network deployment on the ADR performance? What is the impact on the PDR when increasing the number of nodes in uniform and dense deployments of nodes configured with the ADR protocol?

Figure 3.16 shows the results of PDR of the ADR strategy for uniform and dense deployments.

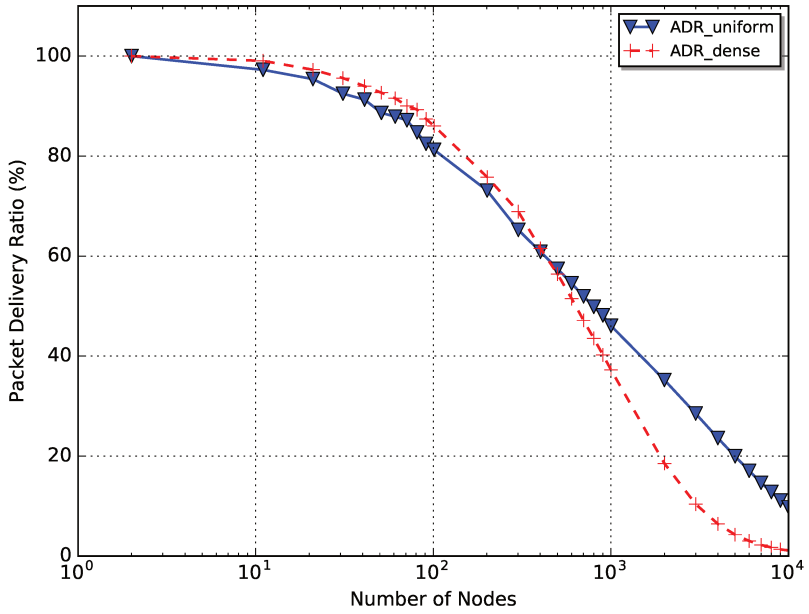

Figure 3.16: Impact of dense deployment on PDR for the ADR strategy.

We observe that PDR in the dense deployment is slightly improved in comparison to the uniform deployment for small and medium networks (up to 400 end-devices). This is because ADR takes advantage of low SFs and their short packet duration for dense deployments where there are more end-devices closer to the gateway. In the case of the uniform deployment, ADR is limited by the deployment because there are more end-devices far from the gateway choosing high SFs and increasing collisions. Beyond 400 end-devices, PDR of the dense deployment begins to decrease rapidly due to low SFs reaching their capacity (i.e., more negative impact due to collisions and packet losses). It shows that low SFs are over-used, high SFs are under-used and the need of a smarter SF allocation strategy. On the other hand, the uniform deployment presents better PDR for large-scale networks thanks to the more balanced distribution of SFs.

What is the impact of the network deployment on the ADR performance? What is the impact on the throughput when increasing the number of nodes in uniform and dense deployments of nodes configured with the ADR protocol?

We also evaluated the impact of the network deployment (i.e., the uniform and dense deployments) on throughput. Figure 3.17 shows throughput results for uniform and dense deployments of the ADR strategy.

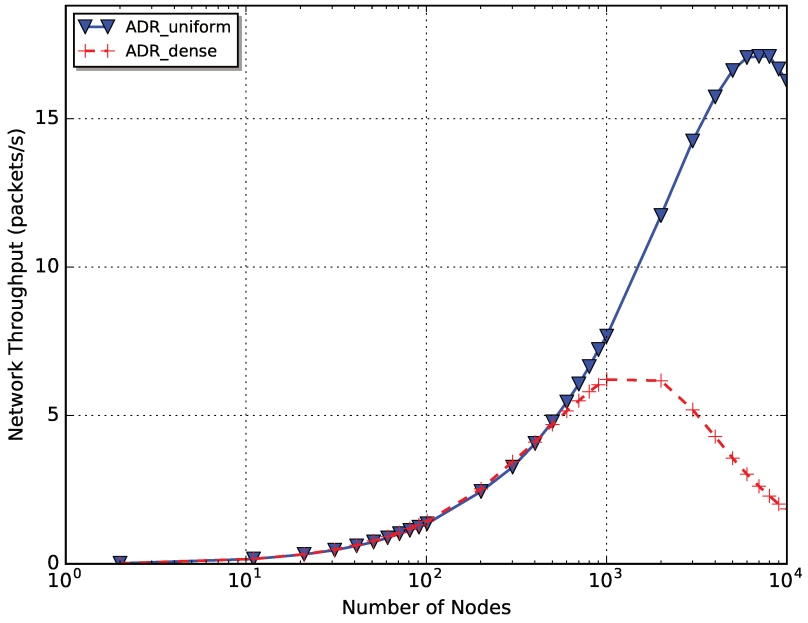

Figure 3.17: Impact of dense deployment on throughput for the ADR strategy.

For networks up to 500 end-devices, throughput is the same for both deployments. Maximum throughput of 17 and 6 packets/sec is achieved for the uniform and dense deployments, respectively. Beyond 500 end-devices, we notice an important decrease in the dense deployments. Throughput in the uniform deployment outperforms the dense deployment because low SFs are saturated in dense deployments, especially in large-scale deployments.

We also investigate the drawbacks of the ADR allocation strategy, i.e., the configuration distribution of SF to determine which SFs are over-used and under-used in a network deployment where nodes are configured by the ADR protocol.

Table 3.19: System Model to analyze drawbacks of the network deployment of nodes configured with the ADR.

Configuration		Network Deployment	
$FrequencyBand$	868 MHz	$AreaofInterest$	circular area $R = D_{max}(SF_{12})$
$Bandwidth$	125 KHz	$Deployment$	uniform
$CodingRate$	4/5	$Multi-GW$	MG_1
$TransmissionPower$	14 dBm	$GWposition$	centered
$SpreadingFactor$	SF_6 to SF_{12}	$PathlossModel$	Okumura Hata
Application			
$ApplicationPeriod$	50-Byte packet every 1 min	$Protocol$	ADR
$Multi-Channel$	1CH	$Bidirectional$	UL only

Simulation parameters are defined in Table 3.19. Note that all parameters are the same of previous analysis except deployment. Here we analyse in detail the uniform deployment with the ADR protocol.

What are the drawbacks of the ADR protocol? What is the impact on the PDR when increasing the number of nodes in uniform deployments of nodes configured with the ADR?

The Adaptive Data Rate strategy allocates SF to a node based on the measurements of uplink SNR, so that nodes close to the gateway will select low SFs (e.g., SF_6) and nodes far away, high SFs (e.g., SF_{12}). If the

majority of deployed nodes are close to the gateway, ADR selects SF_6 for all of them, which means that SF_6 is *over-used* (too many nodes operating at the same SF leading to collisions) and other SFs are *under-used*. If only a part of nodes uses SF_6, and other part uses SF_7 and so on, their transmissions may co-exist without collisions thanks to quasi-orthogonality of the LoRa modulation.

To illustrate this effect of *under-usage* and *over-usage*, Figure 3.18 presents PDR achieved by ADR and the decomposition of PDR into each SF performance. Note that $MG\_1\_ADR\_SFi$ represents PDR of nodes that use SFi in a single gateway deployment configured by the ADR protocol. Curve MG_1_ADR (blue triangles) represents PDR of the total number of nodes (i.e., all nodes configured to all SFs).

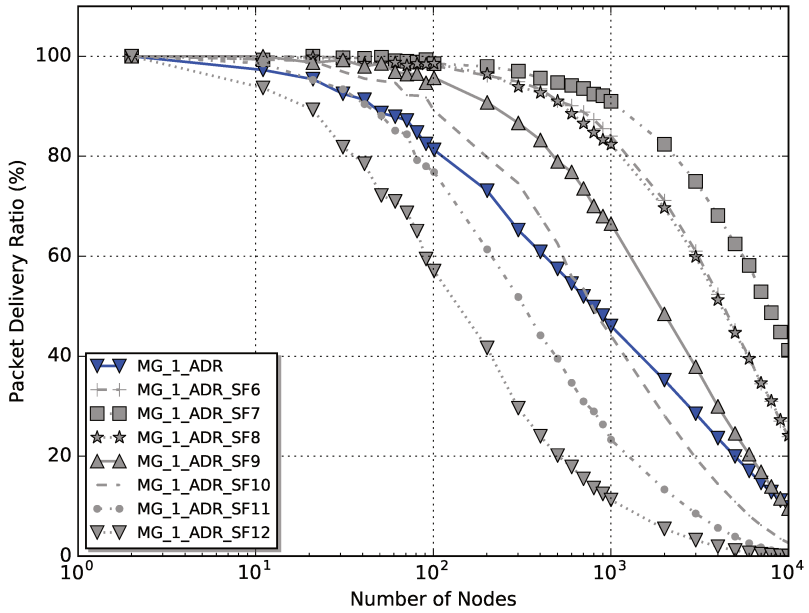

Figure 3.18: PDR achieved by ADR and the decomposition of PDR into each SF: $MG\_1\_ADR\_SFi$ represents PDR of nodes that use SFi. Packets every 60 s, nodes uniformly distributed in a disk of radius $D_{max}(SF_{12}) = 6.1$ km.

We can observe that PDR for each SFi depends on the number of nodes configured with a given value of SFi. The distribution of nodes configured with each SF was presented in Figure 3.12 of the previous section. Table 3.20 shows the configuration distribution of SFs using the ADR protocol.

Table 3.20: Distribution of nodes as a function of SF for a single GW and 1 min traffic intensity using the ADR protocol.

SF_i	6	7	8	9	10	11	12	Total
$\%Nodes$	17.1	5.7	7.7	10.4	14.1	19.1	25.9	100

Regarding the Figure 3.18, there are two regions, above and below curve MG_1_ADR. The curves above MG_1_ADR (i.e., $MG\_1\_ADR\_SF_{6,7,8,9}$) exhibit higher PDR compared to MG_1_ADR, which means that SF=6,7,8,9 are little used with respect to the capacity of each SFi—they are *under-used*, so we need a new allocation strategy to take advantage of them. On the other hand, the curves below MG_1_ADR (i.e., $MG\_1\_ADR\_SF_{11,12}$) represent *over-used* SFs due to network deployment constraints, so we need a smarter strategy to avoid their over-allocation. Note that SF_{10} is *under-used* for deployments up to 1000 end-devices, it is *over-used* beyond this number of end-devices, showing the dependency on the network size.

The figure shows that ADR does not properly take advantage of quasi-orthogonality of the LoRa modulation SFs. So, we need a better strategy that equalizes PDR of each SFi. The appropriate number of nodes configured with each SFi to meet desired requirements and the allocation algorithm taking advantage of it is the goal of our algorithms presented in Chapter 4.

3.4.2 Impact of Pathloss Environment on ADR

In this section we analyze the impact of the environment on the ADR performance in terms of delivered packets and throughput. We evaluate performance of ADR strategy for an open rural environment and a Factory of the Future (FoF) environment.

Table 3.21: System Model to analyze the impact of the environment in deployments of nodes configured with ADR.

Configuration		Network Deployment	
FrequencyBand	868 MHz	*AreaofInterest*	**room 100mx100m**
Bandwidth	125 KHz	*Deployment*	uniform
CodingRate	4/5	$Multi-GW$	MG_1
TransmissionPower	14 dBm	*GWposition*	centered
SpreadingFactor	SF_6 **to** SF_{12}	*PathlossModel*	**Okumura Hata, Tanghe**
Application			
ApplicationPeriod	50Bytes packet every 1 min	*Protocol*	**ADR**
$Multi-Channel$	1CH	*Bidirectional*	UL only

Simulation parameters are defined in Table 3.21. End-devices are uniformly deployed over a square area (i.e., 100 meters x 100 meters room). The FoF environment uses the Tanghe pathloss model and the open rural environment uses the Okumura Hata pathloss model. We perform several simulations with a single gateway for several number of end-devices up to 10000, generating a packet every 1 min.

What is the impact of passing from open to the FoF environment on the ADR performance? What is the impact of the environment on PDR when increasing the number of nodes in deployments of nodes configured with the ADR protocol?

Figure 3.19 shows PDR of ADR as a function of the number of nodes for both environments characterized by their pathloss models.

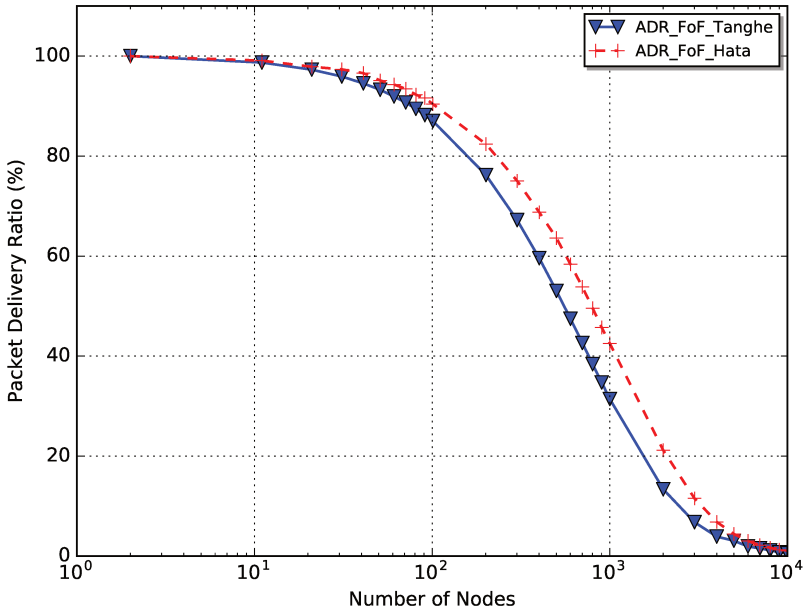

Figure 3.19: PDR in the FoF environment for the ADR strategy.

We observe that PDR of ADR is degraded in the FoF environment using Tanghe compared to the open rural environment that uses Okumura Hata pathloss because ADR is based on the link budget that is impacted by the pathloss model (i.e., Tanghe is more drastic). Note that all end-devices are set up depending on the SNR level, packet loss is due to the minimum SNR to demodulate the signal (i.e., when $SNR_{min}(SF_i)$ is not achieved) but also due to the high use of low SFs increasing collisions. In conclusion, ADR is negatively impacted in the FoF environments using the Tanghe pathloss model compared to the Okumura Hata. This shows the weakness of ADR to more constrained environments.

What is the impact of the environment on the throughput when increasing the number of nodes in deployments of nodes configured with the ADR protocol?

We also evaluated ADR performance in terms of throughput for FoF environments using Tanghe and for open environments using Okumura Hata pathloss model. Figure 3.20 shows the throughput of ADR for both environments.

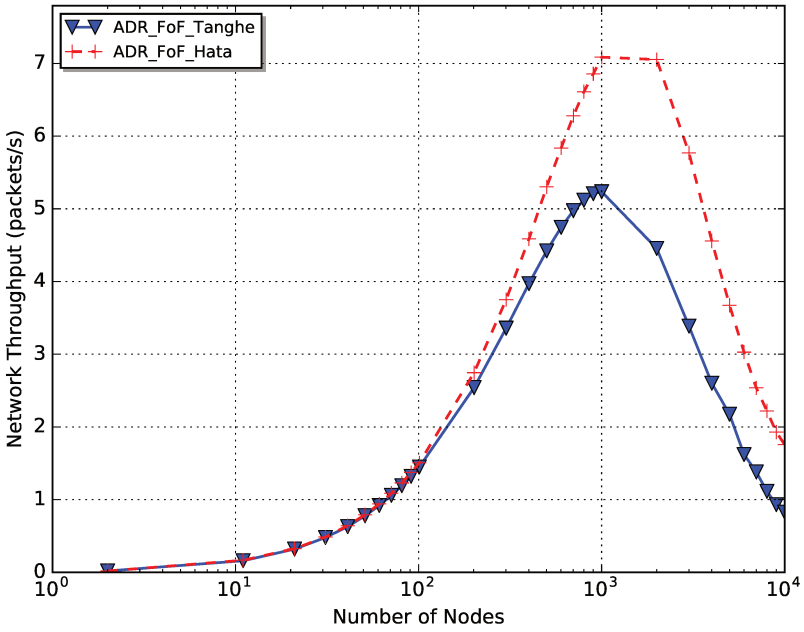

Figure 3.20: Throughput in FoF environment for ADR strategy.

We observe that throughput of ADR in the FoF environment is also degraded because it is more environment constrained (i.e., it considers pathloss, shadowing, and fading). Maximum throughput is almost 5 and 7 packets/sec for Tanghe and Okumura Hata, respectively in 1000 node network. So, we observe a maximum throughput degradation of 25% approximately in the FoF industrial environment.

In this section we conclude that the FoF environment impacts negatively the performance of the ADR protocol due to the fact that this environment is more drastic considering pathloss, shadowing, and fading (e.g., performance is approximately reduced in 25% for 1000 node network). Indeed, our future objective is to provide good connectivity in terms of delivered packets whatever the environment is.

3.4.3 Impact of Multiple Channels on ADR

In this subsection, we analyze the impact of using multiple channels on the ADR performance, i.e., in terms of delivered packets and throughput. We evaluate the scalability when we increase the number of used channels. For example, we would like to know if, when n channels are used, performance will be n times the performance of a single channel.

Table 3.22: System Model to analyze the impact of multiple channels in deployments of nodes configured with ADR.

Configuration		Network Deployment	
$FrequencyBand$	868 MHz	$AreaofInterest$	room 100mx100m
$Bandwidth$	125 KHz	$Deployment$	uniform
$CodingRate$	4/5	$Multi-GW$	MG_1
$TransmissionPower$	14 dBm	$GWposition$	centered
$SpreadingFactor$	SF_6 **to** SF_{12}	$PathlossModel$	Okumura Hata
Application			
$ApplicationPeriod$	50-Byte packet every 1 min	$Protocol$	**ADR**
$Multi-Channel$	**1CH, 8CH**	$Bidirectional$	UL only

Simulation parameters are defined in Table 3.22. End-devices are uniformly deployed in a a square area (i.e., 100 meters x 100 meters room). Note that we evaluate a single gateway scenario in an open rural environment (i.e., Okumura Hata model). Note that the gateway (i.e., the transceiver Semtech SX1301) is capable to operate up to 8 channels in parallel. We assume 8 available channels of 125 KHz. End-devices randomly select the transmission channel among these 8 channels. Note that we investigate ADR performance for scenarios considering one single channel and the 8 assumed channels.

What is the impact of using multiple channels on the PDR when increasing the number of nodes in deployments of nodes configured with the ADR protocol? Is it scalable?

Figure 3.21 presents PDR of ADR using single and multiple channels comparing it with the homogeneous deployment SF_{12}.

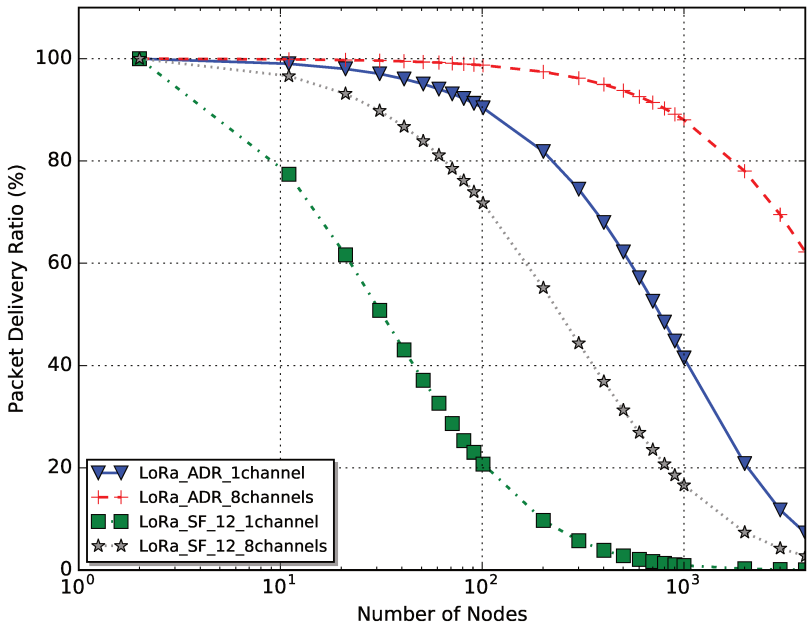

Figure 3.21: PDR of ADR using single and multiple channels.

Increasing the network size (i.e. number of nodes) the gain in terms of PDR of multiple channels increases compared to the single channel. For both deployments (i.e., the ADR protocol and the homogeneous SF_{12}), we observe that network capacity using 8 channels is 8 times the network capacity using the single channel. For example, in the ADR scenario, for approximately 2000 nodes with the single channel we achieve almost 80% of PDR. Increasing the number of used channels to 8, we can increase approximately 8 times the number of deployed nodes ensuring the same level of PDR. It shows the scalability of the use of multiple channels. Regarding the homogeneous SF_{12} deployment, it also improves PDR with multiple channels but it is strongly degraded in large-scale deployments because of the over-usage of SF_{12} increasing packet losses. Then, ADR exploits better all SFs capacities improving PDR using multiple channels compared to the SF_{12} deployment. Indeed, using multiple channels improves scalability of the network. Increasing the capacity of one single channel that supports a certain amount of nodes to multiple channels, the number of supported nodes will increase as many times as the number of channels are used, keeping the same level of PDR.

What is the impact of using multiple channels on throughput when increasing the number of nodes in deployments of nodes configured with the ADR protocol?

We also evaluated throughput of ADR using multiple channels. Figure 3.22 presents throughput comparison of ADR and the homogeneous SF_{12} deployment for single and multiple channels.

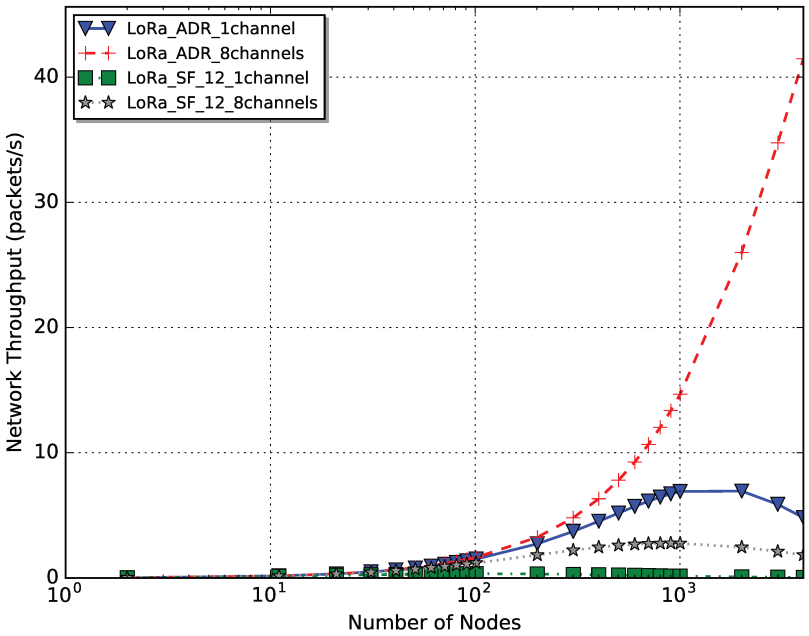

Figure 3.22: Throughput of ADR using single and multiple channels.

Using 8 channels improves the maximum throughput (more than 40 packets/sec) compared to single channel (7 packets/sec) because of multiple channels. Indeed, we expect that the capacity of the 8 channels will be 8 times the capacity of the single channel, i.e., we expect maximum throughput of 56 packets/sec. Furthermore, ADR using single and multiple channels presents the same tendency for networks up to 200 nodes. Beyond it, throughput using 8 channels increases exponentially compared to the single channel that is saturated for 1000 nodes network. ADR using single and multiple channels outperforms the homogeneous SF_{12} deployment that saturates faster due to the long air time of packets.

In this section we conclude that using multiple channels is scalable, i.e., the network capacity using 8 channels is 8 times the network capacity using one single channel ensuring the same level of PDR. Note that the capacity of the network results in the number of nodes the network is capable to serve ensuring a given PDR. Furthermore, multiple channels allows to exploit frequency diversity to reduce the effects of radio signal distortions. Another method to exploit is frequency hopping by rapidly changing the carrier frequency among many different frequencies in a band to avoid interference.

3.4.4 Impact of Uplink and Downlink Communications on ADR

In this section, we investigated the impact of the downlink communication on the performance of the ADR protocol. We evaluate PDR and throughput of network deployments considering only uplink communications and uplink / downlink communications. Note that we evaluate ADR performance using one single channel and multiple channels (e.g., 8 channels).

Table 3.23: System Model to analyze the impact of downlink communication in deployments of nodes set up with ADR.

Configuration		Network Deployment	
FrequencyBand	868 MHz	*AreaofInterest*	room 100mx100m
Bandwidth	125 KHz	*Deployment*	uniform
CodingRate	4/5	*Multi−GW*	MG_1
TransmissionPower	14 dBm	*GWposition*	centered
SpreadingFactor	SF_6 **to** SF_{12}	*PathlossModel*	Okumura Hata
Application			
ApplicationPeriod	50-Byte packet every 1 min	*Protocol*	**ADR**
Multi−Channel	1CH, 8CH	*Bidirectional*	**UL only, UL / DL**

Simulation parameters are defined in Table 3.23. End-devices are uniformly deployed in a square area (i.e., a room of 100 meters x 100 meters). Note that all parameters are equal to the previous section except the bidirectionality, i.e., with and without DL (downlink) in addition to the UL (uplink) communication.

Note that in the ADR of LoRAWAN, the network server will control the data rate and transmission power of the end-device through appropriate MAC commands if the UL ADR bit of the FCrtl (frame control) of the frame header (FHDR) is set. If the DL ADR bit is set, it informs the end-device that the network server is in a position to send ADR commands. If an end-device optimizes its parameters, it periodically needs to validate that the network still receives the UL frames. Each time the UL frame counter is incremented without considering repeated transmissions, the end-device increments an ADR_ACK_CNT counter. When this counter exceeds an ADR_ACK_LIMIT limit without any DL response, it sets the ADR ACK request bit (ADRACKReq). So, the network is required to respond with a DL frame within the next ADR_ACK_DELAY frames. If any received DL frame following an UL frame, the ADR_ACK_CNT counter is reset. If no reply is received within the next ADR_ACK_DELAY UL frames, the end-device must try to gain connectivity switching its parameters. To evaluate the impact of these DL frames, we assume the ADR_ACK_LIMIT limit equal to 64. The duration of the DL response depends on the configuration parameters, we assume the same parameters of the UL frame. We also assume that reception occurs in the receive window RX1.

What is the impact of downlink communication on the PDR when increasing the number of nodes in deployments of nodes configured with the ADR protocol?

Figure 3.23 shows PDR of network deployments with and without downlink communication for scenarios using one single channel and 8 channels.

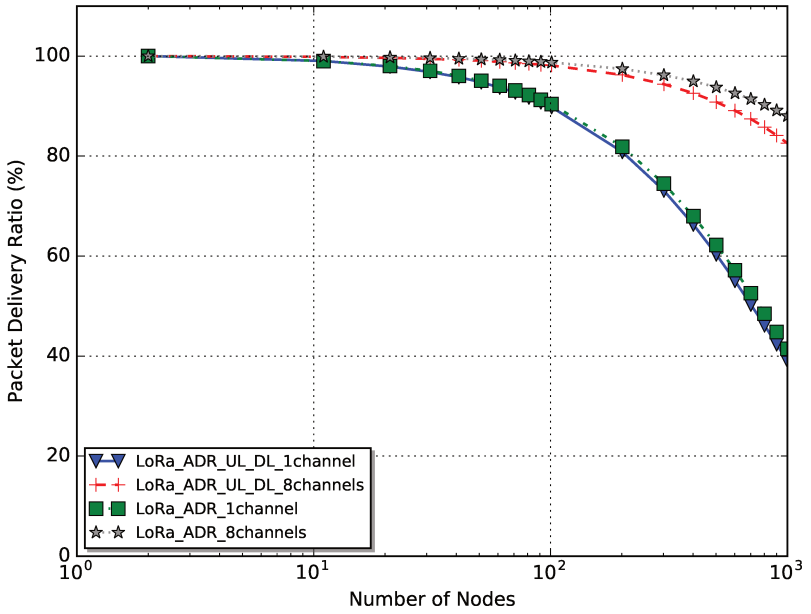

Figure 3.23: Impact of the downlink transmissions on PDR of ADR for single and multiple channels.

We compare uplink based communication with uplink-downlink (receive window RX1 in the LoRaWAN specification) based communications. For single channel, downlink transmissions slightly degrades PDR. For multiple channels, the negative impact is more important as long as the number of nodes increases. This is because several packets are lost in the gateway transceiver in all channels when it transmits downlink packets on a single channel. Increasing the network size up to 1000 nodes, could reduce PDR by 7%. This degradation increases with the network size. In conclusion, PDR using multiple channels is impacted by downlink communications, especially for large-scale networks because one single downlink transmission disable all channels for reception at the gateway.

What is the impact of downlink communication on the throughput when increasing the number of nodes in deployments of nodes configured with the ADR protocol?

Analyzing the throughput, Figure 3.24 presents the impact of the downlink transmissions on the ADR performance using single and multiple channels.

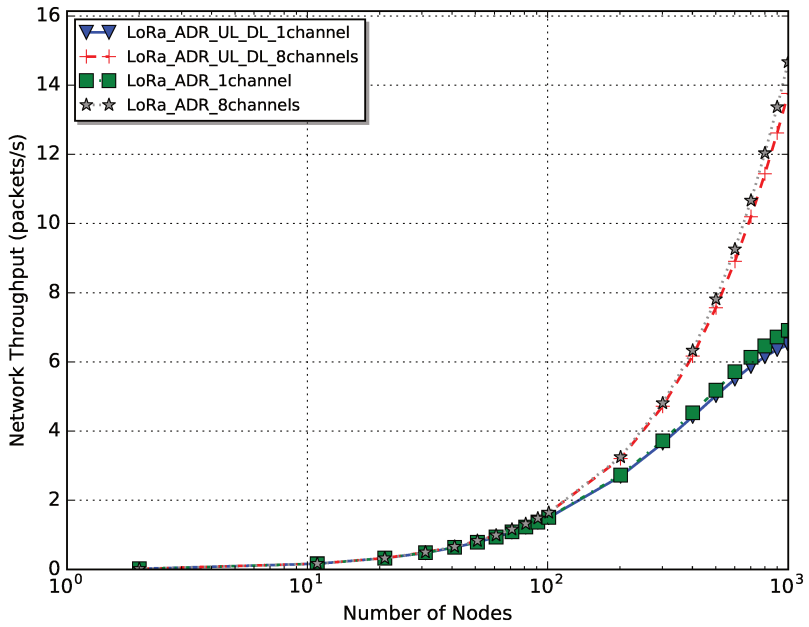

Figure 3.24: Impact of the downlink transmissions on throughput of ADR for single and multiple channels.

Increasing the number of nodes, increases the negative impact of the downlink transmissions. Again, this is because the reception of packets is negatively impacted in all channels when there is a downlink transmission on any of the single channels at the gateway level. In conclusion, throughput is also impacted by downlink communications especially using multiple channels in large-scale networks. We expect more significant negative impact on throughput for larger number of nodes on the network deployment.

In this section we conclude that performance is impacted by downlink communications, especially for large-scale networks and in the scenarios using multiple channels due to all channels being disabled for reception at the gateway when a downlink transmission occurs on a single channel.

3.5 Network Densification and Topology Adaptation

In this section, we investigate network densification and topology adaptation that are important issues in the LoRa network research. Increasing the number of gateways seems to be a good strategy. However, interference can have a big impact on the network performance. Thus, in this analysis we look for the optimal number of gateways and the best SF configuration for a given number of end-devices to assure a given level of reliability in multiple gateways deployments. We propose an adaptation strategy for nodes with homogeneous communication parameters.

We presented the metrics to evaluate multiple gateway deployments in Subsection 3.1.6. In this section we present the network densification, its impact on homogeneous deployments, an adaptation strategy proposition, and the impact of the network densification on ADR.

3.5.1 Multiple Gateways Deployments

Here, we present the network deployment of multiple gateways, i.e., 3, 7, and 9 gateways. For example, Figure 3.25 shows MG deployments of 1000 nodes configured with SF_6 (configurations denoted by $MG_{3,7,9}SF_6$ for 3, 7 or 9 GWs respectively). A black triangle represents a gateway and stars correspond to nodes with the color depending on their PDR level. Non-covered nodes are in red whereas green nodes benefit from good PDR (up to 80%). Regarding the defined metrics, Figure 3.25 shows that the Covered Nodes Ratio is 53.3%, 97.5% and 100% for 3, 7, or 9 GWs, respectively. Redundancy increases with the number of GWs from 0.5 for MG_3SF_6 to 1.28 for MG_9SF_6. Connected PDR is 75.50 %, 82.16% and 88.98% for 3, 7, or 9 GWs, respectively. We can observe that increasing the number of GWs increases coverage and enhances PDR.

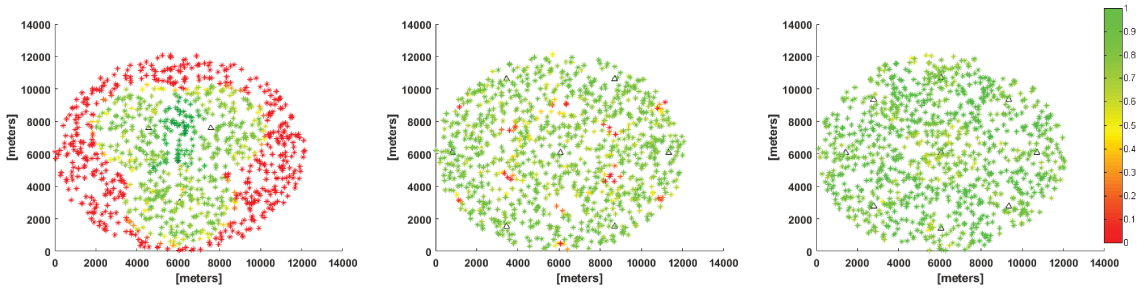

(a) 3 GWs (b) 7 GWs (c) 9 GWs

Figure 3.25: Uniform deployments of 1000 nodes in a Multi-GW network, nodes configured with SF_6 (configuration denoted by MG_3SF_6, MG_7SF_6 and MG_9SF_6)

However, we need to investigate the impact of the network densification on the performance for each SF configuration taking into account the constraints of the network deployment.

3.5.2 Impact of Network Densification

Here, we analyze the impact of increasing the number of GWs, i.e., the network densification in several scenarios of deployments of nodes with homogeneous configuration parameters.

Table 3.24: System Model to analyze the impact of the network densification in deployments of nodes configured with homogeneous parameters.

Configuration		Network Deployment	
$FrequencyBand$	868 MHz	$AreaofInterest$	circular area $R = D_{max}(SF_{12})$
$Bandwidth$	125 KHz	$Deployment$	uniform
$CodingRate$	4/5	$Multi-GW$	MG_3, MG_7, MG_9
$TransmissionPower$	14 dBm	$GWposition$	circles covering circle geometry
$SpreadingFactor$	SF_i only	$PathlossModel$	Okumura Hata
Application			
$ApplicationPeriod$	50-Byte packet every 1 min	$Protocol$	Homogeneous
$Multi-Channel$	1CH	$Bidirectional$	UL only

Simulation parameters are defined in Table 3.24. End-devices are uniformly deployed in a circular area of $R = D_{max}(SF_{12})$. We analyse the impact of increasing the number of gateways on the performance. Gateways are positioned following the circles covering circle geometry. MG_iSF_j defines a network deployment with i gateways and end-devices configured with the SF_j homogeneous strategy. We investigate multiple gateway deployments performing several simulations for several number of end-devices up to 10000, generating a packet every 60 sec. Note that the protocol is the homogeneous SF_i strategy but in multiple gateway scenarios. Note also that we assume open rural environment with a single channel without the downlink communication effect.

What is the impact of the network densification on PDR when increasing the number of nodes in deployments of nodes configured with homogeneous parameters?

Figure 3.26 presents the Network PDR for MG_jSF_i deployments, where all nodes are deployed with the same SF_i in a circular area of radius equal to $D_{max}(SF_{12})$. It shows that the Ratio of Covered Nodes highly impacts Network PDR of networks with low SFs.

For example, in a SF_6 deployment (MG_3SF_6), even if SF_6 has higher capacity, the network performance for sparse networks (up to 100 nodes) is drastically reduced because only 53.3% of the nodes are covered. We can also observe this impact for $MG_3SF_{7,8,9,10}$ deployments (note that PDR for a network with 1 node is equal to the Ratio of Covered Nodes). Thus, network PDR highly depends on the position of the gateways and the network coverage. Network PDRs of all $MG_{7,9}SF_i$ are only impacted by Connected PDR (see Figures 3.26(b) and 3.26(c)) because the Ratio of Covered Nodes is 100% for all MG_jSF_i (except for MG_7SF_6 with 95.90%).

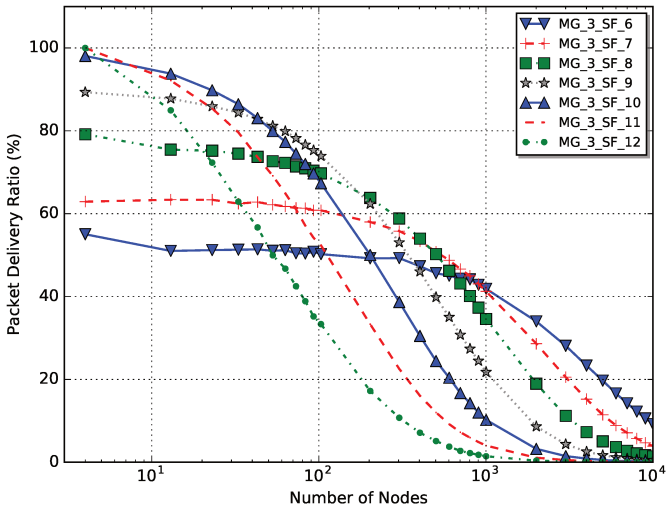

(a) 3 GWs

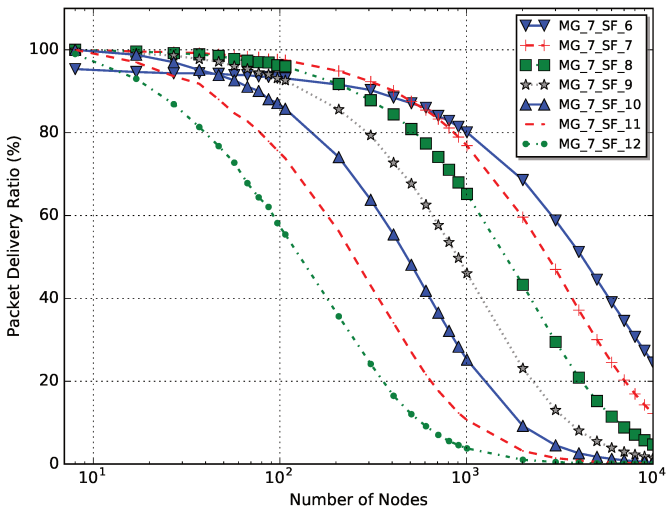

(b) 7 GWs

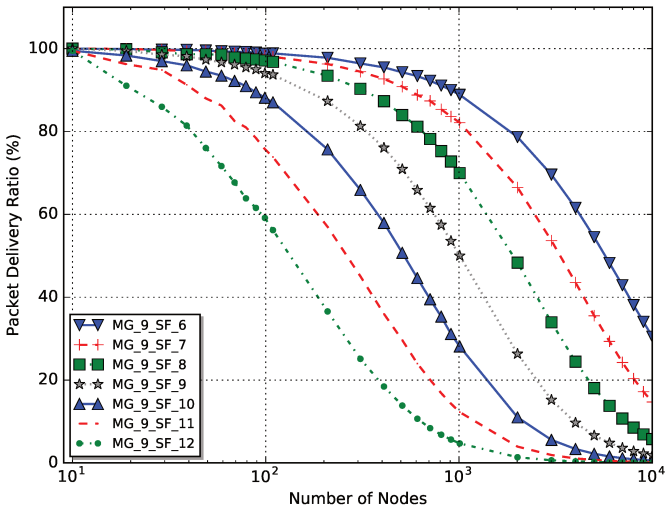

(c) 9 GWs

Figure 3.26: Network PDR for Multi-GW deployments in a disk of $D_{max}(SF_{12})$ radius.

What is the impact of the network densification on the throughput when increasing the number of nodes in deployments of nodes configured with homogeneous parameters?

Figure 3.27 shows the network throughput for multiple gateway deployments. We observe higher throughput for lower SFs due to the higher spectral efficiency of low SFs.

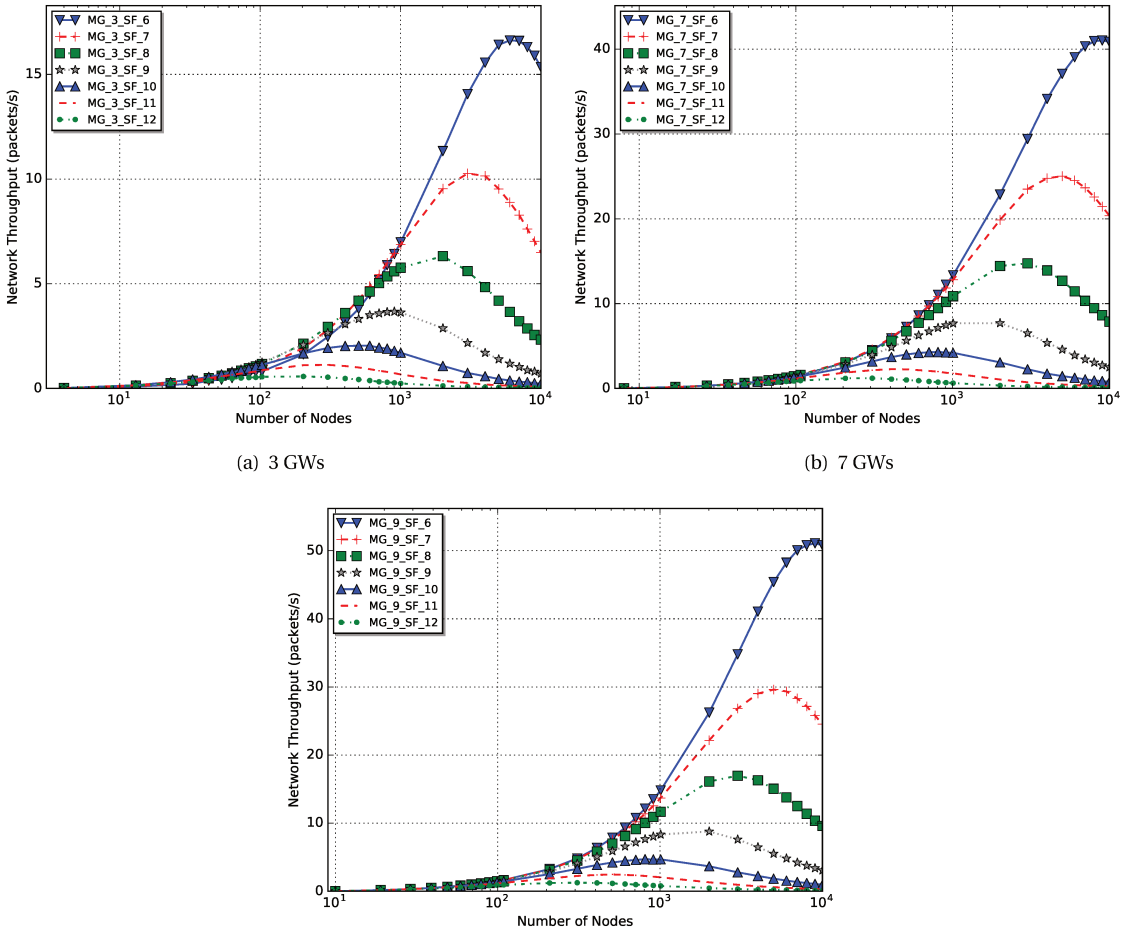

(a) 3 GWs

(b) 7 GWs

(c) 9 GWs

Figure 3.27: Network throughput for Multi-GW deployments in a disk of $D_{max}(SF_{12})$ radius.

We observe that the throughput increases due to more intensive usage of the spectrum until reaching a maximum. This maximum throughput is 17, 41 and 51 packets/second for $MG_{3,7,9}SF_6$, respectively. Beyond this point, the effect of the collisions becomes more important, then throughput starts to decrease.

Which SF configuration maximizes PDR? How to adapt SF according to the network size?

Figure 3.28 shows Network PDR for MG deployments of 100 and 1000 nodes in a disk of radius equal to $D_{max}(SF_{12})$ as a function of the number of GWs and SF.

In sparse networks (e.g., with 100 nodes), increasing the number of GW improves PDR thanks to redundancy. However, for more than 7 GWs, there is no additional gain. Regarding the deployments with 1, 3, 7, and 9 GWs, the best PDR is achieved for SF_{10}, SF_9, SF_7, and SF_6, respectively.

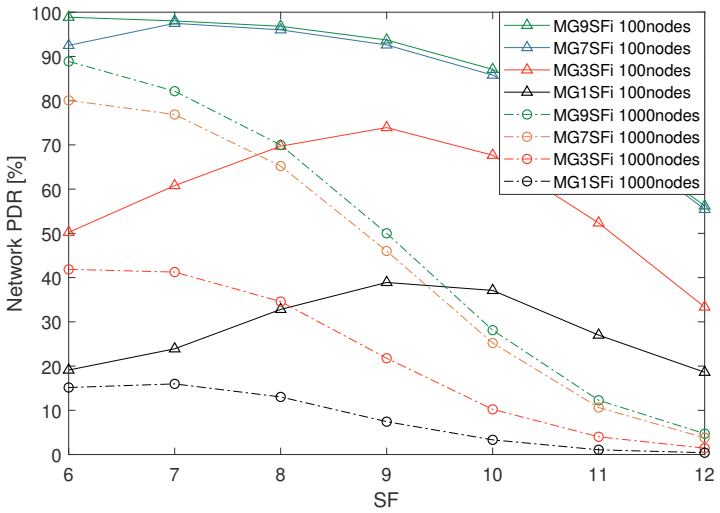

Figure 3.28: Network PDR for Multi-GW $MG_{7,9}SFi$, for different SF_i configurations of 100 and 1000 nodes.

In dense networks (e.g., with 1000 nodes), the higher SF, the faster each GW reaches its maximum capacity, so for 1, 3, 7, and 9 GWs, the best PDR is reached for SF_6. Then, low SFs (MG_iSF_6 and MG_iSF_7) presents higher reliability compared to high SFs.

To conclude, by limiting the size of each GW (i.e., the number of covered nodes), GW can better take advantage of the spectrum spatial reuse and can serve them with better PDR, especially for a large number of end-devices.

3.5.3 Adaptation Strategy

What are the optimal spreading factor configurations and how many gateways are needed to ensure a given reliability for small to large network deployments?

Based on the analysis of Figure 3.26, Figure 3.29 illustrates the Multi-GW strategy. It provides the required number of gateways and the optimal SF_i configuration as a function of the number of nodes assuring different levels of PDR (from 0% to 100%, i.e., from red to green). Red for network PDR of 0% and Dark Green for network PDR of 100%).

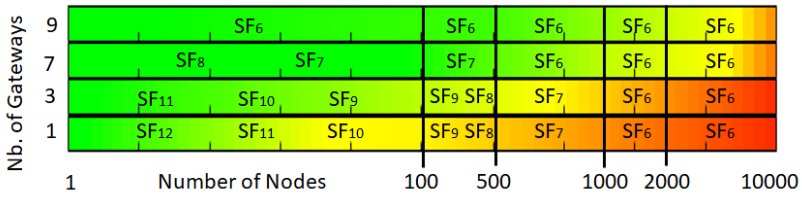

Figure 3.29: Multi-GW strategy.

When the number of nodes increases, we have to decrease SF and increase the number of GWs to keep the required level of Network PDR. For up to 100 nodes, the optimal number of required GWs is 3 and the strategy is to adapt SF from SF_{11} to SF_{10}, then to SF_9 according to the number of nodes ($MG_3SF_{11,10,9}$ in Figure 3.26(a)).

For a medium size network (between 100 and 500 nodes), 7 GWs are required and the optimal strategy is to configure all nodes with SF_7. For larger networks (beyond 500 and up to 1000 nodes), 9 GWs are required with the optimal SF configuration of SF_6 to assure PDR of 80%.

3.5.4 Impact of Network Densification on ADR

Here, we evaluate the impact of the network densification, increasing the number of gateways, in several scenarios of deployments of nodes with the ADR protocol.

Table 3.25: System Model to analyze the impact of network densification in deployments of nodes configured with ADR.

Configuration		Network Deployment	
$FrequencyBand$	868 MHz	$AreaofInterest$	circular area $R = D_{max}(SF_{12})$
$Bandwidth$	125 KHz	$Deployment$	uniform
$CodingRate$	4/5	$Multi-GW$	MG_3, MG_7, MG_9
$TransmissionPower$	14 dBm	$GWposition$	circles covering circle geometry
$SpreadingFactor$	SF_6 to SF_{12}	$PathlossModel$	Okumura Hata
Application			
$ApplicationPeriod$	50-Byte packet every 1 min	$Protocol$	ADR
$Multi-Channel$	1CH	$Bidirectional$	UL only

Simulation parameters are defined in Table 3.25. All simulation parameters are equal to the previous section except the protocol. In this investigation, we consider the ADR protocol. Note that $MG_j ADR$ defines a network deployment with j gateways and the end-devices configured using the ADR protocol.

What is the impact of the network densification on the PDR when increasing the number of nodes in deployments of nodes configured with ADR?

Figures 3.30 and 3.31 present Network PDR and throughput for SF_6, SF_{12} homogeneous deployments, and MG$_j$ADR for 3, 7, or 9 GWs. In Figure 3.30(a), MG$_3$ADR improves PDR compared to SF_6 and SF_{12} homogeneous deployments because ADR exploits all SFs taking advantage of their quasi-orthogonality. In Figure 3.30(b), MG$_7$ADR configures with SF_6 the majority of nodes, so its PDR is closer to MG$_9$SF$_6$. In Figure 3.30(c), MG$_9$ADR and MG$_9$SF$_6$ present similar performance because having 9 GWs allows ADR to set up all nodes with SF6. MG$_j$ADR does not maintain its performance for over-sized number of GWs as also observed in other work [96] and Figure 3.32.

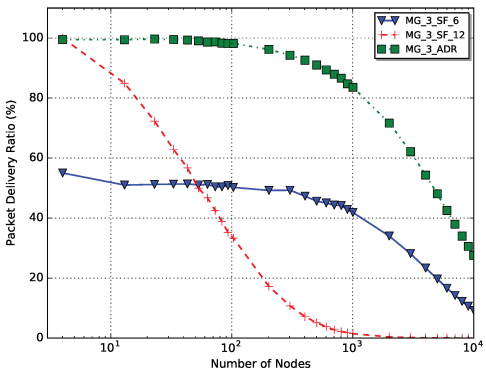

(a) 3 GWs

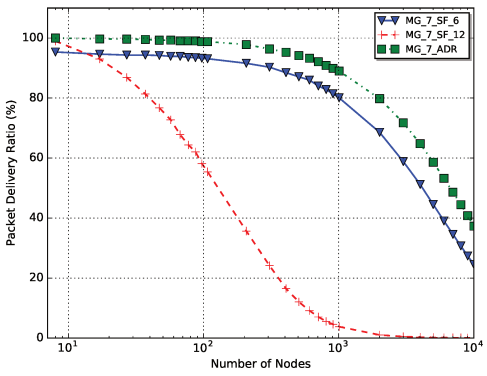

(b) 7 GWs

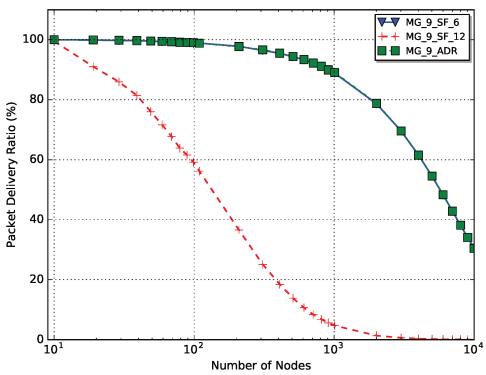

(c) 9 GWs

Figure 3.30: Network PDR for Multi-GW ADR deployments in a disk of radius equal to $D_{max}(SF_{12})$.

What is the impact of the network densification on the throughput when increasing the number of nodes in deployments of nodes configured with ADR?

We also evaluated throughput of the ADR protocol in multiple gateway deployments. Figure 3.31 shows the network throughput for 3, 7, and 9 gateways in terms of number of packets received per second.

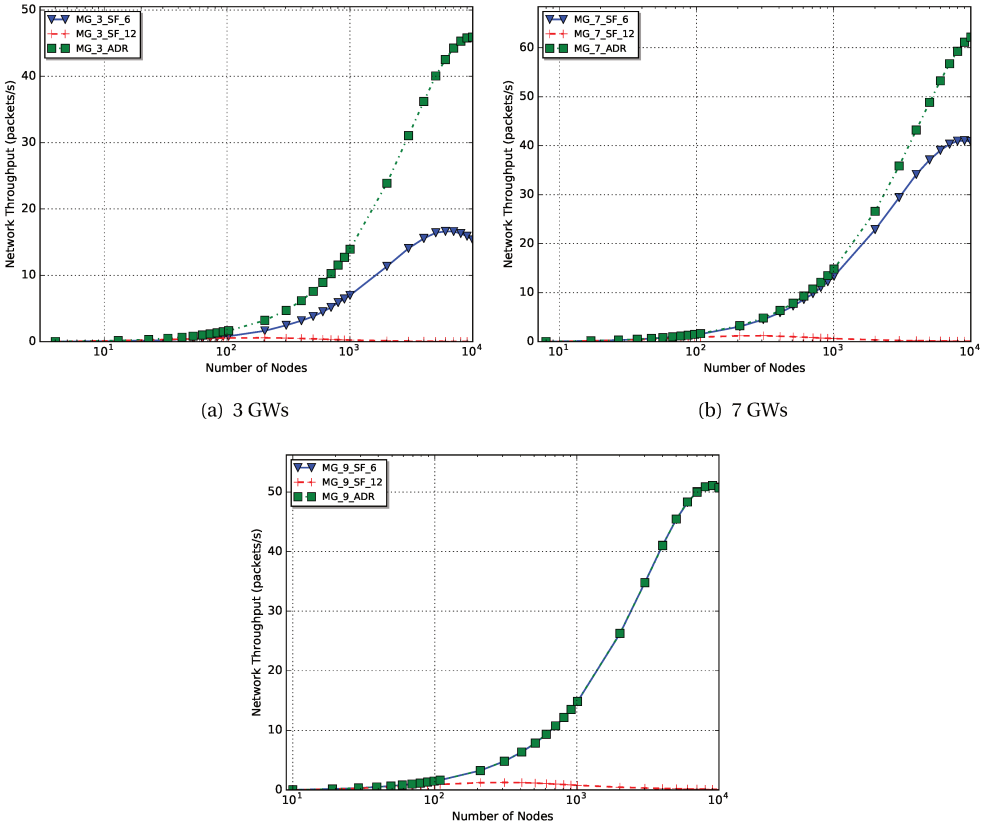

(a) 3 GWs

(b) 7 GWs

(c) 9 GWs

Figure 3.31: Network throughput for Multi-GW ADR deployments in a disk of radius equal to $D_{max}(SF_{12})$.

Increasing the number of nodes, throughput increases achieving the maximum. We observe that maximums for 3 and 7 gateways are greater than throughput of the homogeneous SF_6 and SF_{12}. Regarding the deployment with 9 gateways, we observe that throughput of ADR is almost the same as the homogeneous SF_6 because the ADR protocol configures the majority of devices with SF_6 since the network densification is increased, i.e., any device can reach a diversity of gateways with at least one of the 9 gateways close to it.

In conclusion, Figure 3.32 compares the performance in terms of PDR of MG$_j$ADR for 1,3, 7 or 9 GWs.

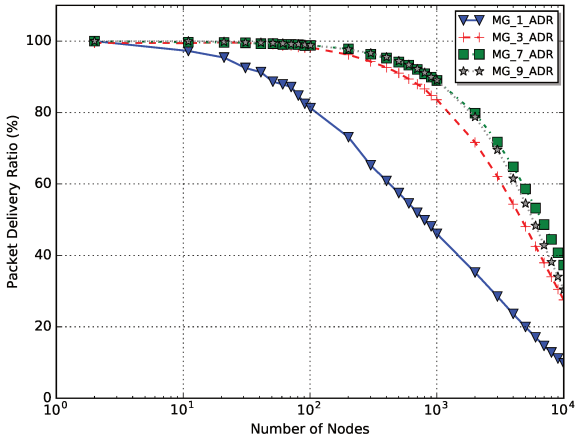

Figure 3.32: Network PDR of MG$_j$ADR strategies for different number of GWs.

We observe that over-sizing the number of GWs degrades Network PDR of MG$_j$ADR because when densifying the network, MG$_j$ADR configures most of the nodes with SF_6 and saturates it faster. This drawback shows the need of better allocation strategies.

Conclusion

In this chapter, we have investigated homogeneous (i.e., deployment of nodes configured with the same SF) and heterogeneous (i.e., deployment of nodes configured with different SF) networks for large scale deployments, SFs allocations, and performance in terms of PDR and throughput. Simulation results compare the performance for homogeneous and heterogeneous deployments as a function of the number of nodes and traffic intensity.

First, we have analyzed homogeneous deployments for different SFs from SF_6 to SF_{12}. We investigated the capacity of each SF. Simulations show better performance for the SF_6 deployment because of its short air time but reduced cell coverage. Second, we investigated the impact of the quasi-orthogonality of SF in heterogeneous deployments. We have compared heterogeneous and homogeneous in uniform deployments: the deployment that selects its LoRa configuration according to its link budget (ADR in steady state) results in the best PDR and throughput due to the use of all SFs exploiting orthogonality. The results clearly show the benefits of heterogeneity for large scale network deployments. Evaluating the multi-homogeneous deployment, which is dense closer to the center, we found that it is possible to improve or degrade ADR performance depending on the network size. This shows the need of adaptive SF allocation strategies according to the deployment density and network size.

We also evaluated ADR performance and limitations. Indeed, we investigated ADR behavior following different criteria (i.e., environment, multi-channel, downlink communication). ADR performs better in dense deployments compared to uniform deployments for medium size networks because ADR takes advantage of the low SFs and their short packet duration. For larger networks, the performance of ADR in dense deployment decreases rapidly due to saturation of low SFs causing more collisions and packet losses. ADR is negatively impacted in FoF environments using Tanghe pathloss model compared to Okumura Hata. This shows the weakness of ADR in more constrained environments. ADR exploits better all SFs capacities improving PDR using multiple channels compared to the single one. However, using multiple channels is more impacted by downlink communications. ADR does not exploit properly the quasi-orthogonality of SFs (i.e., under and over usage of SFs). Thus, we need a strategy that equitably balances PDR of each SFi.

Finally, we evaluated network densification and topology adaptation. By limiting the size of each GW (i.e., the number of covered nodes), GW can better take advantage of the spatial reuse and can serve them with better PDR, especially for a large number of nodes. Multi-GW adaptation considers the required number of gateways and the optimal SF_i configuration to assure sufficient PDR for different network sizes.

In the following chapter, we plan to enhance allocation strategies according to PDR of each GW. The distributed decision module can use several estimated metrics (based on PDR, spectrum occupancy, gateway load, redundancy) to provide better performance. Indeed, we look for a strategy that does not depend on the environment.

Efficient Spreading Factor Allocation in Massive Access LoRa Multi Gateway Adaptive Networks

This chapter is partially adapted from:

- *M. Nunez, A. Guizar, M. Maman, A. Duda.* Toward a Self-Deployment of LoRa Networks: Link and Topology Adaptation. *In IEEE 15th International Conference on Wireless and Mobile Computing, Networking and Communications (WiMob). IEEE, 2019.* [98]
- *M. Nunez, M. Maman, A. Duda.* Spreading Factor Allocation for LoRa Nodes Progressively Joining a Multi-Gateway Adaptive Network. *(submitted to IEEE Globecom 2020).*

Contents

Introduction

The massive access problem in the LoRa technology involves two aspects: link coordination and resource allocation. Massive deployments requires link coordination through MAC protocols in order to avoid collisions. Varying LoRa communication parameters (TP, SF, BW, CR, Channel) results in different transmission qualities. Thus, in this chapter we focus on resource allocation, i.e., efficiently allocating resources to end-devices based on the deployed environment to improve massive access and scalability.

In the previous chapter, we evaluated the performance and limitations of massive access in LoRa networks for different application cases or traffic intensities. We investigated the capacity of each SF in homogeneous deployments and the impact of the quasi-orthogonality in heterogeneous deployments. We also evaluated the limitations of ADR and we showed the need of smarter resource allocation strategies to adapt the end-devices communication parameters and to self-deploy LoRa networks.

In this chapter, the objective is to improve the network transmission quality for large-scale deployments optimizing efficiently the resource allocation of spreading factor to the end-devices. Furthermore, we look to improve the network density placing multiple gateways for different network deployments (uniform and dense end-devices placements).

First, we present several strategies to *deploy* LoRa networks by adapting the communication parameter spreading factor at the initialization, *when all nodes join the network*. We propose improvements to ADR, the classical spreading factor allocation mechanism of LoRaWAN: (i) enhanced link adaptation (ELA), and (ii) joint adaptation (MGELA) strategies. They improve the network capacity and transmission quality in terms of packet delivery ratio. Second, we present a strategy to *self-deploy* LoRa networks by adapting the spreading factor *in the course of time when nodes progressively join the network* based on different metrics. We propose a progressive joining strategy based on link, network, and distribution metrics of previously joined end-devices to set up the configuration of joining end-devices to self-deploy LoRa networks according to their network size.

Note that we consider a centralized architecture, where the network server senses, analyzes, takes a decision and requests to the node for the adaptation. When a node requests to join the network, and if the network server accepts its request, the network server replies with an adaptation request containing the optimal configuration for the node. Hence, each node sets up its configuration once per simulation when it joins the network. We consider a first arrived first served approach. Each node joins the network gradually and selects its best configuration according to the current status of the network keeping good level of transmission quality. Note that use the simulation model already defined in previous chapter.

4.1 Enhanced Link Adaptation

How to enhance the SF allocation strategy? How to still improve the allocation strategy in more general scenarios independent on the environment / context?

Spreading factor allocation to different end-devices is an important issue in LoRa networks. ADR does not exploit all the potential of LoRa technology and presents limitations as we showed in previous chapter. Here, we look for improving the spreading factor allocation strategy exploiting the under-used SFs and limiting usage of over-used SFs. We present our proposal: the Enhanced Link Adaptation (ELA) and we compare it with ADR.

4.1.1 ELA Algorithm

We propose an adaptive strategy called Enhanced Link Adaptation (ELA) to exploit the maximum capacity of GW exploiting all SFs and their quasi-orthogonality. Algorithm 1 describes ELA.

Algorithm 1 Enhanced Link Adaptation (ELA)

$\%NmaxSF_{j=6,...,12} = [41.3, 24.8, 16.5, 8.3, 5.4, 2.5, 1.2]$
$SNR_{req,SF=6,...,12} = -[5, 7.5, 10, 12.5, 15, 17.5, 20] dB$
$marg = 3dB$
procedure $ELA(0)$
    return $[NSF_6, ..., NSF_{12}] = 0$
procedure $ELA(N)$
    $[NSF_6, ..., NSF_{12}] = ELA(N-1)$
    For node N
    $SINR_N = SINR(N, GW)$
    Choose $SF_k \mid k = Min(j \mid SINR_j \geq SNR_{req,SF_j} + marg) \wedge ((NSF_j + 1)/N < \%NmaxSF_j))$
    $SF_N \leftarrow SF_k$
    $NSF_k \leftarrow NSF_k + 1$
    return $[NSF_6, ..., NSF_{12}]$

When node N wants to join the network, it sends a request to the network server. If the network server accepts the joining, it executes the procedure ELA(N) and defines the optimal SF configuration (SF_k) for node N (i.e., SF_N) according to its link budget and the capacity of each SF. We calculated the capacity of each SF for application period (AP) equal to 60 sec to assure PDR of 90%. Hence, Table 4.26 provides the percentage of nodes to allocate to each SF in order to take advantage of the maximum capacity of the GW. Indeed, the table shows the capacity of each SF for AP equal to 60 sec to assure a PDR of 90% and extends the values obtained elsewhere [42].

Table 4.26: Distribution of nodes as a function of SF for a single GW and 1 min traffic intensity.

SF_i	6	7	8	9	10	11	12	Total
$\%Nodes$	41.3	24.8	16.5	8.3	5.4	2.5	1.2	100

Thus, according to the Signal Interference Noise Ratio ($SINR_N$) of node N, it chooses the optimal SF_k according to the distribution ($\%NmaxSF_k$) of each configuration SF_k. If the capacity of SF_k is reached, then it checks the availability to be configured with SF_{k+1}, and so on up to SF_{12}. When the capacity of all SFs are reached, the network server makes a trade-off between the optimal configuration and the distribution of the nodes on all the SFs according to Table 4.26 (i.e., it keeps the number of nodes configured with each SF proportional to the percentage of nodes supported by each SF if it is possible, otherwise it takes the optimal configuration according to its link budget).

4.1.2 ELA Gain Compared to ADR

In this section, we simulated several single GW deployments for three strategies: (i) LoRaSF_6 where all the nodes are configured with SF_6, (ii) ADR, and (iii) ELA. The objective is to show the gain of ELA and to compare it with the ADR performance.

Table 4.27: System Model to analyze ELA performance compared to ADR.

Configuration		Network Deployment	
$FrequencyBand$	868 MHz	$AreaofInterest$	circular area $R = D_{max}(SF_6)$
$Bandwidth$	125 KHz	$Deployment$	uniform
$CodingRate$	4/5	$Multi-GW$	MG_1
$TransmissionPower$	14 dBm	$GWposition$	centered
$SpreadingFactor$	SF_6 to SF_{12}	$PathlossModel$	Okumura Hata
Application			
$ApplicationPeriod$	50-Byte packet every 1 min	$Protocol$	ELA
$Multi-Channel$	1CH	$Bidirectional$	UL only

Simulation parameters are defined in Table 4.27. End-devices are uniformly deployed over a circular area of radius $D_{max}(SF_6)$. We consider one single gateway placed at the center of the deployment. The protocol is the ELA algorithm. The application makes that end-devices generate 50-Byte packets every 60 sec. Note that we assume open rural environment with a single channel without the downlink communication effect.

What is the gain of ELA compared to ADR? What is the impact on the PDR when increasing the number of nodes in uniform deployments of nodes configures with ELA?

Figure 4.1 compares PDR of ELA, ADR, and the LoRaSF_6 strategies for different network deployments increasing the number of end-devices.

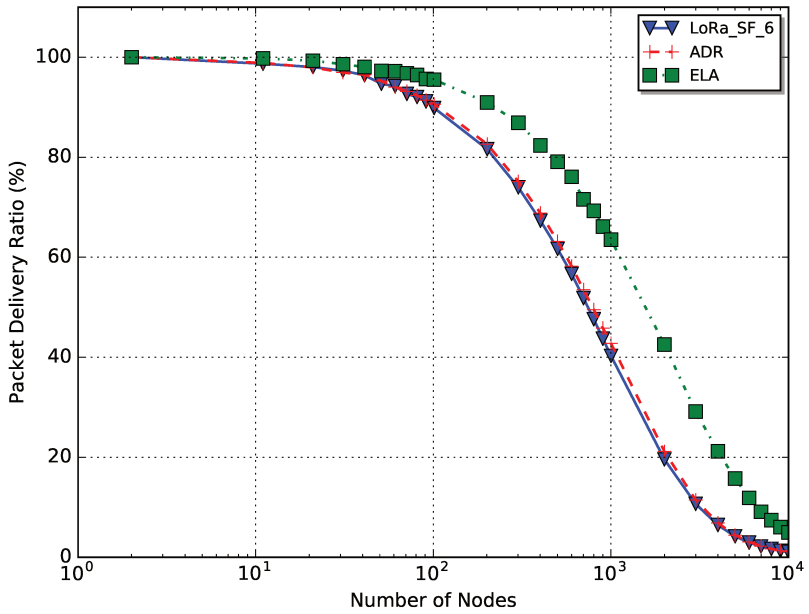

Figure 4.1: Comparison of 3 link adaptation strategies for devices generating a packet each 60 s in a disk of radius $D_{max}(SF_6)$.

We observe that ADR has the same performance than $LoRaSF_6$ (where all the nodes are configured with SF_6) because the selection of SF is only based on the link budget. Thus, all the devices select SF_6 whereas ELA estimates that a large number of nodes use the SF_6 configuration and exploits other configurations to decrease the number of collisions improving PDR.

The link adaptation algorithm must select the configuration according to the scenario criteria (e.g., network congestion) and the radio environment (e.g., link budget, level of interference). The ELA strategy optimizes the network performance with a better use of each configuration (i.e., taking into account the current load and the capacity of each SF). Thus, ELA is adapted to more complex deployments and provides a fairer distribution of the configuration than ADR, which is highly dependent on the topology propagation model and the type of deployment.

4.2 ELA Performance Evaluation

In this section, the objective is to evaluate the ELA strategy performance in different scenarios impacted by: (i) network deployment, (ii) pathloss environment, (iii) multiple channels, and (iv) downlink communications.

We evaluated the impact of these issues on ELA in single gateway deployments. We studied the impact of the network deployment: in uniform and dense deployments. We also evaluate different environments as open rural and the Factory of the Future (FoF). Furthermore, we studied the impact of using multiple channels instead of using a single channel. Finally, we evaluate the impact of downlink communication instead of only considering uplink communication.

4.2.1 Impact of Network Deployment on ELA

We evaluate the ELA strategy in terms of reliability and throughput for uniform and dense deployments.

Table 4.28: System Model to analyze the impact of network deployment on ELA.

Configuration		Network Deployment	
$FrequencyBand$	868 MHz	$AreaofInterest$	**circular area** $R = D_{max}(SF_{12})$
$Bandwidth$	125 KHz	$Deployment$	**uniform, dense**
$CodingRate$	4/5	$Multi-GW$	MG_1
$TransmissionPower$	14 dBm	$GWposition$	centered
$SpreadingFactor$	SF_6 **to** SF_{12}	$PathlossModel$	Okumura Hata
Application			
$ApplicationPeriod$	50Bytes packet every 1 min	$Protocol$	**ELA**
$Multi-Channel$	1CH	$Bidirectional$	UL only

Simulation parameters are defined in Table 4.28. End-devices are deployed over an area of a circle of $R = D_{max}(SF_{12})$. We analyze the impact of dense deployments closer to the gateway and compare it with the uniform deployment. We performed several simulations for several numbers of end-devices (up to 10,000) generating a packet every 60 sec.

What is the impact of network deployment on the ELA performance? What is the impact on the ELA PDR when increasing the number of nodes in uniform and dense deployment scenarios?

Figure 4.2 shows PDR of the ELA strategy for uniform and dense deployments.

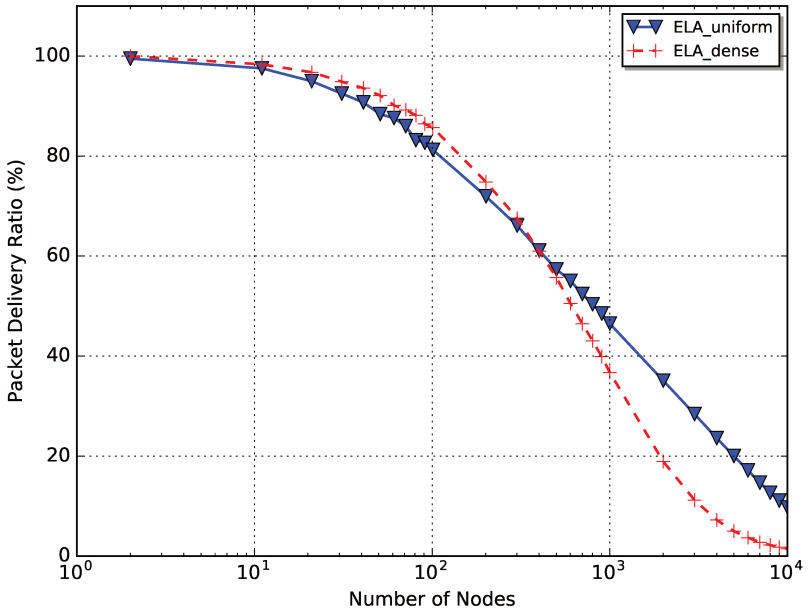

Figure 4.2: PDR of ELA in uniform and dense deployments.

We observe performance for small and medium networks (up to 500 end-devices). ELA in dense deployments slightly outperforms ELA in uniform deployments because it better exploits closer nodes with low SFs. For larger network deployments (beyond 500 nodes), performance of ELA in the dense deployment decreases faster due to the over-charge of end-devices close to the gateway increasing collisions. Contrarily to ELA in the dense deployment, ELA in the uniform deployment allocates SFs more efficiently due to the uniform distribution.

In conclusion, ELA presents good performance in terms of PDR for network deployments of up to 500 end-devices in dense deployments. Beyond this number of end-devices, ELA in uniform deployments better exploits SF allocation improving PDR compared to dense deployments. Indeed, one is better for small networks and the other is better for larger networks because of the configuration distribution of SFs.

What is the impact of network deployment on the ELA performance? What is the impact on the ELA throughput when increasing the number of nodes in uniform and dense deployment scenarios?

We also evaluated the network throughput of ELA in uniform and dense deployments. Figure 4.3 shows the throughput for different number of end-devices.

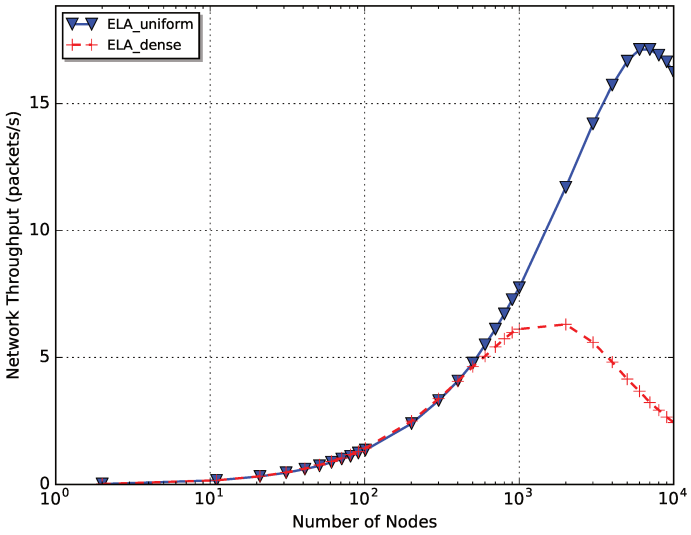

Figure 4.3: Throughput of ELA in uniform and dense deployments.

We observe the maximum throughput of 17 and 6 packets/sec for uniform and dense deployments, respectively. We notice maximum throughputs are achieved for 6000 and 2000 end-devices, respectively. For networks of up to 500 nodes, ELA presents the same tendency in throughput for both deployments. Beyond 500 nodes, ELA in dense deployments saturates faster than ELA in uniform deployments because in dense deployments, low SFs start to be over-used, due to high density close to GW, increasing collisions.

In conclusion, the network deployment impacts the network throughput for large scale networks, more than 500 nodes: ELA in dense deployments is more impacted by collisions than ELA in uniform deployments. Note that ELA has similar performance compared with ADR, evaluated in the previous chapter, for deployments in a circular area of $R = D_{max}(SF_{12})$ with a single gateway due to the constraint of the deployment on this area. Then, to relax this constraint and show the gain of ELA: (i) we will evaluate smaller areas with a single gateway and (ii) we will increase the number of gateways over the largest circular area.

4.2.2 Impact of Pathloss Environment on ELA

In the previous chapter, we evaluated performance of ADR in different environments. We found that PDR of ADR is negatively impacted in FoF environments using Tanghe pathloss model compared to open rural environments (using Okumura Hata). Here, we analyze our proposal ELA in the FoF environment using both pathloss propagation models.

Table 4.29: System Model to analyze the impact of the pathloss environment on ELA.

Configuration		Network Deployment	
$FrequencyBand$	868 MHz	$AreaofInterest$	**room 100mx100m**
$Bandwidth$	125 KHz	$Deployment$	uniform
$CodingRate$	4/5	$Multi-GW$	MG_1
$TransmissionPower$	14 dBm	$GWposition$	centered
$SpreadingFactor$	SF_6 **to** SF_{12}	$PathlossModel$	**Okumura Hata, Tanghe**
Application			
$ApplicationPeriod$	50Bytes packet every 1 min	$Protocol$	**ELA**
$Multi-Channel$	1CH	$Bidirectional$	UL only

Simulation parameters are defined in Table 4.29. End-devices are uniformly deployed over a square area of 100 meters x 100 meters. The FoF environment uses the Tanghe pathloss modes whereas the open environment uses the Okumura Hata pathloss model. We perform several simulations with a single gateway for several number of end-devices generating a packet every 1 minute. Note that the protocol is the enhanced link adaptation.

What is the impact of passing from open to FoF environment on the ELA performance? What is the impact of the pathloss environment on PDR when increasing the number of nodes in deployments of nodes configured with ELA?

Figure 4.4 shows PDR of ELA for different numbers of end-devices for both pathloss models.

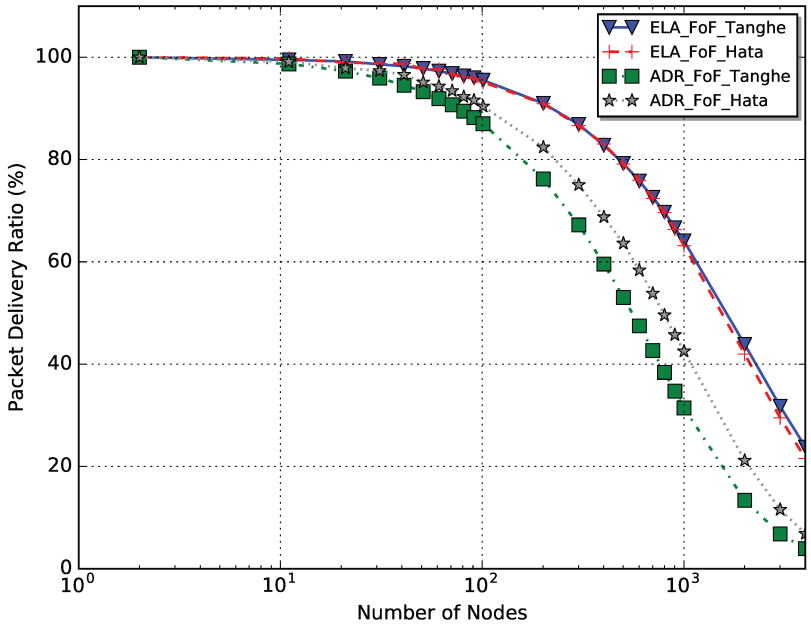

Figure 4.4: PDR of ELA in the FoF environment.

Different to ADR, we observe that PDR of ELA is not degraded in the FoF environment using Tangue compared to the open rural environment using Okumura Hata because ELA exploits the use of all available SFs taking advantage of the quasi-orthogonality of SFs. In conclusion, ELA is not negatively impacted in FoF environments using Tanghe compared to open rural environments using Okumura Hata, which is not the case for ADR. This shows the robustness of ELA to more constrained environments.

What is the impact of the pathloss environment on the throughput when increasing the number of nodes in deployments of nodes configured with ELA?

Furthermore, we also evaluated the performance of ELA in terms of throughput for FoF environments using Tanghe and Okumura Hata pathloss models. Figure 4.5 shows the throughput of ELA for both pathloss models.

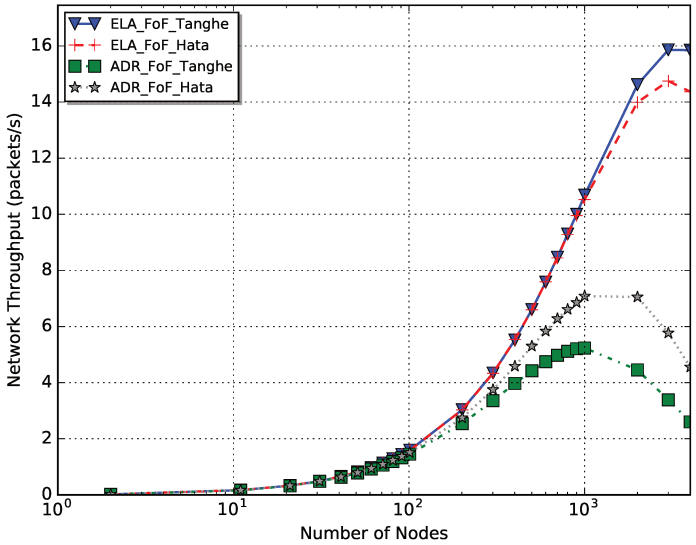

Figure 4.5: Throughput of ELA in the FoF environment.

We observe that throughput of ELA using Tanghe is slightly better than ELA using Okumura Hata. Maximum throughput are 16 and 15 packets/sec for Tangue and Okumura Hata respectively for 3000 end-devices. However, ELA improves considerably the throughput of ADR, e.g., 7 and 5 packets/sec for Okumura Hata and Tangue, respectively (for 1000 end-devices).

In this section, we conclude that the FoF environment impacts negatively the performance of ADR due to this environment being more drastic considering pathloss, shadowing, and fading. However, ELA performance is not impacted negatively in the FoF environment because it exploits the use of all SFs taking advantage of their quasi-orthogonality. Indeed, ELA performance is slightly degraded for large-scale networks, e.g., more than 1000 end-devices. Then, ELA is more robust compared to ADR compared to more constrained environments.

4.2.3 Impact of Multiple Channels on ELA

In this section, we analyze the impact of using multiple channels instead of a single one on the ELA performance. We evaluate the scalability when increasing the number of used channels. Indeed, we would like to know if the capacity will be n times the capacity of a single channel when n channels are used.

Table 4.30: System Model to analyze the impact of using multiple channels on ELA.

Configuration		Network Deployment	
$FrequencyBand$	868 MHz	$AreaofInterest$	room 100mx100m
$Bandwidth$	125 KHz	$Deployment$	uniform
$CodingRate$	4/5	$Multi-GW$	MG_1
$TransmissionPower$	14 dBm	$GWposition$	centered
$SpreadingFactor$	SF_6 **to** SF_{12}	$PathlossModel$	Okumura Hata
Application			
$ApplicationPeriod$	50-Byte packet every 1 min	$Protocol$	**ELA**
$Multi-Channel$	**1CH, 8CH**	$Bidirectional$	UL only

Simulation parameters are defined in Table 4.30. End-devices are uniformly deployed in a square area (i.e., a room of 100 meters x 100 meters). Note that we evaluate a single gateway scenario considering the Okumura Hata pathloss model. Note also that the gateway is the transceiver Semtech SX1301 that is capable to operate up to 8 channels in parallel. Then, we assume 8 available channels of 125 kHz. End-devices randomly selects the transmission channel among these 8 channels.

What is the impact of using multiple channels on the PDR when increasing the number of nodes in deployments of nodes configured with ELA? Is it scalable?

Figure 4.6 shows PDR of ELA using single and multiple channels.

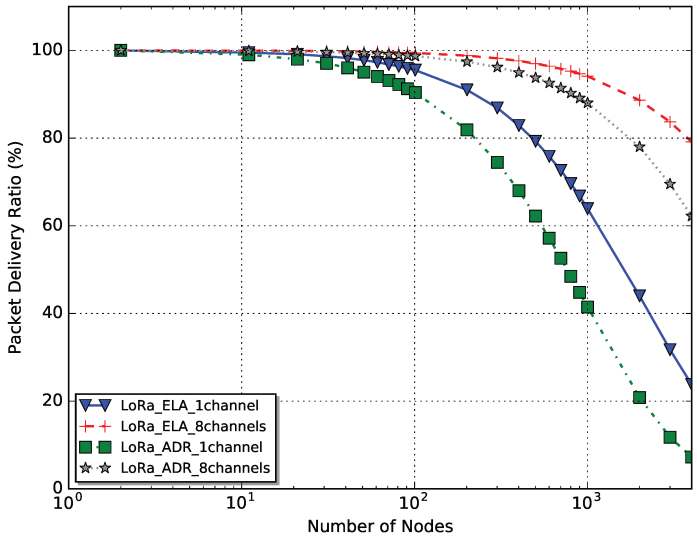

Figure 4.6: PDR of ELA using single and multiple channels.

As long as the network size in terms of the number of nodes increases, the gain of multiple channels becomes more important, increasing PDR. For 100 end-devices, the improvement is from 95% to 100% PDR. For 1000 end-devices, it is from 62% to 95% PDR, and for large-scale networks (4000 end-devices) from 22% to 80%. Moreover, taking results in previous chapter of ADR with multiple channels, ELA with 8 channel outperforms ADR with 8 channels in terms of PDR (60% of ADR improved while the improvement of ELA is up to 80%) due to better SF utilisation (i.e., SF configuration distribution). Then, ELA exploits better all SFs capacities improving PDR using multiple channels compared to the ADR deployment. Indeed, using multiple channels improves scalability of the network. Increasing the capacity of one single channel that supports a certain amount of nodes to multiple channels, the number of supported nodes will increase as many times as the number of channels are used, keeping the same level of PDR.

What is the impact of using multiple channels on throughput when increasing the number of nodes in deployments of nodes configured with ELA?

We also evaluated the throughput of ELA in multiple channels. Figure 4.7 shows the throughput of ELA for single and multiple channels.

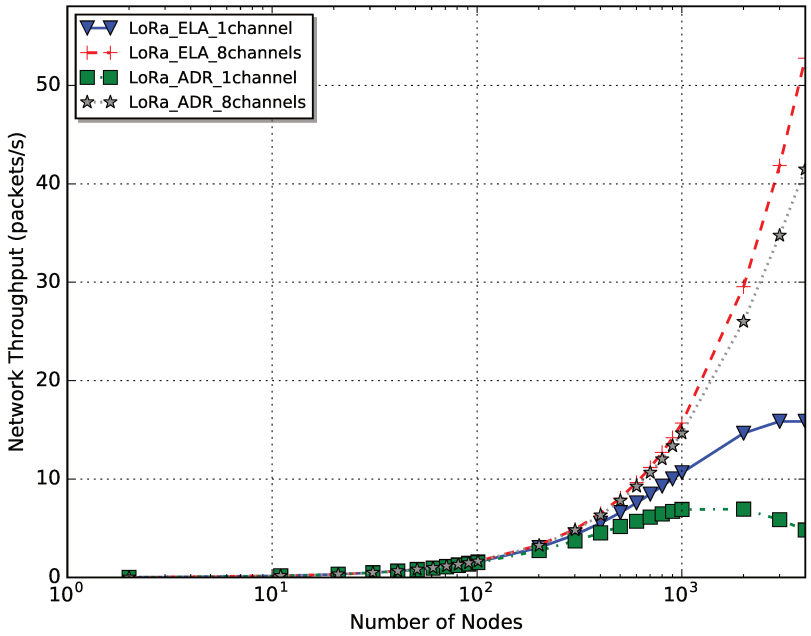

Figure 4.7: Throughput of ELA using single and multiple channels.

Using 8 channels improves maximum throughput (more than 50 packets/sec) considerably compared to the single channel (16 packets/sec) because of better spectral efficiency and more available bandwidth. Throughput gain using 8 channels becomes more important for increased network size. For large-scale networks, there is an improvement from 16 to more than 50 packets/sec. Indeed, we expect that the capacity of the 8 channels will be 8 times the capacity of one single channel, i.e., we expect a maximum of 128 packets/sec using the ELA strategy.

In this section, we conclude that using multiple channels with the ELA strategy is more scalable than using it with the ADR strategy. The network capacity using 8 channels is 8 times the network capacity of one single channel ensuring the same level of PDR. Note that the capacity of the network results in the number of nodes the network is capable to manage to ensure a given PDR. Furthermore, multiple channels allows to exploit frequency diversity to reduce the effects of radio signal distortions. Another method to exploit is frequency hopping by rapidly changing the carrier frequency among many different frequencies in a band to avoid interference.

4.2.4 Impact of Uplink and Downlink Communications on ELA

In this section, we investigate the impact of the downlink communication on the performance of the ELA strategy. We evaluate PDR and throughput of network deployments considering only uplink communications and uplink / downlink communications. Note that we evaluate ELA using single and multiple channels (i.e., 8 channels).

Table 4.31: System Model to analyze the impact of uplink and downlink communications on ELA.

Configuration		Network Deployment	
$FrequencyBand$	868 MHz	$AreaofInterest$	room 100mx100m
$Bandwidth$	125 KHz	$Deployment$	uniform
$CodingRate$	4/5	$Multi-GW$	MG_1
$TransmissionPower$	14 dBm	$GWposition$	centered
$SpreadingFactor$	SF_6 **to** SF_{12}	$PathlossModel$	Okumura Hata
Application			
$ApplicationPeriod$	50Bytes packet every 1 min	$Protocol$	**ELA**
$Multi-Channel$	1CH, 8CH	$Bidirectional$	**UL only, UL / DL**

Simulation parameters are defined in Table 4.31. End-devices are uniformly deployed in a square area (i.e., a room of 100 meters x 100 meters). Note that all parameters are equal to the previous section except the bidirectionality, i.e., with and without DL (downlink) in addition to the UL (uplink) communication.

Note that we defined in Subsection 3.4.4 the assumptions for downlink communications in ADR. Similarly to ADR, in ELA we assume the ACK_LIMIT limit equal to 64 to evaluate the impact of these DL frames. The duration of the DL response depends on the configuration parameters, we assume the same parameters of the UL frame. We also assume that reception occurs in the receive window RX1. Note also that if an end-device optimizes its parameters, it periodically needs to validate that the network still receives the UL frames. Each time the UL frame counter is incremented without considering repeated transmissions, the end-device increments an ACK_CNT counter. When this counter exceeds an ACK_LIMIT limit without any DL response, it sets the ACK request bit (ACKReq). So, the network is required to respond with a DL frame within the next ADR_ACK_DELAY frames.

What is the impact of downlink communication on the PDR when increasing the number of nodes in deployments of nodes configured with ELA?

Figure 4.8 shows PDR of network deployments with and without downlink communication for scenarios configured with ELA using single and multiple channels.

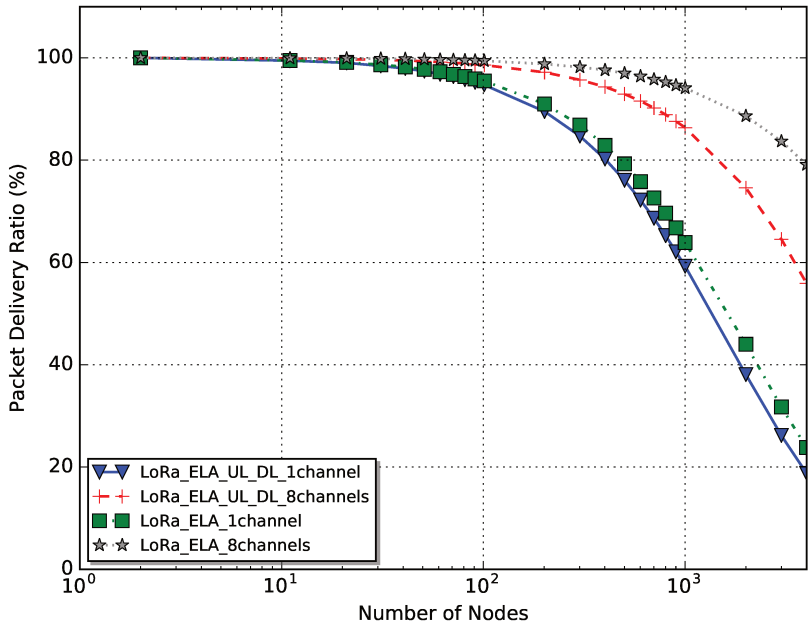

Figure 4.8: Impact of the downlink transmission on PDR of ELA for single and multiple channels.

For a single channel, downlink transmissions slightly degrades PDR, especially for more than 100 end-devices. For 8 channels, there is more important degradation of PDR as long as the number of end-devices increases. This is due to the limitation of the gateway transceiver of loosing packets in reception in all channels (i.e., 8 channels) during the downlink transmission on one channel. Increasing the network size up to 1000 nodes, downlink transmissions could reduce PDR by 10%. This degradation could be 20% for larger networks (e.g., 4000 nodes). In conclusion, using multiple channels is strongly impacted by downlink communications, especially for large-scale deployments, in terms of PDR.

What is the impact of downlink communication on the throughput when increasing the number of nodes in deployment of nodes configures with ELA?

Regarding the throughput, Figure 4.9 shows the impact of downlink transmissions on the ELA performance using single and multiple channels.

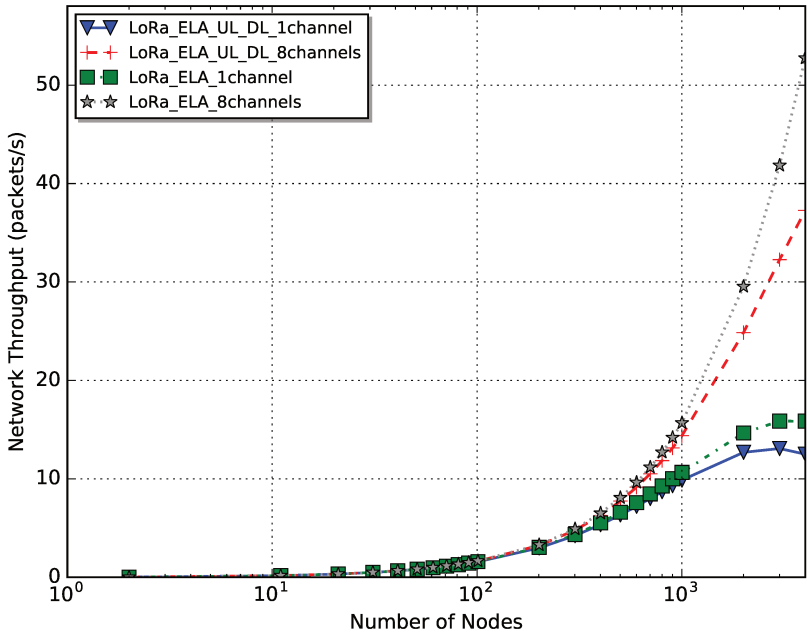

Figure 4.9: Impact of the downlink transmission on throughput of ELA for single and multiple channels.

As long as the network size increases, the negative impact of the downlink transmission increases, especially for multiple channels. This is because packets are lost in all channels by the gateway when a downlink transmission occurs. In conclusion, throughput is also strongly degraded by downlink communications using multiple channels in large-scale networks. We expect more significant negative impact on throughput for larger number of nodes on the network deployment.

In this section we conclude that performance is impacted by downlink communications, especially for large-scale networks and in the scenarios using multiple channels due to all channels being disabled for reception at the gateway when a downlink transmission occurs on a single channel. Note that ADR presents similar tendency but ELA improves the ADR performance.

4.3 Enhanced Link and Topology Adaptation

In this section, we extend our ELA approach to a Multi-GW network deployments by taking into account the capacity of each GW according to the percentage of nodes supported by each SF per GW. The objective is to investigate the network densification and topology adaptation using the ELA strategy. We look for the optimal number of gateways and the best SF configuration for a given number of end-devices to assure a given level of reliability in multiple gateway deployments. We propose an adaptation strategy for nodes configured with ELA. The proposed Multi-GW Enhanced Link Adaptation (MG$_j$ELA) strategy is described

in Algorithm 2. First, according to the $SINR_N$ of node N, the network server selects the best GW to communicate with. Second, it chooses the SF configuration using the ELA algorithm, making a trade-off between the optimal SF and the network load as described in Algorithm 1.

Algorithm 2 Multi-GW Enhanced Link Adaptation (MG$_j$ELA)

1: GW: $k \epsilon [1, ..., M]$
2: **procedure** $MGELA(0, M)$
3: return $[NSF_6, ..., NSF_{12}]_{k=1,...,M} = 0$
4: **procedure** $MGELA(N, M)$
5: $[NSF_6, ..., NSF_{12}]_{k=1,...,M} = MGELA(N-1, M)$
6: For node N
7: Choose the best GW_m, $m = k \mid Max(SINR(N, GW_k))$
8: $[NSF_6, ..., NSF_{12}]_m \leftarrow ELA(N_m)$
9: return $[NSF_6, ..., NSF_{12}]_{k=1,...,M}$

4.3.1 Impact of Network Densification

Here, we analyze the impact of increasing the number of gateways, i.e., the network densification, using the Enhanced Link and Topology Adaptation strategy (MGELA).

Table 4.32: System Model to analyze the impact of network densification on the enhanced link and topology strategies (MG_jELA).

Configuration		Network Deployment	
$FrequencyBand$	868 MHz	$Areaof Interest$	circular area $R = D_{max}(SF_{12})$
$Bandwidth$	125 KHz	$Deployment$	uniform
$CodingRate$	4/5	$Multi-GW$	MG_3, MG_7, MG_9
$TransmissionPower$	14 dBm	$GW position$	circles covering circle geometry
$SpreadingFactor$	SF_6 to SF_{12}	$PathlossModel$	Okumura Hata
Application			
$ApplicationPeriod$	50-Byte packet every 1 min	$Protocol$	ELA
$Multi-Channel$	1CH	$Bidirectional$	UL only

Simulation parameters are defined in Table 4.32. Note that we return to end-devices uniformly deployed in a circular area of $R = D_{max}(SF_{12})$ because it is more interesting to analyze large-scale deployments on this area. We analyze the impact of increasing the number of gateways on the performance. Gateways are positioned following the circles covering circle geometry. MG_jELA refers to a network deployment with j gateways and end-devices configured with the MG_jELA algorithm. We investigate multiple gateway deployments performing several simulations for several number of end-devices up to 10000, generating a packet every 60 sec. Note that the protocol is the ELA strategy but in multiple gateway scenarios. Note also that we assume open rural environment with a single channel without the downlink communication effect.

What is the impact of the network densification on PDR when increasing the number of nodes configured with the MG_jELA strategy?

Figure 4.10 shows Network PDR for MG$_j$ELA and MG$_j$ADR strategies for 3, 7, and 9 gateways deployed in a disk of radius $D_{max}(SF_{12})$. The figure also shows the homogeneous deployments configured with SF_6 and SF_{12} as reference to compare MG$_j$ELA and MG$_j$ADR strategies.

In Figure 4.10(a), MG$_3$ADR and MG$_3$ELA show similar performance due to the limitation in coverage using low SFs. In Fig 4.10(c), MG$_9$ADR and MG$_9$SF$_6$ present similar performance because having 9 GWs allows ADR to set up all nodes with SF6. The proposed MG$_j$ELA outperforms MG_jSF_i in terms of network PDR. MG$_j$ELA keeps good performance for an over-sized number of GWs, which is not always the case for MG$_j$ADR. This drawback has been also observed elsewhere [96].

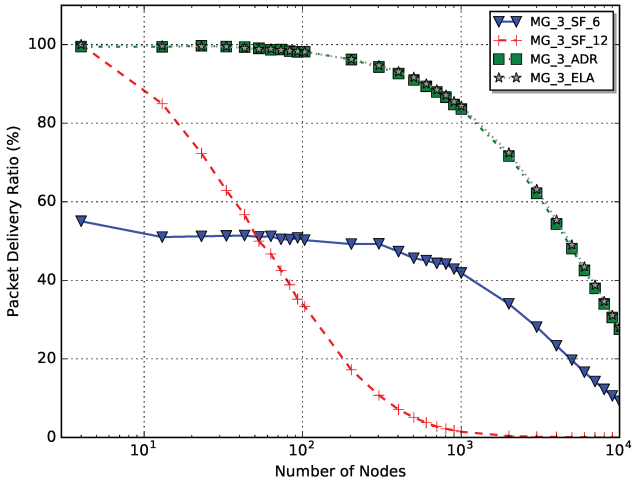

(a) 3 GWs

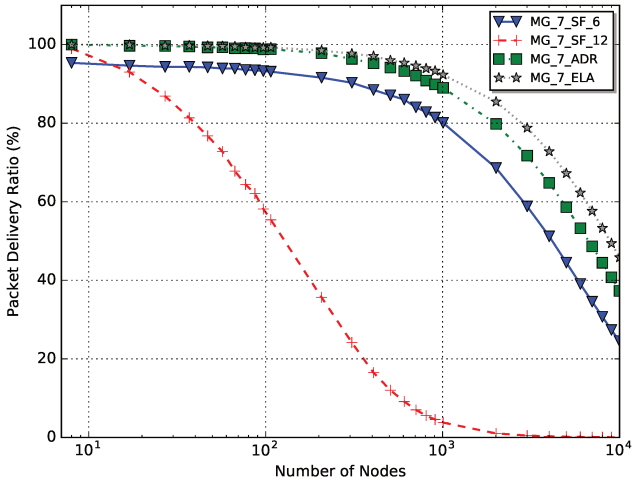

(b) 7 GWs

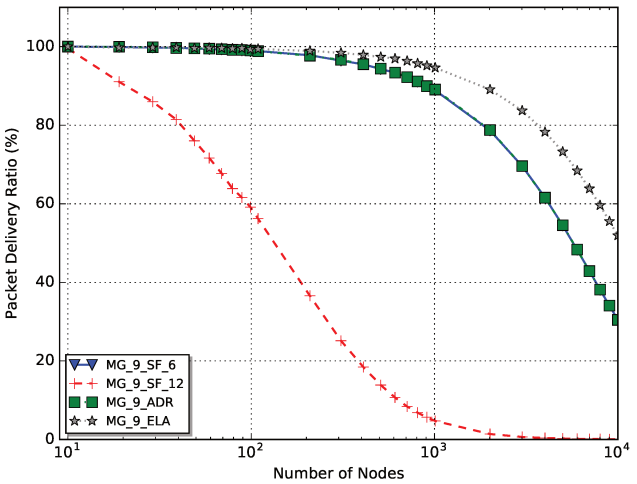

(c) 9 GWs

Figure 4.10: Network PDR for Multi-GW ADR and ELA deployments in a disk of radius equal to $D_{max}(SF_{12})$.

What is the impact of the network densification on the throughput when increasing the number of nodes in deployments of nodes configured with the MG_jELA strategy?

We also evaluated throughput for 3, 7, and 9 gateways. Figure 4.11 shows the network throughput in packets per second for MG$_j$ELA and MG$_j$ADR strategies.

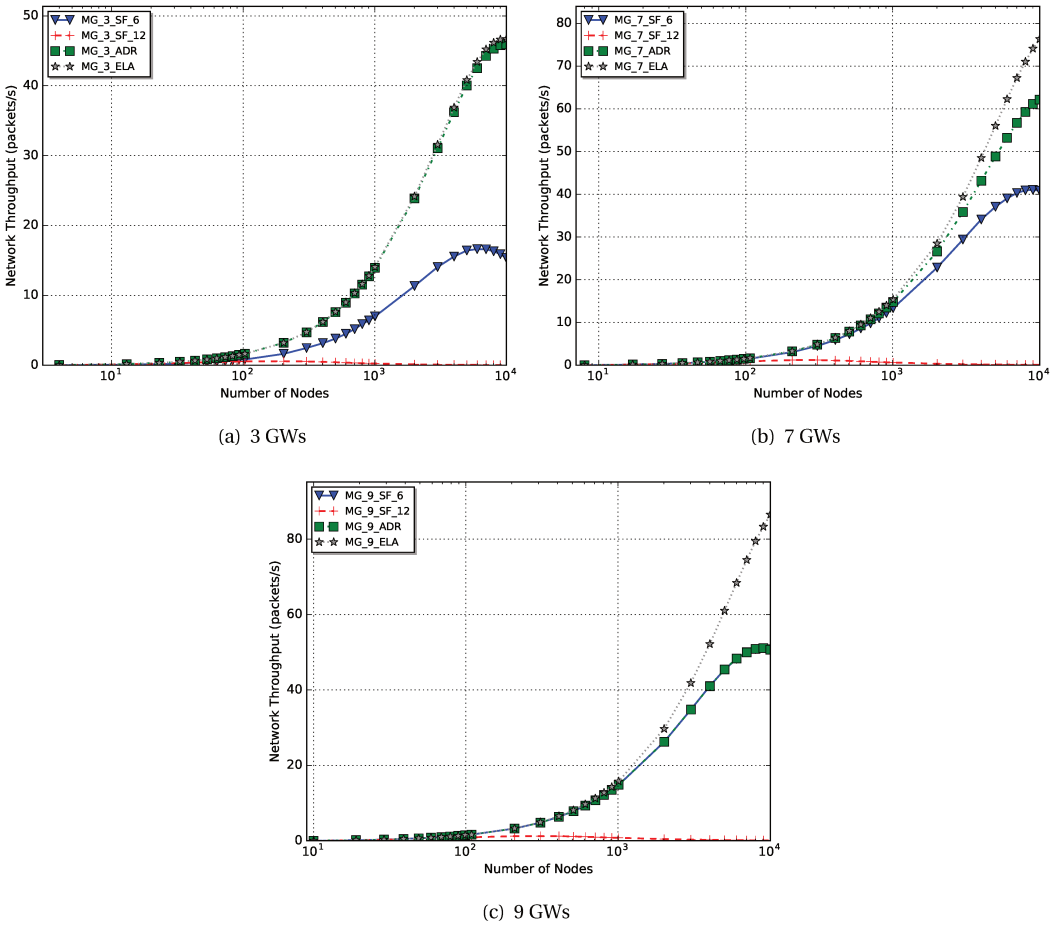

(a) 3 GWs

(b) 7 GWs

(c) 9 GWs

Figure 4.11: Network throughput for Multi-GW ADR and ELA deployments in a disk of radius equal to $D_{max}(SF_{12})$.

Increasing the number of nodes, throughput increases achieving the maximum. We observe that maximums for 3, 7, and 9 gateways are greater than throughput of the homogeneous SF_6 and SF_{12}. Regarding the deployment with 9 gateways, we observe that throughput of ADR is almost the same to the homogeneous SF_6 because the ADR protocol configures the majority of devices with SF_6 since the network densification is increased, i.e., any device can reach a diversity of gateways with at least one of the 9 gateways close to it. On the other hand, throughput of ELA improves the ADR one due to better SF configuration distribution.

We observe in Figure 4.11(a), MG$_3$ADR and MG$_3$ELA show similar tendency due to the limitation in coverage using low SFs. In Fig 4.11(b), MG$_7$ELA outperforms MG$_7$ADR because with 7 gateways the constraint of the network deployment is relaxed. In Fig 4.11(c), MG$_9$ADR and MG$_9$SF$_6$ present similar tendency because having 9 GWs allows ADR to set up all nodes with SF6. The proposed MG$_j$ELA outperforms MG_jSF_i in terms of network throughput. MG$_j$ELA keeps good performance for an over-sized number of GWs, which is not always the case for MG$_j$ADR (e.g., 9 gateways).

What is the impact of network densification on performance of the MG_jELA strategy compared to the ADR strategy when increasing the number of nodes?

In conclusion, Figure 4.12 compares the performance of MG$_j$ADR and MG$_j$ELA for 1-3-7-9 GWs network deployments.

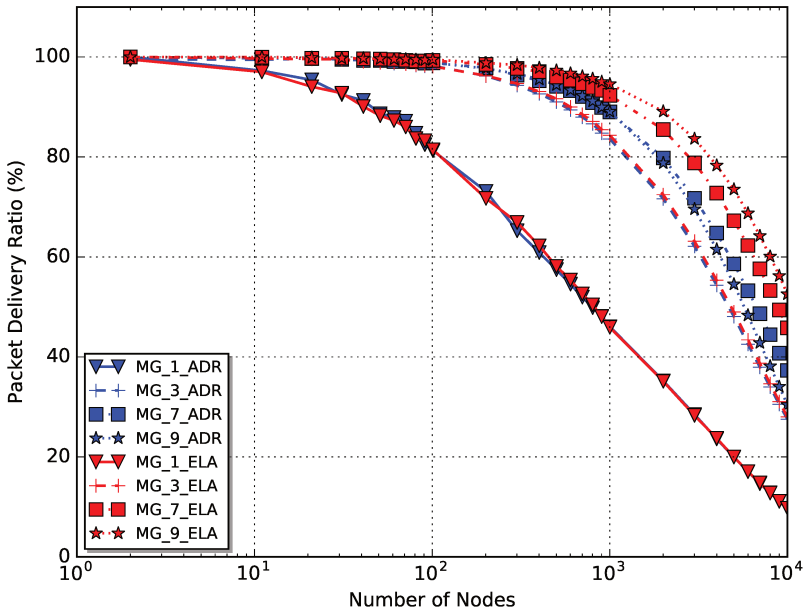

Figure 4.12: Network PDR of MG$_j$ADR and MG$_j$ELA strategies for different number of GWs.

On one hand, we observe that over-sizing the number of GWs degrades Network PDR of MG$_j$ADR because MG$_j$ADR configures most of the nodes with SF_6 and saturates faster. On the other hand, MG$_j$ELA takes advantage of the infrastructure densification and exploits the capacity of the unused SFs (i.e., better SF configuration distribution). Thus, when the number of GWs increases, Network PDR is improved.

4.3.2 Adaptation Strategy

How many gateways are needed to ensure a given reliability for small to large network deployments?

Figure 4.13 illustrates the required number of GWs for the MG$_j$ELA strategy as a function of the number of deployed nodes to assure different levels of reliability (PDR from 0% to 100%, i.e., from red to green).

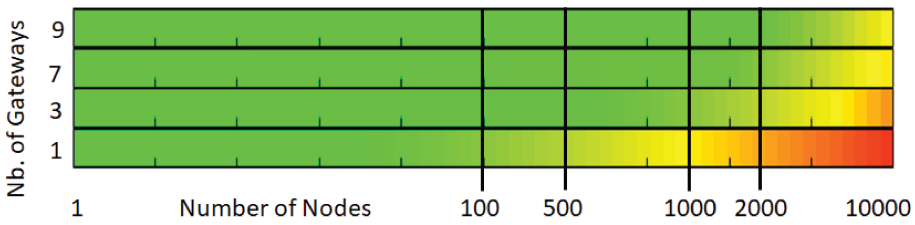

Figure 4.13: Multi-GW ELA (MG$_j$ELA) strategy.

It shows that a single GW can assure 80% PDR for up to 100 deployed nodes and 3 GWs for up to 1000 nodes. By comparing Figures 3.29 and 4.13, we observe that the MG$_j$ELA strategy reduces the number of GW and improves the performance. To assure a high reliability (i.e., more than 80%) for the 500 node deployment, 9 GWs are required with the optimal SF_6 configuration (MG_9SF_6) whereas MG$_j$ELA needs only 3 GWs.

4.4 Nodes Progressively Joining Network

We can define three methodologies to maximize the network performance. First, we have the *global maximization* in which the central entity has a global knowledge of the network. It could apply brute force method by analyzing all the possibilities and combinations of configurations to find the maximum. The algorithm by Slabicki et al. [42] proposes to sort nodes according to the increasing distance from the gateway before allocating SF, which is an important constraint in real deployments. Second, the *iterative maximization* improves the performance link by link after the initialization of the network and could take a lot of time

to converge [46, 96]. Finally, we have *nodes progressively joining maximization* in which they progressively join the network and select their configuration according to the current state of the network (i.e., composed of the nodes already accepted in the network). We assume that already accepted nodes cannot change their decision on the parameter configuration after the joining procedure. This approach uses a distributed decision based on multiple estimated metrics available at the gateways.

In this section, we consider the last approach (*nodes progressively joining*) because it is more realistic and takes advantage of the current network statistics readily estimated from experimental gateway measurement. The following subsections present the allocation algorithms according to the defined metrics, the evaluation of their performance in uniform and dense deployments, and the performance comparison with respect to ADR.

4.4.1 Enhanced Link and Network Distribution Adaptation

In this subsection, we define the Enhanced Link Network Distribution (ELNDA) algorithm based on multiple metrics and multiple criteria. It takes into account:

1. the link budget with the selected gateway that could be the closest one, the most reliable one in terms of PDR, or the least congested one.
2. the multi-connectivity or multiple paths through the gateways.
3. the network distribution to exploit all SFs effectively giving fair use of each SF per GW in multi-gateway deployments.

The proposed allocation algorithm is based on different metrics such as the selected link PDR, network PDR, and the network distribution (capacity of the gateway and SFs), respectively represented by $Metric_L$, $Metric_N$, and $Metric_D$. The objective is to allocate SF to new end-devices joining the network so they obtain maximal PDR. ELNDA controls the weight of the different metrics with α and β parameters that are link and network distribution weights respectively.

The ELNDA algorithm looks for maximizing PDR based on the currently estimated metrics for the network size (number of end-devices that already joined the network) to define the SF configuration of end-devices joining the network. We evaluate our proposal for the uniform deployment of nodes and also for more realistic deployments such as a more dense deployment in the center of the area of interest. Furthermore, we compare our proposal with ADR.

Equation 4.32 defines the ELNDA. We look for SF that maximizes PDR taking into account the multiple metrics and the optimal values of α and β.

$$ELNDA(\alpha,\beta) = \beta[\alpha(Metric_{\mathrm{L}}) + (1-\alpha)(Metric_{\mathrm{N}})] + (1-\beta)(Metric_{\mathrm{D}}) \tag{4.32}$$

where:

- α is the *link weight*, $\alpha \in [0,1]$.
- β is the *network distribution weight*, $\beta \in [0,1]$.
- $Metric_L$ is the link quality metric according to the selected GW and the selected SF. It considers the estimated average PDR of all the nodes that already joined the network with the same SF. Equation 4.33 defines this metric, where $\widehat{PDR}$ is the average estimated PDR.

$$Metric_{\mathrm{L}} = \widehat{PDR}(GW_{selected}, SF_i) \tag{4.33}$$

We compute PDR regarding the selected GW: (i) the closest GW to the end-device, (ii) the GW with the best PDR, or (iii) the least congested GW.

- $Metric_N$ is the network link quality metric according to the network infrastructure (i.e., taking into account the node connectivity with one or several GWs) and the selected SF. This metric considers the probability that at least one GW correctly receives the packet. Equation 4.34 defines this metric, where M is the number of GWs in the network.

$$Metric_{\mathrm{N}} = 1 - \prod_{j \in GW}^{M} (1 - \widehat{PDR}(j, SF_i)) \tag{4.34}$$

  We recall that the higher SF, the larger the number of GWs in the communication range of the node.

- $Metric_D$: is the distribution metric that aims to balance the load of each SF. It measures the difference between the percentage of the maximum number of nodes that should be configured with each SF (i.e., $\%Nmax(SF_i)$) and the percentage of nodes that are really configured with each SF for the selected GW (i.e., $A(SF_i)$).

  Equation 4.35 defines the distribution metric for the closest GW.

$$Metric_{\mathrm{D}} = \frac{\%Nmax(SF_i) - A(SF_i)}{MAX(\%Nmax(SF_i) - A(SF_i))} \tag{4.35}$$

  where,

$$A(SF_i) = \frac{Number\_nodes(SF_i, GW_{closest})}{Number\_nodes(GW_{closest})} \tag{4.36}$$

  This metric aims to fairly exploit all the SFs by allocating the least used SF to the new end-devices. The percentage of nodes for each SF to guarantee a fair level of PDR of 90% is given in Table 4.33.

Table 4.33: Distribution of nodes as a function of SF for a single GW and traffic intensity corresponding to one packet every 1 min.

SF_i	6	7	8	9	10	11	12
$\%Nmax(SF_i)$	41.3	24.8	16.5	8.3	5.4	2.5	1.2

Note that the average estimated PDR ($\widehat{PDR}$) is evaluated by each gateway for each SF and takes into account all the nodes that are currently accepted in the network.

We discuss the behavior of different metric combinations depending on the value of α and β. We evaluate performance of ELNDA for multiple gateway deployments.

An end-device should choose the closest gateway or the best one in terms of PDR as selected gateway (i.e., $Metric_L$ with $\alpha = 1$ and $\beta = 1$)?

Table 4.34: System Model to analyze the performance of $Metric_L$, i.e., ELNDA(α=1, β=1) in the nodes progressively joining network.

Configuration		Network Deployment	
$FrequencyBand$	868 MHz	$AreaofInterest$	circular area $R = D_{max}(SF_{12})$
$Bandwidth$	125 KHz	$Deployment$	uniform
$CodingRate$	4/5	$Multi-GW$	MG_1, MG_3, MG_7, MG_9
$TransmissionPower$	14 dBm	$GWposition$	circles covering circle geometry
$SpreadingFactor$	SF_6 to SF_{12}	$PathlossModel$	Okumura Hata
Application			
$ApplicationPeriod$	50-Byte packet every 1 min	$Protocol$	ELNDA(α=1, β=1)
$Multi-Channel$	1CH	$Bidirectional$	UL only

Simulation parameters are defined in Table 4.34. The frequency band is 868 MHz, the bandwidth is 125 kHz, the coding rate is 4/5, the transmit power is 14 dBm, and the spreading factor is selected among SF_6 up to SF_{12}. The area of deployment is a circular area with radius $R = D_{max}(SF_{12})$, it is an uniform deployment, MG_j means that there are j gateways positioned according to the circles covering circle geometry, and the pathloss model is the Okumura Hata. The application (AP) transmits 50-Byte packets every 1 min to stress the single channel and only the uplink communication is considered. Note that we analyze the performance of $Metric_L$ that is equal to ELNDA(α=1, β=1).

A node joining the network selects its SF configuration according to the selected gateway to communicate with. This gateway could be the closest or the one which offers the best packet delivery ratio between all gateways. Thus, performance in terms of PDR when choosing the closest or the best gateway for several uniform deployments of nodes and 1-3-7-9 gateways are shown in Figure 4.14.

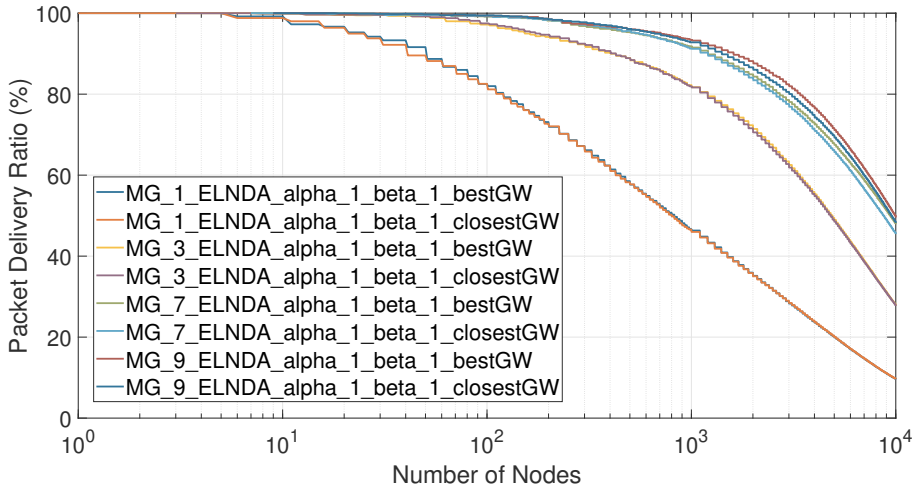

Figure 4.14: ELNDA($\alpha = 1$, $\beta = 1$) for the closest and the best GW.

For 1 gateway deployments, there is no difference when choosing the gateway, which is normal. For multiple gateways, selecting the best gateway with ELNDA($\alpha = 1$ and $\beta = 1$) to take decision on choosing SF improves PDR compared to the closest one. So, the closest gateway is not necessarily the selected gateway that an end-device should communicate with. This is because the selected gateway depends on the nodes configuration around the gateways that impacts PDR.

To conclude, ELNDA($\alpha = 1$, $\beta = 1$) is a first method to balance the SF allocation. $Metric_L$ with the selection of the best gateway improves the PDR for uniform deployments of end-devices and multiple gateways. Thereafter, we will only evaluate the best gateway.

An end-device should decide its SF according to a selected GW (i.e., $Metric_L$ with $\alpha = 1$ and $\beta = 1$) or according to the network infrastructure quality (i.e., $Metric_N$ with $\alpha = 0$ and $\beta = 1$)?

Table 4.35: System Model to analyze the performance using $Metric_L$ and $Metric_N$ in the nodes progressively joining network.

Configuration		Network Deployment	
FrequencyBand	868 MHz	*AreaofInterest*	circular area $R = D_{max}(SF_{12})$
Bandwidth	125 KHz	*Deployment*	uniform
CodingRate	4/5	*Multi – GW*	MG_1, MG_3, MG_9
TransmissionPower	14 dBm	*GWposition*	circles covering circle geometry
SpreadingFactor	SF_6 **to** SF_{12}	*PathlossModel*	Okumura Hata
Application			
ApplicationPeriod	50-Byte packet every 1 min	*Protocol*	**ELNDA(α=0 or 1, β=1)**
Multi – Channel	1CH	*Bidirectional*	UL only

Simulation parameters are defined in Table 4.35. Note that all parameters are the same of previous analysis except the protocol, it is ELNDA(α=0 or 1, β=1). Indeed, we evaluate $Metric_L$ with $\alpha = 1$ and $\beta = 1$ and $Metric_N$ with $\alpha = 0$ and $\beta = 1$. Note also that we evaluated PDR performance for 1-3-7-9 gateways but we do not show results for 7 gateways to make figures more readable.

At the beginning of the simulation, a node joins the network and each GW estimates statistics for each SF. Based on the estimated PDR, our algorithm makes the decision on the optimal SF to configure on the joining end-device. On the one hand, the accuracy of $Metric_L$ ($\alpha = 1$ and $\beta = 1$) depends on the granularity of the estimated PDR, the duration of the windows for transmitting and receiving packets to calculate the statistics, and the traffic intensity of the end-devices. On the other hand, $Metric_N$ ($\alpha = 0$ and $\beta = 1$)

takes into account the connectivity with several GWs in the communication range of the end-device. The accuracy of this metric indirectly depends on the estimated PDR.

In uniform deployment scenarios, Figure 4.15 shows PDR for 1, 3, 9 GWs for ELNDA ($\alpha = 0$, $\beta = 1$), ELNDA ($\alpha = 1$, $\beta = 1$), and ADR.

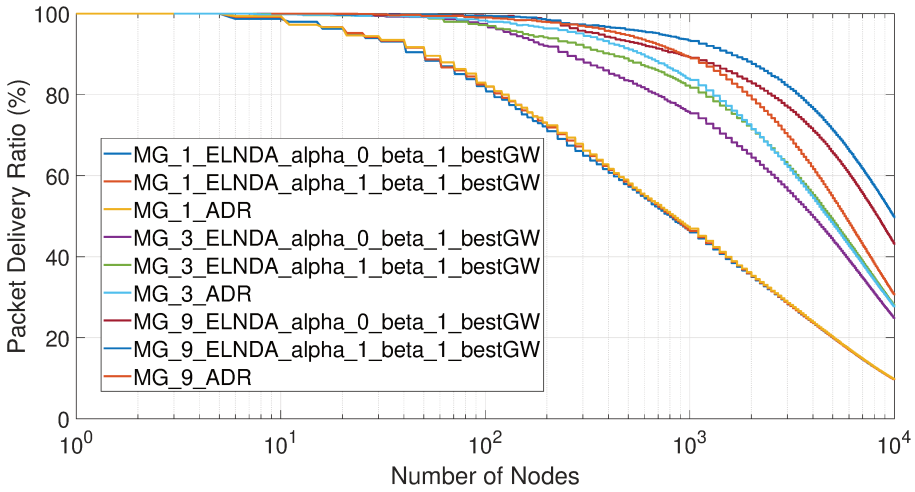

Figure 4.15: PDR of ELNDA for $\alpha = 0$, $\alpha = 1$ and $\beta = 1$, and ADR in uniform deployment scenarios of 1, 3, 9 GWs.

For a single GW, $Metric_L$ ($\alpha = 1$ and $\beta = 1$), $Metric_N$ ($\alpha = 0$ and $\beta = 1$), and ADR provide the same level of performance because the selection of SF is mainly constrained by the deployment. Indeed, a large portion of end-devices is far from the GW and overuses high SFs. For multiple GWs, $Metric_L$ is more interesting than $Metric_N$ because it better exploits the multi-GW context. Moreover, $Metric_L$ outperforms ADR thanks to a better SF allocation. In fact, with 9 GWs, ADR mainly exploits SF_6 whereas $Metric_L$ reduces the load of low SFs and also exploits high SFs. We observe that ADR provides good performance for sparse networks but ELNDA becomes more important for large-scale deployments (e.g., 10,000 end-devices).

What is the impact of dense deployments on ELNDA(α,β) compared to ADR?

Table 4.36: System Model to analyze the impact of dense deployments on the performance of ELNDA(α,β) compared to the existing solution ADR, in the nodes progressively joining network.

Configuration		Network Deployment	
FrequencyBand	868 MHz	*AreaofInterest*	circular area $R = D_{max}(SF_{12})$
Bandwidth	125 KHz	*Deployment*	**dense**
CodingRate	4/5	*Multi−GW*	MG_1, MG_3, MG_9
TransmissionPower	14 dBm	*GWposition*	circles covering circle geometry
SpreadingFactor	SF_6 **to** SF_{12}	*PathlossModel*	Okumura Hata
Application			
ApplicationPeriod	50-Byte packet every 1 min	*Protocol*	**ELNDA(α=0 or 1, β=1)**
Multi−Channel	1CH	*Bidirectional*	UL only

Simulation parameters are defined in Table 4.36. Note that all parameters are the same of previous analysis except the deployment. Here, we investigate $Metric_L$ with $\alpha = 1$, $\beta = 1$, and $Metric_N$ with $\alpha = 0$ and $\beta = 1$, in dense deployments.

Figure 4.16 shows PDR for 1, 3, and 9 GWs for $Metric_L$, $Metric_N$ and ADR for more realistic deployments, i.e., denser at the center of the area of interest.

For a single GW, ADR, $Metric_L$ ($\alpha = 1$ and $\beta = 1$) and $Metric_N$ ($\alpha = 0$ and $\beta = 1$) still provide the same level of performance. For multiple GWs, $Metric_L$ is more interesting than $Metric_N$ and better exploits the multi-GW context than ADR for large-scale deployments. ELNDA is impacted for a small number of end-devices but performs better for an increasing number of devices, because it does not base the adaptation merely on link quality.

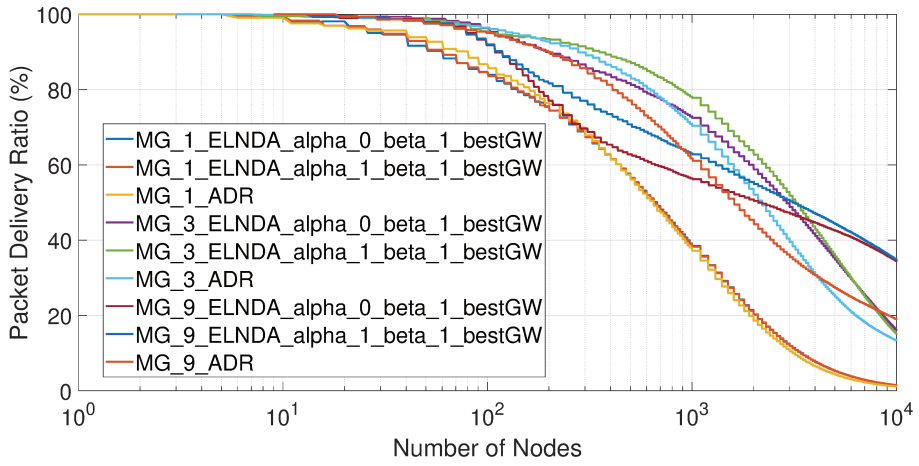

Figure 4.16: PDR of ELNDA for $\alpha = 0$, $\alpha = 1$ and $\beta = 1$, and ADR in dense deployment scenarios of 1, 3, and 9 GWs.

We notice that for the small scale scenario, 3 GW deployments have better PDR than 9 GW deployments because of better placement of the GWs. Indeed, they better exploit each SF capacity and the quasi-orthogonality between SFs to provide better link quality (e.g., reducing inter-GW distance at the range of low SFs implies that ADR set low SFs to nodes, without exploiting the others). For large-scale deployments, ELNDA in 9 GW scenarios results in a more reliable network than in the case of 3 GW because it better exploits the spatial reuse in the multi-GWs context, so it benefits from larger network capacity than for 3 GWs in the large-scale scenario.

To conclude, it is more interesting to take into account the metric based on the link quality with the selected GW ($Metric_L$) than the metric related to the network infrastructure ($Metric_N$) for both uniform and dense multiple gateway deployments.

In dense deployments, ADR is more interesting for small size networks whereas ELNDA becomes better for large-scale networks.

What is the optimal weight α between the link quality with the selected GW and the network link quality to maximize PDR for uniform deployments?

Here we analyze the impact of varying the link weight (α). We evaluated the ELNDA for many α values between 0 and 1 ($\alpha = 0 : 0.1 : 1$) for 9 gateways in uniform deployments.

Table 4.37: System Model to analyze the optimal α between the link quality and the network link quality in uniform deployments.

Configuration		Network Deployment	
FrequencyBand	868 MHz	*AreaofInterest*	circular area $R = D_{max}(SF_{12})$
Bandwidth	125 KHz	*Deployment*	**uniform**
CodingRate	4/5	*Multi – GW*	MG_9
TransmissionPower	14 dBm	*GWposition*	circles covering circle geometry
SpreadingFactor	SF_6 **to** SF_{12}	*PathlossModel*	Okumura Hata
Application			
ApplicationPeriod	50-Byte packet every 1 min	*Protocol*	**ELNDA(α=0:0.1:1, β=1)**
Multi – Channel	1CH	*Bidirectional*	UL only

Simulation parameters are defined in Table 4.37. Note that all parameters are the same of previous analysis except the protocol, it is ELNDA(α=0:0.1:1, β=1). Indeed, we evaluate more in detail the impact of α in uniform deployments to find the optimal α trading-off the $Metric_L$ ($\alpha = 1$ and $\beta = 1$) and the $Metric_N$ ($\alpha = 0$ and $\beta = 1$). Note also that we focus on investigate PDR performance for 9 gateways.

Figure 4.17 shows PDR for the best gateway as the selected gateway in 9 gateways uniform deployment.

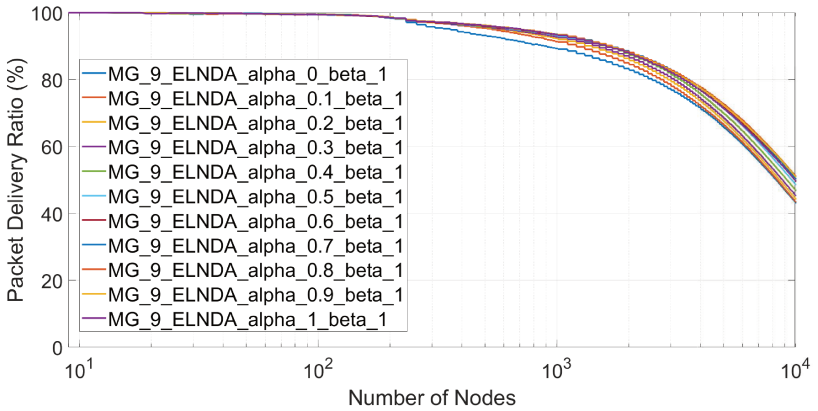

Figure 4.17: PDR of ELNDA for $\alpha = 0 : 0.1 : 1$ and $\beta = 1$ in 9 GWs uniform deployment.

We observe that $\alpha = 0$ presents the smallest PDR in both deployments. Increasing α until 0.8 increases the PDR. Then, increasing α until 1 keeps it at the same level of reliability.

What is the optimal weight α between the link quality with the selected GW and the network link quality to maximize PDR for dense deployments?

Here we analyze the impact of varying the link weight α. We evaluated the ELNDA for many α values between 0 and 1 ($\alpha = 0 : 0.1 : 1$) for 9 gateways in dense deployments.

Table 4.38: System Model to analyze the optimal α between the link quality and the network link quality in dense deployments.

Configuration		Network Deployment	
$FrequencyBand$	868 MHz	$AreaofInterest$	circular area $R = D_{max}(SF_{12})$
$Bandwidth$	125 KHz	$Deployment$	**dense**
$CodingRate$	4/5	$Multi-GW$	MG_9
$TransmissionPower$	14 dBm	$GWposition$	circles covering circle geometry
$SpreadingFactor$	SF_6 **to** SF_{12}	$PathlossModel$	Okumura Hata
Application			
$ApplicationPeriod$	50-Byte packet every 1 min	$Protocol$	**ELNDA(α=0:0.1:1, β=1)**
$Multi-Channel$	1CH	$Bidirectional$	UL only

Simulation parameters are defined in Table 4.38. Note that all parameters are the same of previous analysis except the deployment. Here, we evaluate more in detail the impact of α in dense deployments to find the optimal α trading-off the $Metric_L$ ($\alpha = 1$ and $\beta = 1$) and the $Metric_N$ ($\alpha = 0$ and $\beta = 1$).

Figure 4.18 shows PDR for the best gateway as the selected gateway in 9 gateways dense deployment.

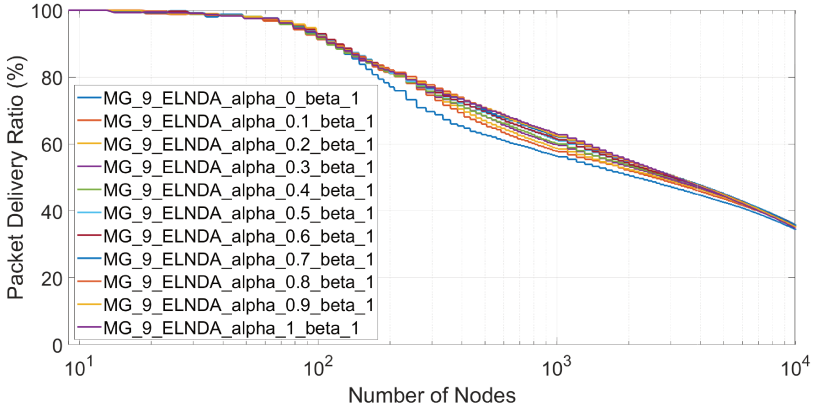

Figure 4.18: PDR of ELNDA for $\alpha = 0 : 0.1 : 1$ and $\beta = 1$ in 9 GWs dense deployment.

We observe similar tendency as in uniform deployment, i.e., $\alpha = 0$ presents the smallest PDR in both deployments. Increasing α until 0.8 increases the PDR. Then, increasing α until 1 keeps it at the same level of reliability.

To conclude, link weight $\alpha \in [0.5-1.0]$ optimizes network PDR in uniform and dense deployments thanks to the optimal use of link and network PDR metrics.

Hereafter, we consider the optimal value of $\alpha = 0.8$, the best GW as the selected GW, and 9 GWs.

What is the impact of only using the network distribution metric ($\beta = 0$) or using the optimal link quality metric based on the estimated PDR ($\alpha = 0.8$ and $\beta = 1$) in uniform deployments? Does a mixed metric ($\alpha = 0.8$ and $\beta = 0.5$) optimize PDR?

ELNDA($\beta = 0$) is only based on the percentage of the utilization of each SF per GW, $Metric_D$, whereas ELNDA($\alpha = 0.8, \beta = 1$) balances selected link and network metrics based on estimated PDR. ELNDA($\alpha = 0.8, \beta = 0.5$) balances the three metrics: $Metric_L$, $Metric_N$, and $Metric_D$ according to α and β.

Table 4.39: System Model to analyze the impact of only using the network distribution metric or using the link quality based on the estimated PDR in uniform deployments.

Configuration		Network Deployment	
$FrequencyBand$	868 MHz	$AreaofInterest$	circular area $R = D_{max}(SF_{12})$
$Bandwidth$	125 KHz	$Deployment$	**uniform**
$CodingRate$	4/5	$Multi-GW$	MG_9
$TransmissionPower$	14 dBm	$GWposition$	circles covering circle geometry
$SpreadingFactor$	SF_6 **to** SF_{12}	$PathlossModel$	Okumura Hata
Application			
$ApplicationPeriod$	50-Byte packet every 1 min	$Protocol$	**ELNDA(α=0.8, β=0, 0.5, 1)**
$Multi-Channel$	1CH	$Bidirectional$	UL only

Simulation parameters are defined in Table 4.39. Note that all parameters are the same of previous analysis except the protocol, here it is ELNDA(α=0.8, β=0-0.5-1). Indeed, we evaluate the impact of balancing $Metric_L$, $Metric_N$, and $Metric_D$. Note also that we focus on investigate PDR performance for 9 gateways.

In uniform deployments, Figure 4.19 shows PDR in the 9 GWs deployment with ELNDA($\alpha = 0.8, \beta = 0-0.5-1$) and ADR.

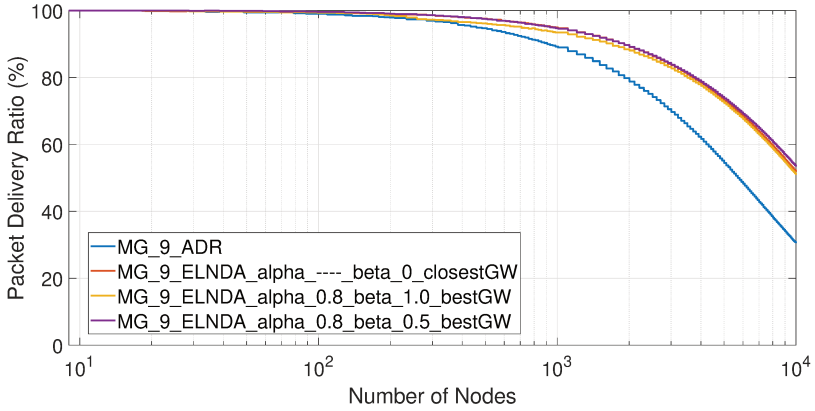

Figure 4.19: PDR comparison of ELNDA ($\alpha = 0.8, \beta = 0-0.5-1$) and ADR in a uniform deployment scenario of 9 GWs.

We observe two zones: less than 100 nodes, and beyond. For the first zone, PDRs for all three values of β are almost the same (i.e., 100%). Beyond 100 nodes, we observe that balancing $Metric_L$ and $Metric_N$ (i.e. $\beta = 1$) improves ADR. ELNDA based only on the $Metric_D$ (i.e. $\beta = 0$) presents same tendency and similar PDR because the uniform deployment. ELNDA($\alpha = 0.8, \beta = 0.5$) slightly outperforms the others with $\beta = 0-1$.

To conclude, we observed PDR improvement for different combinations of the metrics compared to ADR, especially ELNDA($\alpha = 0.8, \beta = 0.5$). However, we have considered the uniform deployment of nodes. Hence,

we need to analyze the impact of our proposed strategy ELNDA in more realistic deployment scenarios (i.e., network deployment denser at the center as in a typical city).

What is the impact of only using the network distribution metric ($\beta = 0$) or using the optimal link quality metric based on the estimated PDR ($\alpha = 0.8$ and $\beta = 1$) in dense deployments? Does a mixed metric ($\alpha = 0.8$ and $\beta = 0.5$) optimize PDR?

Table 4.40: System Model to analyze the impact of only using the network distribution metric or using the link quality based on the estimated PDR in dense deployments.

Configuration		Network Deployment	
$FrequencyBand$	868 MHz	$AreaofInterest$	circular area $R = D_{max}(SF_{12})$
$Bandwidth$	125 KHz	$Deployment$	**dense**
$CodingRate$	4/5	$Multi-GW$	MG_9
$TransmissionPower$	14 dBm	$GWposition$	circles covering circle geometry
$SpreadingFactor$	SF_6 **to** SF_{12}	$PathlossModel$	Okumura Hata
Application			
$ApplicationPeriod$	50-Byte packet every 1 min	$Protocol$	**ELNDA(α=0.8, β=0, 0.5, 1)**
$Multi-Channel$	1CH	$Bidirectional$	UL only

Simulation parameters are defined in Table 4.40. Note that all parameters are the same of previous analysis except the deployment. Indeed, we evaluate the impact of balancing $Metric_L$, $Metric_N$, and $Metric_D$ in dense deployments.

For dense deployment scenarios, Figure 4.20 shows PDR in the 9 GW deployment with ELNDA ($\alpha = 0.8, \beta = 0 - 0.5 - 1$) and ADR.

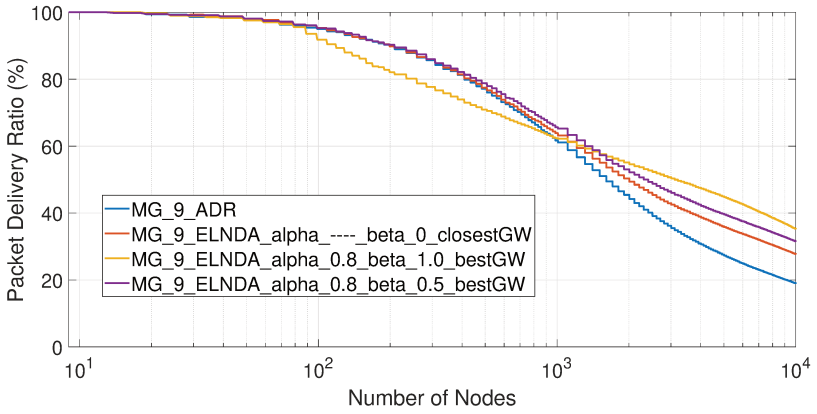

Figure 4.20: PDR comparison of ELNDA ($\alpha = 0.8, \beta = 0 - 0.5 - 1$) and ADR in a dense deployment scenario of 9 GWs.

We observe three zones: less than 100 nodes, up to 1000 nodes, and beyond 1000 nodes. For the first zone, PDR for all three values of β is the same and has the same tendency. Up to 1000 nodes, we observe that balancing $Metric_L$ and $Metric_N$, i.e., ELNDA($\beta = 1$), is not interesting due to the impact of the granularity of estimating PDR for these metrics. Its PDR is degraded compared to the others including ADR. The problem is that it recovers the average metric for each SF and not for its own PDR depending on the selected GW and its availability. We also observe that balancing $Metric_L$, $Metric_N$, and $Metric_D$, i.e., ELNDA($\alpha = 0.8, \beta = 0.5$), slightly outperforms the others becoming more important with an increasing number of nodes joining the network. Beyond 1000 nodes, we observe that leaving out $Metric_D$ and balancing link quality and network infrastructure metrics, i.e., ELNDA($\alpha = 0.8, \beta = 1$), becomes more interesting, outperforming the others.

To conclude, we have evaluated the impact of balancing three metrics: $Metric_L$, $Metric_N$, and $Metric_D$ to improve network reliability. We found that mixing the three metrics, ELNDA($\beta = 0.5$), is interesting for network deployments up to 1000 nodes. Beyond this point, the link and network metrics based on the estimated PDR ($Metric_L$ and $Metric_N$) outperform ADR and mixing the three metrics improves PDR. Thus, we need an algorithm taking the right combination of the metrics according to the network conditions such

as the network size—it is a dynamic *network distribution weight* β varying with $\beta = f(number\_of\_nodes)$, the number of nodes.

4.4.2 Adaptive β According to the Network Size

In this section, we propose to adapt the *network distribution weight* β depending on the number of end-devices (network size). β depends on the network size, network densification, gateway placement, and deployment density. In this work, we consider the fixed locations of GWs, the number of GWs, and the deployment density. We propose dynamic β that varies as a function of the number of joining end-devices. The objective is to adapt the network depending on its size, allocating optimally SFs to the joining end-devices based on a decision taking into account mixed metrics to maximize PDR or minimize the performance degradation.

Equation 4.37 defines dynamic β for three different network sizes: (i) small, i.e., up to 500 nodes. (ii) medium, i.e., up to 1500 nodes, and (iii) large, i.e., up to 10,000 nodes.

$$\beta = \begin{cases} 0.1 & if\ (nb\_nodes < 500) \\ 0.5 & if\ (500 \leq nb\_nodes < 1500) \\ 0.9 & if\ (nb\_nodes \geq 1500) \end{cases} \tag{4.37}$$

Table 4.41: System Model to analyze the adaptive β according to the network size.

Configuration		Network Deployment	
FrequencyBand	868 MHz	*AreaofInterest*	circular area $R = D_{max}(SF_{12})$
Bandwidth	125 KHz	*Deployment*	**dense**
CodingRate	4/5	*Multi−GW*	MG_9
TransmissionPower	14 dBm	*GWposition*	circles covering circle geometry
SpreadingFactor	SF_6 **to** SF_{12}	*PathlossModel*	Okumura Hata
Application			
ApplicationPeriod	50-Byte packet every 1 min	*Protocol*	**ELNDA(α=0.8, β=f(network size))**
Multi−Channel	1CH	*Bidirectional*	UL only

Simulation parameters are defined in Table 4.41. Note that all parameters are the same of previous analysis except the protocol. Indeed, we evaluate the ELNDA (α=0.8, β=f(network size)) in dense deployments.

Figure 4.21 shows the same curves as in Figure 4.20 but replacing ELNDA ($\beta = 0.5$) with dynamic β.

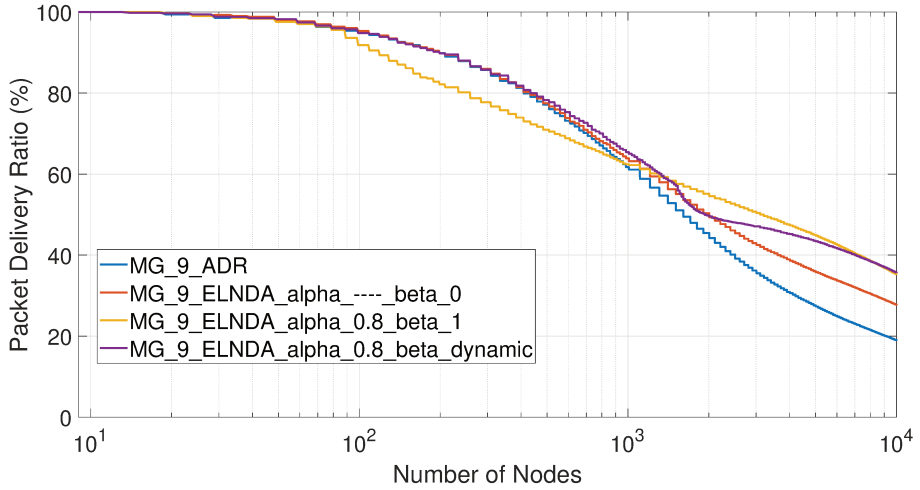

Figure 4.21: PDR of ADR, ELNDA($\beta = 0$), ELNDA ($\beta = 1$), and dynamic β in dense deployment scenarios of 9GWs.

We observe that dynamic β results in improved PDR for both small and large networks. It considers network distribution for small networks and switches to $Metric_L$ and $Metric_N$ when the network becomes larger. It is an interesting alternative to balance the three metrics according to the network size. Note that a

transition period appears because only new joining nodes change the value of β and the already deployed nodes do not change their configurations. Then, after a certain number of nodes joining the network, dynamic β achieves the same performance as ELNDA ($\beta = 1$).

Conclusion

In this chapter, we have investigated how to make LoRa network deployments easier by considering all network parameters, such as devices heterogeneity, network topology, density deployment, and traffic intensity.

We have proposed two approaches for adaptation of LoRa networks to different scenarios: link adaptation (i.e., each node selects its configuration according to its link budget but also according to the network load), and joint optimization: link and topology adaptation (i.e., densifying the network infrastructure by increasing the number of gateways).

The ELA strategy selects the configuration according to the scenario criteria (e.g., network congestion) and the radio environment (e.g., link budget) and optimizes a single gateway capacity with a better usage of each SF configuration according to each SF capacity. It is suitable for more complex deployments and fairer distribution of the configuration compared to ADR, which is only based on the link budget highly dependent on the propagation model and the type of deployment.

Multi-GW adaptation provides the required number of gateways and the optimal SF_i configuration to assure a high reliability for different network sizes. The densification of the network infrastructure maximizes the overall capacity of the LoRa Multi-GW network for different SF configurations. We also propose the joint Multi-GW ELA (MG_jELA) strategy that improves the transmission quality and outperforms Multi-GW ADR by exploiting the quasi-orthogonality of various SFs, the spatial reuse of the communication and the capacity of the GW according to each SF capacity.

Moreover, we investigate how to provide good transmission quality in LoRa networks by considering the scenario with nodes progressively joining the network and we propose an algorithm to improve network performance by effectively allocating a spreading factor (SF) to end-devices in realistic multi-gateway deployments. The algorithm performs better than ADR and enhances LoRa deployments by adapting the communication parameters of end-devices in function of the network size and estimated metrics. The allocation decision is based on different metrics: link packet delivery ratio (PDR), network PDR, and network distribution of SF per gateway. The network server can easily compute the estimated metrics from gateway measurements.

For nodes progressively joining networks, we have investigated the problem of how to allocate SFs in realistic deployments by considering all different network parameters. We have proposed an adaptation algorithm that effectively allocates SF to progressively joining nodes. The algorithm is based on three metrics (link quality with respect to a selected GW or to the network infrastructure, and network distribution of SF) and their combination related to the *link weight* and the *network distribution weight*.

For uniform deployments, the link quality metric is more interesting than the network metric. ELNDA improves network reliability in terms of PDR because of fair SF allocation. It outperforms ADR especially for an increasing number of GWs. For dense deployments, the mixed link and network metric is more interesting for large-scale networks whereas ADR is better for small networks. Indeed, for less congested networks, it is preferable to maximize the robustness of links to better support new joining nodes than minimizing the PDR degradation. Then, we have evaluated the impact of balancing the three metrics. For networks of up to 1000 nodes, the mixed metric ELNDA($\beta = 0.5$) is interesting. For larger networks, it is more interesting to leave out the metric network distribution ELNDA($\beta = 1$).

Last but not least, we have proposed ELNDA based on dynamic β that changes according to the network size. It properly exploits the metrics regardless of the level of congestion or the size of the network passing by a transition period and achieving optimal PDR.

Conclusion

In this chapter, we summarize our work concluding this thesis and highlighting the most important results. Then we discuss future research directions.

The objective of this thesis was to ensure IoT communication with high reliability, energy-efficiency, and robustness to interference to make WSNs deployments easier by self-deploying and adapting WSNs to the context. In this thesis, we started by comparing different LPWANs to focus on the LoRa technology. It offers several degrees of freedom on its communication parameters making it a good candidate for adaptive networks. Then, we theoretically evaluated energy consumption of LoRa networks showing the interest to focus on LoRa for adaptive networks and we also proposed adaptation strategies. Next, we investigated performance and limitations of LoRa networks identifying drawbacks of ADR. This investigation allowed us to propose enhancements by allocating SF optimally to improve reliability and fairness taking into account deployment constraints and exploiting LoRa properties. We highlight below the contributions of this thesis.

LPWANs and LoRa

This thesis presented a short overview of principal LPWAN technologies for IoT. Among these technologies, we have looked for the one suitable for adaptive networks to self-deploy WSNs. We found the LoRa technology as a good candidate for several reasons such as the degrees of freedom of its communication parameters, the robustness to interference, the openness and maturity of the technology. Thus, we presented more in detail the LoRa technology (PHY layer) and the LoRaWAN specification (MAC layer). We also presented the Adaptive Data Rate (ADR) mechanism of LoRaWAN on node and in the network. However, a deep analysis of the flexibility of LoRa communication parameters was required to understand the trade-offs when changing one parameter.

LoRa Deployments

We also discussed current real LoRa deployments for many applications in smart cities and smart meters reducing operation costs and improving people's life. Several studies provided insights of LoRa performance and limitations. We concluded that we need to take into account the capture effect and imperfect orthogonality of spreading factors as well as performance analysis in massive network deployments. The reviewed literature indicates the interest of heterogeneous deployments and optimal spreading factor allocation strategies to improve network performance.

Adaptation Approaches

We discussed link and topology adaptation approaches. Several studies agreed that nodes should be configured according to their radio environment, but also to the scenario criteria taking into account the network load and energy efficiency. We identified some insights to adapt the link considering fairer distribution of the spreading factors. We exploit the spatial reuse of the communication by densifying the network infrastructure increasing the redundancy. We also exploit the quasi-orthogonality of different spreading factors and the capacity of gateways for each spreading factor. Finally, we propose an algorithm to self-adapt nodes progressively joining a network based on several metrics.

LoRa for Adaptive Networks

We investigated energy consumption of sending a 50 byte packet with various LoRa configurations for star and mesh topologies. The goal was to exploit the LoRa technology by adapting its parameters (i.e., spreading factor, bandwidth, and transmitted power). We computed energy consumption based on the transceiver data sheet Semtech SX1276.

For the star topology, we observed that increasing SF has a more significant impact on energy consumption than increasing P_{tx}, that also makes the communication range longer. The best strategy is firstly to adapt the transmission power and then to increment the spreading factor to obtain the optimal energy consumption. When the bandwidth is considered, our results showed that the optimal energy consumption is for BW = 500 kHz up to a range of 3 km. Beyond 3 km, we adapt BW according to the data rate and range constraints.

For the mesh topology, the energy consumption is optimized by exploiting different radio configurations and the network topology (e.g., the number of hops, the network density, the cell coverage).

In dense networks, the proposed strategy consists of setting the spreading factor to SF6 and progressively increasing the transmitted power with the inter-relay distance. In the case of sparse networks, we recommend to adapt SF until reach the (SF=12, P_{tx} = 14 dBm) configuration.

According to the topology comparison, we showed that a global strategy exploiting both topologies exists and the trade-off between the star and mesh strategies depends on end-to-end distance D (i.e., the network coverage) and inter-relay distance d (i.e., the network density). Adapting the topology and the LoRa radio parameters permits to maintain low energy consumption and to extend the range of communication.

To evaluate our proposals, we have developed a LoRa module based on improved WSNet simulator, including a spectrum usage abstraction, the co-channel rejection due to the quasi-orthogonality of SFs and the gateway capture effect. Thanks to our realistic network simulator, we have considered the hidden and exposed terminal problems present in star of stars topology and provided a good transmission quality by exploiting the right level of redundancy.

LoRa Performance Analysis

We have investigated homogeneous and heterogeneous networks for large scale deployments, SFs allocations, and performance in terms of PDR and throughput. Simulation results compared the performance for homogeneous and heterogeneous deployments as a function of the number of nodes and traffic intensity.

First, we have analyzed homogeneous deployments for different SFs from SF_6 to SF_{12}. Simulations show better performance for the SF_6 deployment because of its short air time but reduced cell coverage. Second, we have compared heterogeneous and homogeneous in uniform deployments: the deployment that selects its LoRa configuration according to its link budget (ADR) results in the best PDR and throughput due to the use of all SFs exploiting orthogonality. The results clearly showed the benefits of heterogeneity for large scale network deployments. Evaluating the multi-homogeneous deployment, dense closer to the center, we found that it is possible to improve or degrade ADR performance depending on the network size. This shows the need of adaptive SF allocation strategies according to the deployment density and the network size.

We also evaluated ADR performance and limitations. ADR performs better in dense deployments compared to uniform deployments for medium size networks because ADR takes advantage of low SFs and their short packet duration. For larger networks, performance of ADR in dense deployments decreases rapidly due to saturation of low SFs causing more collisions and packet losses. ADR is negatively impacted in FoF environments using Tanghe pathloss model compared to open rural environment using Okumura Hata. This shows the weakness of ADR to more constrained environments, it is dependant on the environment. ADR exploits better all SFs capacities improving PDR using multiple channels compared to a single one. It increases scalability as many times as channels are used. However, when using multiple channels, ADR is more impacted by the downlink communications. ADR does not exploit properly the quasi-orthogonality of SFs (i.e., under and over usage of SFs). Thus, we need a strategy that balances equitably PDR of each SFi.

We evaluated network densification and topology adaptation. By limiting the size of each GW (i.e., the number of covered nodes), GW can better take advantage of the spatial reuse and can serve them with better PDR, especially for a larger number of nodes. Multi-GW adaptation considers the required number of gateways and the optimal SF_i configuration to assure sufficient PDR for different network sizes.

Efficient Spreading Factor Allocation

We have investigated how to make LoRa network deployments easier by considering all network parameters, such as device heterogeneity, network topology, density deployment, and traffic intensity.

We have proposed two approaches for adaptation of LoRa networks to different scenarios: link adaptation (i.e., each node selects its configuration according to its link budget but also according to the network load), and joint optimization: link and topology adaptation (i.e., densifying the network infrastructure by increasing the number of gateways).

The ELA strategy selects the configuration according to the scenario criteria (e.g., network congestion) and the radio environment (e.g., link budget) and optimizes a single gateway capacity with a better use of each SF configuration according to each SF capacity. It is suitable for more complex deployments and fairer distribution of the configuration compared to ADR, which is only based on the link budget highly dependent on the propagation model and the type of deployment.

Multi-GW adaptation provides the required number of gateways and the optimal SF_i configuration to assure a high reliability for different network sizes. The densification of the network infrastructure maximizes the overall capacity of the LoRa Multi-GW network for different SF configurations. We also proposed the joint Multi-GW ELA (MG_jELA) strategy, which improves the transmission quality and outperforms Multi-GW ADR by exploiting the quasi-orthogonality of various SFs, the spatial reuse of the communication and the capacity of the GW according to each SF capacity.

Nodes Progressively Joining the Network

We considered the scenario with nodes progressively joining the network. We proposed an algorithm to improve network performance by effectively allocating SF to end-devices in realistic multi-gateway deployments. The algorithm performed better than ADR and enhanced LoRa deployments by adapting the communication parameters of end-devices in function of the network size and estimated metrics. The allocation decision is based on different metrics: link packet delivery ratio (PDR), network PDR, and network distribution of SF per gateway. The network server can easily compute the estimated metrics and a combination of these metrics from gateway measurements.

For uniform deployments, the link quality metric is more interesting than the network metric. ELNDA improves network reliability in terms of PDR because of fair SF allocation. It outperformed ADR especially for an increasing number of GWs. For dense deployments, the mixed link and network metric is more interesting for large-scale networks whereas ADR is better for small networks. Indeed, for less congested networks, it is preferable to maximize the robustness of links to better support new joining nodes than to minimize the PDR degradation. Then, we have evaluated the impact of balancing the three metrics. For networks up to 1000 nodes, the mixed metric ELNDA($\beta = 0.5$) is interesting. For larger networks, it is more interesting leaving out the metric network distribution ELNDA($\beta = 1$).

Last but not least, we have proposed ELNDA based on dynamic β that changes according to the network size. It properly exploits the metrics regardless of the level of congestion or the size of the network passing by a transition period and achieving optimal PDR.

Future Directions

During this thesis, we selected different directions to perform our investigations allowing us to constitute a stage of work in the domain of LoRa networks. However, it is only a first step in LoRa adaptive networks. Therefore, additional investigation is necessary to adapt a network deployment. We present some research direction below:

Mesh networks: We analytically investigated the energy efficiency in LoRa mesh topology showing the dependency on the network density and network coverage. However, further investigation is necessary in LoRa mesh networks allowing multihop networking between nodes to extend coverage. Indeed, we need to consider MAC and routing protocols in a network simulator, then validate it in real deployments.

Machine Learning: Network performance could be still improved by adapting the network with machine learning techniques for link coordination and resource allocation by tuning parameters.

Experimental validation: We need to experimentally validate our proposals on large scale LoRa deployments. Indeed, our proposal can be integrated into current deployments. However, further studies should investigate and validate LoRa deployments with mobile nodes taking into account the effect of the interference from other technologies (as it operates in an unlicensed band) and the negative effect of downlink communications. Actually, dynamic re-transmission policies are needed to improve link coordination and resource allocation.

Optimal placement of the gateways: Another interesting issue for future work is the optimal placement of gateways depending on the use case and application. I think we can define a reuse distance between gateways depending on load traffic and network density to optimize LoRa performance.

Bandwidth and coding rate adaptation: Future research should consider bandwidth and coding rate adaptation depending on the environment or the application. Future studies are needed to determine if it is still possible to improve LoRa performance. I think adapting these parameters will improve performance.

In this thesis we investigated three bandwidths: 125, 250, and 500 KHz. Nevertheless, the LoRa standard also defines smaller bandwidths: 7.8125, 15.625, 31.25, and 62.5 KHz. It should be interesting to adapt this parameter exploiting the orthogonality between LoRa signals with different bandwidths. For example, a LoRa signal using SF_7 and BW=125 KHz is not orthogonal with a signal using SF_9 and BW=250 KHz. Table 5.42 shows the orthogonality of different combinations of BWs and SFs, where 'x' represents the non orthogonal combinations.

Table 5.42: Orthogonality for different combinations of BWs and SFs.

BW [KHz]		125							250							500						
	SF	6	7	8	9	10	11	12	6	7	8	9	10	11	12	6	7	8	9	10	11	12
125	6	x									x									x		
	7		x									x									x	
	8			x									x									x
	9				x									x								
	10					x									x							
	11						x															
	12							x														
250	6								x									x				
	7									x									x			
	8	x									x									x		
	9		x									x									x	
	10			x									x									x
	11				x									x								
	12					x									x							
500	6															x						
	7																x					
	8								x									x				
	9									x									x			
	10	x									x									x		
	11		x									x									x	
	12			x									x									x

Bibliography

[1] DELOITTE : The Future of Connectivity in IoT Deployments, 2018. 11

[2] ERICSSON : Ericsson Mobility Report, 2017. 11

[3] GROWTHENABLER : Market Pulse Report, Internet of Things (IoT), 2017. 11

[4] J. LIN, W. YU, N. ZHANG, X. YANG, H. ZHANG et W. ZHAO : A Survey on Internet of Things: Architecture, Enabling Technologies, Security and Privacy, and Applications. *IEEE Internet of Things Journal*, 4 (5):1125–1142, Oct 2017. ISSN 2372-2541. 11

[5] A. AL-FUQAHA, M. GUIZANI, M. MOHAMMADI, M. ALEDHARI et M. AYYASH : Internet of Things: A Survey on Enabling Technologies, Protocols, and Applications. *IEEE Communications Surveys Tutorials*, 17(4):2347–2376, Fourthquarter 2015. ISSN 2373-745X. 11

[6] J. A. STANKOVIC : Research Directions for the Internet of Things. *IEEE Internet of Things Journal*, 1 (1):3–9, Feb 2014. ISSN 2372-2541. 11

[7] NORTHSTREAM : Massive IoT: Different Technologies for Different Needs. *White Paper*, 2017. 11

[8] 5G AMERICAS : LTE Progress Leading to the 5G Massive Internet of Things, 2017. 11

[9] Jothi Prasanna Shanmuga SUNDARAM, Wan DU et Zhiwei ZHAO : A Survey on LoRa Networking: Research Problems, Current Solutions and Open Issues. *ArXiv*, abs/1908.10195, 2019. 11, 15, 16, 34

[10] S. CHEN, R. MA, H. CHEN, H. ZHANG, W. MENG et J. LIU : Machine-to-Machine Communications in Ultra-Dense Networks—A Survey. *IEEE Communications Surveys Tutorials*, 19(3):1478–1503, thirdquarter 2017. ISSN 2373-745X. 11

[11] Usman RAZA, Parag KULKARNI et Mahesh SOORIYABANDARA : Low Power Wide Area Networks: An Overview. *IEEE Communications Surveys & Tutorials*, 19(2):855–873, 2017. 11, 22, 24

[12] H. WANG et A. O. FAPOJUWO : A Survey of Enabling Technologies of Low Power and Long Range Machine-to-Machine Communications. *IEEE Communications Surveys Tutorials*, 19(4):2621–2639, Fourthquarter 2017. ISSN 2373-745X. 11

[13] J. C. ZUNIGA : Sigfox system description. *LPWAN@IETF97*, 2016. 11

[14] Lorenzo VANGELISTA, Andrea ZANELLA et Michele ZORZI : Long-Range IoT Technologies: The Dawn of LoRa™. *In 1st EAI International Conference on Future access enablers of ubiquitous and intelligent infrastructures*, pages 51–58, 09 2015. ISBN 978-3-319-27071-5. 11

[15] J. LEE, Y. KIM, Y. KWAK, J. ZHANG, A. PAPASAKELLARIOU, T. NOVLAN, C. SUN et Y. LI : LTE-Advanced in 3GPP Rel.-13/14: An Evolution Toward 5G. *IEEE Communications Magazine*, 54(3):36–42, March 2016. ISSN 1558-1896. 11

[16] M. MEZZAVILLA, M. ZHANG, M. POLESE, R. FORD, S. DUTTA, S. RANGAN et M. ZORZI : End-to-End Simulation of 5G mmWave Networks. *IEEE Communications Surveys Tutorials*, 20(3):2237–2263, thirdquarter 2018. ISSN 2373-745X. 11

[17] D. FLORE : 3GPP Standards for the Internet-of-Things., 2016. 11

[18] INGENU : How RPMA Works? *White paper.*, 2016. 11

[19] William WEBB : Understanding Weightless: Technology, Equipment, and Network Deployment for M2M Communications in White Space, 2012. 11

[20] J. BARDYN, T. MELLY, O. SELLER et N. SORNIN : IoT: The Era of LPWAN is Starting Now. *In ESSCIRC Conference 2016: 42nd European Solid-State Circuits Conference*, pages 25–30, Sep. 2016. 11

[21] SEMTECH : Smart Buildings Transformed Using Semtech's LoRa Technology. *White paper*, 2017. 11, 41

[22] SEMTECH : Smart Cities Transformed Using Semtech's LoRa Technology. *White paper*, 2017. 11, 41

[23] SEMTECH : Revolutionising Smart Agriculture Using Semtech's LoRa Technology. *White paper*, 2017. 11, 41

[24] SEMTECH : Real-World LoRaWAN Network Capacity for Electrical Metering Applications. *White paper*, 2017. 11, 41

[25] SEMTECH : Lora Technology: Mallorca Develops First LoRaWAN Smart Island. *Tech. Rep.*, 2018. 11, 41

[26] SEMTECH : Lora Technology: Transforming Golf Courses With IoT. *Tech. Rep.*, 2018. 11, 41

[27] W. DU, Z. XING, M. LI, B. HE, L. H. C. CHUA et H. MIAO : Optimal Sensor Placement and Measurement of Wind for Water Quality Studies in Urban Reservoirs. *In IPSN-14 Proceedings of the 13th International Symposium on Information Processing in Sensor Networks*, pages 167–178, April 2014. 12, 41

[28] Wan DU, Zikun XING, Bingsheng HE, Lloyd CHUA et Haiyan MIAO : Sensor placement and measurement of wind for water quality studies in urban reservoirs, 02 2015. 12

[29] W. DU, J. C. LIANDO, H. ZHANG et M. LI : Pando: Fountain-Enabled Fast Data Dissemination With Constructive Interference. *IEEE/ACM Transactions on Networking*, 25(2):820–833, April 2017. ISSN 1558-2566. 12

[30] Wan DU, Jansen LIANDO et Huanle ZHANG : When Pipelines Meet Fountain: Fast Data Dissemination in Wireless Sensor Networks. *In 2015 13th ACM Conference*, pages 365–378, 11 2015. 12

[31] Steven J JOHNSTON, Philip BASFORD, Florentin BULOT, Mihaela APETROAIE-CRISTEA, Natasha H. C EASTON, Charlie DAVENPORT, Gavin FOSTER, Matthew LOXHAM, Andrew K. R MORRIS et Simon J COX : City Scale Particulate Matter Monitoring Using LoRaWAN Based Air Quality IoT Devices. *Sensors (Basel, Switzerland) vol. 19,1 209.*, 01 2019. 12, 41

[32] S. J. JOHNSTON, P. J. BASFORD, F. M. J. BULOT, M. APETROAIE-CRISTEA, G. L. FOSTERX, M. LOXHAMZ et S. J. COX : IoT Deployment for City Scale Air Quality Monitoring with Low-Power Wide Area Networks. *In 2018 Global Internet of Things Summit (GIoTS)*, pages 1–6, June 2018. 12

[33] J. PARK, Y. OH, H. BYUN et C. KIM : Low Cost Fine-Grained Air Quality Monitoring System Using LoRa WAN. *In 2019 International Conference on Information Networking (ICOIN)*, pages 439–441, Jan 2019. 12

[34] B. REYNDERS, W. MEERT et S. POLLIN : Range and Coexistence Analysis of Long Range Unlicensed Communication. *In 2016 23rd International Conference on Telecommunications (ICT)*, pages 1–6, May 2016. 12, 32, 41

[35] Ferran ADELANTADO, Xavier VILAJOSANA, Pere TUSET-PEIRO, Borja MARTINEZ, Joan MELIA-SEGUI et Thomas WATTEYNE : Understanding the Limits of LoRaWAN. *IEEE Communications Magazine*, 55 (9):34–40, 2017. 12

[36] Juha PETÄJÄJÄRVI, Konstantin MIKHAYLOV, Marko PETTISSALO, Janne JANHUNEN et Jari IINATTI : Performance of a Low-Power Wide-Area Network Based on LoRa Technology: Doppler Robustness, Scalability, and Coverage. *International Journal of Distributed Sensor Networks*, 13(3), mar 2017. 12, 42

[37] Jetmir HAXHIBEQIRI, Floris Van den ABEELE, Ingrid MOERMAN et Jeroen HOEBEKE : LoRa Scalability: A Simulation Model Based on Interference Measurements. *Sensors*, 17(6):1193, may 2017. 12, 34, 41

[38] CEA-LETI : WSNet Simulator v4.0. https://github.com/CEA-Leti/wsnet/, 2018. 14

[39] Adwait DONGARE, Revathy NARAYANAN, Akshay GADRE, Anh LUONG, Artur BALANUTA, Swarun KUMAR, Bob IANNUCCI et Anthony ROWE : Charm: Exploiting Geographical Diversity through Coherent Combining in Low-Power Wide-Area Networks. *The International Conference on Information Processing in Sensor Networks (IPSN)*, pages 60–71, 04 2018. 16

[40] SEMTECH : SX1301 Transceiver. https://www.semtech.com/products/wireless-rf/lora-gateways/SX1301, 2018. 16, 32

[41] V. HAUSER et T. HÉGR : Proposal of Adaptive Data Rate Algorithm for LoRaWAN-Based Infrastructure. *In 2017 IEEE 5th International Conference on Future Internet of Things and Cloud (FiCloud)*, pages 85–90, Aug 2017. 16, 43

[42] M. SLABICKI, G. PREMSANKAR et M. Di FRANCESCO : Adaptive Configuration of LoRa Networks for Dense IoT Deployments. *In NOMS 2018 - 2018 IEEE/IFIP Network Operations and Management Symposium*, pages 1–9, April 2018. 16, 43, 44, 97, 109

[43] B. REYNDERS, W. MEERT et S. POLLIN : Power and Spreading Factor Control in Low Power Wide Area Networks. *In IEEE International Conference on Communications (ICC)*, pages 1–6, 2017. 16, 43, 44

[44] L. AMICHI, M. KANEKO, N. E. RACHKIDY et A. GUITTON : Spreading Factor Allocation Strategy for LoRa Networks Under Imperfect Orthogonality. *In ICC 2019 - 2019 IEEE International Conference on Communications (ICC)*, pages 1–7, May 2019. 16, 43

[45] F. CUOMO, M. CAMPO, A. CAPONI, G. BIANCHI, G. ROSSINI et P. PISANI : EXPLoRa: Extending the Performance of LoRa by Suitable Spreading Factor Allocations. *In 2017 IEEE 13th International Conference on Wireless and Mobile Computing, Networking and Communications (WiMob)*, pages 1–8, Oct 2017. 16, 43, 44

[46] F. CUOMO, J. C. C. GÁMEZ, A. MAURIZIO, L. SCIPIONE, M. CAMPO, A. CAPONI, G. BIANCHI, G. ROSSINI et P. PISANI : Towards Traffic-Oriented Spreading Factor Allocations in LoRaWAN Systems. *In 2018 17th Annual Mediterranean Ad Hoc Networking Workshop (Med-Hoc-Net)*, pages 1–8, June 2018. 16, 43, 44, 110

[47] Raouf KERKOUCHE, Réda ALAMI, Raphaël FÉRAUD, Nadège VARSIER et Patrick MAILLÉ : Node-Based Optimization of LoRa Transmissions with Multi-Armed Bandit Algorithms. *In 25th International Conference on Telecommunications (ICT)*, pages 521–526, 2018. URL https://doi.org/10.1109/ICT.2018.8464949. 16, 43, 44

[48] Amin AZARI et Cicek CAVDAR : Self-Organized Low-Power IoT Networks: A Distributed Learning Approach. *CoRR*, 2018. URL http://arxiv.org/abs/1807.09333. 16, 43

[49] F. SFORZA : Communication Systems, 2013. URL https://patents.google.com/patent/US8406275. 22

[50] Semtech, 2013. URL https://www.semtech.com/. 22

[51] ETSI EN 300.220 : Electromagnetic compatibility and Radio spectrum Matters (ERM); Short Range Devices (SRD); Radio equipment to be used in the 25 MHz to 1 000 MHz frequency range with power levels ranging up to 500 mW; Part 1: Technical characteristics and test methods Europe. Standard, European Telecommunications Standards Institute, Sophia Antipolis, FR, janvier 2012. 22

[52] Waspmote Sigfox Networking Guide, 2015. URL https://www.libelium.com/downloads/documentation/sigfox_networking_guide.pdf. 23

[53] Rpma Technology for the Internet of Things, 2016. URL https://theinternetofthings.report/all-resources.aspx?Vendor=whitePaper. 23

[54] T. MYERS, D. WERNER, K. SINSUAN, J. WILSON, S. REULAND, P. SINGLER et M. HUOVILA : Light Monitoring System Using a Random Phase Multiple Access System, 2013. URL https://patents.google.com/patent/US8477830. 23

[55] D. FLORE : 3GPP Standards for the Internet of Things, 2016. URL https://www.3gpp.org/news-events/3pp-news/1766-iot_progress. 24

[56] Kais MEKKI, Eddy BAJIC, Frederic CHAXEL et Fernand MEYER : "A Comparative Study of LPWAN Technologies for Large-Scale IoT Deployment". *ICT Express*, 5(1):1 – 7, 2019. ISSN 2405-9595. URL http://www.sciencedirect.com/science/article/pii/S2405959517302953. 24, 25

[57] Weiping SUN, Munhwan CHOI et Sunghyun CHOI : IEEE 802.11ah A Long Range 802.11 WLAN at Sub 1 GHz. *Journal of ICT Standardization*, 1:83–107, 01 2013. 24

[58] T. ADAME, A. BEL, B. BELLALTA, J. BARCELO, J. GONZALEZ et M. OLIVER : Capacity Analysis of IEEE 802.11ah WLANs for M2M Communications. *Lecture Notes in Computer Science*, page 139–155, 2013. ISSN 1611-3349. URL http://dx.doi.org/10.1007/978-3-319-03871-1_13. 24

[59] S. BHANDARI, S. K. SHARMA et X. WANG : Device Grouping for Fast and Efficient Channel Access in IEEE 802.11ah Based IoT Networks. *In 2018 IEEE International Conference on Communications Workshops (ICC Workshops)*, pages 1–6, May 2018. 25

[60] Elodie MORIN : *Interoperability of Adaptive Low Power Consumption Communication Protocol for Sensor Networks*. Theses, Université Grenoble Alpes, avril 2018. URL https://tel.archives-ouvertes.fr/tel-01903194. 25

[61] O. SELLER et N. SORNIN : Low Power Long Range Transmitter, 2014. URL https://patents.google.com/patent/US20140219329A1/en. 27

[62] SEMTECH : AN1200.22 LoRa Modulation Basics. http://wiki.lahoud.fr/lib/exe/fetch.php?media=an1200.22.pdf., 2015. 27, 34

[63] Andrzej Duda MARTIN HEUSSE : LoRa Basics, 2020. Accessed on 2020-4-2. 29, 30

[64] SEMTECH : SX1272/3/6/7/8: Modem Designer's Guide. https://www.semtech.com/uploads/documents/LoraDesignGuideSTD.pdf, 2013. 32

[65] SEMTECH : SX1276 137 MHz to 1020 MHz Low Power Long Range Transceiver. http://www.semtech.com/wireless-rf/rf-transceivers/sx1276/, 2015. 32, 51

[66] C. GOURSAUD et J. M. GORCE : Dedicated Networks for IoT: PHY / MAC State of the Art and Challenges. *EAI Endorsed Transactions on Internet of Things*, 15(1), 10 2015. 33, 42

[67] Jansen C. LIANDO, Amalinda GAMAGE, Agustinus W. TENGOURTIUS et Mo LI : Known and Unknown Facts of LoRa: Experiences from a Large-Scale Measurement Study. *ACM Trans. Sen. Netw.*, 15(2):16:1–16:35, février 2019. ISSN 1550-4859. URL http://doi.acm.org/10.1145/3293534. 34

[68] R. EL CHALL, S. LAHOUD et M. EL HELOU : LoRaWAN Network: Radio Propagation Models and Performance Evaluation in Various Environments in Lebanon. *IEEE Internet of Things Journal*, 6(2):2366–2378, April 2019. ISSN 2372-2541. 34

[69] N. SORNIN, M. LUIS, T. EIRICH, T. KRAMP et O. HERSENT : LoRaWAN Specification v1.0 LoRa Alliance. https://www.lora-alliance.org/resource-hub/lorawantm-specification-v10, 2015. 34, 35, 50, 51

[70] ERTÜRK, AYDIN, BÜYÜKAKKAŞLAR et EVIRGEN : A Survey on LoRaWAN Architecture, Protocol and Technologies. *Future Internet*, 11(10):216, 2019. 35

[71] Shengyang LI, Usman RAZA et Aftab KHAN : How Agile is the Adaptive Data Rate Mechanism of LoRaWAN? *CoRR*, abs/1808.09286, 2018. URL http://arxiv.org/abs/1808.09286. 38, 39

[72] SEMTECH : Smart Parking. *White paper*, 2017. 41

[73] SEMTECH : Smart Lighting. *White paper*, 2017. 41

[74] Mohamed AREF et Axel SIKORA : Free Space Range Measurements with Semtech LoRaTM Technology. *In The 2nd IEEE International Symposium on Wireless Systems within the Conferences on Intelligent Data Acquisition and Advanced Computing Systems*, 2014. 41

[75] J. PETÄJÄJÄRVI, K. MIKHAYLOV, M. HÄMÄLÄINEN et J. IINATTI : Evaluation of LoRa LPWAN Technology for Remote Health and Wellbeing Monitoring. *In 2016 10th International Symposium on Medical Information and Communication Technology (ISMICT)*, pages 1–5, March 2016. 41

[76] Juha PETÄJÄJÄRVI, Konstantin MIKHAYLOV, Antti ROIVAINEN et Tuomo HANNINEN : On the Coverage of LPWANs: Range Evaluation and Channel Attenuation and Model for LoRa Technology. *In 2015 14th International Conference on ITS Telecommunications (ITST)*. IEEE, 2015. 41

[77] A. J. WIXTED, P. KINNAIRD, H. LARIJANI, A. TAIT, A. AHMADINIA et N. STRACHAN : Evaluation of LoRa and LoRaWAN for Wireless Sensor Networks. *In IEEE SENSORS*, 2016. 41

[78] W. SAN-UM, P. LEKBUNYASIN, M. KODYOO, W. WONGSUWAN, J. MAKFAK et J. KERDSRI : A Long-Range Low-Power Wireless Sensor Network Based on U-LoRa Technology for Tactical Troops Tracking Systems. *In 2017 Third Asian Conference on Defence Technology (ACDT)*, pages 32–35, Jan 2017. 41

[79] Lingling LI, Jiuchun REN et Qian ZHU : On the Application of LoRa LPWAN Technology in Sailing Monitoring System. *In 2017 13th Annual Conference on Wireless On-demand Network Systems and Services (WONS)*, 2017. 41

[80] Norbert BLENN et Fernando A. KUIPERS : LoRaWAN in the Wild: Measurements from The Things Network. *CoRR*, 2017. URL http://arxiv.org/abs/1706.03086. 41

[81] T. TO et A. DUDA : Simulation of LoRa in NS-3: Improving LoRa Performance with CSMA. *In 2018 IEEE International Conference on Communications (ICC)*, pages 1–7, May 2018. 41

[82] CATTANI : An Experimental Evaluation of the Reliability of LoRa Long-Range Low-Power Wireless Communication. *Journal of Sensor and Actuator Networks*, 6(2):7, jun 2017. 42

[83] Luca FELTRIN, Chiara BURATTI, Enrico VINCIARELLI, Roberto De BONIS et Roberto VERDONE : LoRaWAN: Evaluation of Link- and System-Level Performance. *IEEE Internet of Things Journal*, 5 (3):2249–2258, jun 2018. 42

[84] A. WARET, M. KANEKO, A. GUITTON et N. EL RACHKIDY : LoRa Throughput Analysis With Imperfect Spreading Factor Orthogonality . *IEEE Wireless Communications Letters*, 8(2):408–411, April 2019. ISSN 2162-2345. 42

[85] Konstantin MIKHAYLOV, Juha PETAJAJARVI et Tuomo HANNINEN : Analysis of Capacity and Scalability of the LoRa and Low and Power Wide and Area Network and Technology. *European Wireless 2016*, European Wireless 2016. 42

[86] Martin BOR, John VIDLER et Utz ROEDIG : LoRa for the Internet of Things. *In Proceedings of the 2016 International Conference on Embedded Wireless Systems and Networks*, EWSN '16, pages 361–366, USA, 2016. Junction Publishing. ISBN 978-0-9949886-0-7. URL http://dl.acm.org/citation.cfm?id=2893711.2893802. 42

[87] Moises NUNEZ, Arturo GUIZAR, Mickael MAMAN et Andrzej DUDA : Evaluating LoRa Energy Efficiency for Adaptive Networks: From Star to Mesh Topologies. *In IEEE 13th International Conference on Wireless and Mobile Computing, Networking and Communications (WiMob)*. IEEE, 2017. 42, 44, 49

[88] Martin C. BOR, Utz ROEDIG, Thiemo VOIGT et Juan M. ALONSO : Do LoRa Low-Power Wide-Area Networks Scale? *In Proceedings of the 19th ACM International Conference on Modeling, Analysis and Simulation of Wireless and Mobile Systems*. ACM Press, 2016. 42, 44

[89] Orestis GEORGIOU et Usman RAZA : Low Power Wide Area Network Analysis: Can LoRa Scale? *IEEE Wireless Communications Letters*, 6(2):162–165, apr 2017. 42

[90] Daniele CROCE, Michele GUCCIARDO, Stefano MANGIONE, Giuseppe SANTAROMITA et Ilenia TINNIRELLO : Impact of LoRa Imperfect Orthogonality: Analysis of Link-Level Performance. *IEEE Communications Letters*, 22(4):796–799, apr 2018. 42

[91] Floris Van den ABEELE, Jetmir HAXHIBEQIRI, Ingrid MOERMAN et Jeroen HOEBEKE : Scalability Analysis of Large-Scale LoRaWAN Networks in NS-3. *IEEE Internet of Things Journal*, 4(6), dec 2017. 43

[92] Jin-Taek LIM et Youngnam HAN : Spreading Factor Allocation for Massive Connectivity in LoRa Systems. *IEEE Communications Letters*, 22(4):800–803, apr 2018. 43

[93] S. ABBOUD, N. EL RACHKIDY, A. GUITTON et H. SAFA : Gateway Selection for Downlink Communication in LoRaWAN. *In 2019 IEEE Wireless Communications and Networking Conference (WCNC)*, pages 1–6, April 2019. 44

[94] Thiemo VOIGT, Martin BOR, Utz ROEDIG et Juan ALONSO : Mitigating Inter-Network Interference in LoRa Networks. *In Proceedings of the 2017 International Conference on Embedded Wireless Systems and Networks*, pages 323–328, USA, 2017. Junction Publishing. ISBN 978-0-9949886-1-4. URL http://dl.acm.org/citation.cfm?id=3108009.3108093. 44

[95] Christelle CAILLOUET, Martin HEUSSE et Franck ROUSSEAU : Optimal SF Allocation in LoRaWAN Considering Physical Capture and Imperfect Orthogonality. *In GLOBECOM 2019 - IEEE Global Communications Conference*, Waikoloa, United States, décembre 2019. URL https://hal.inria.fr/hal-02267218. 44

[96] F. CUOMO, M. CAMPO, E. BASSETTI, L. CARTELLA, F. SOLE et G. BIANCHI : Adaptive Mitigation of the Air-Time Pressure in LoRa Multi-Gateway Architectures. *In 24th European Wireless 2018*, pages 1–6, May 2018. 44, 91, 106, 110

[97] M. N. OCHOA, L. SURATY, M. MAMAN et A. DUDA : Large Scale LoRa Networks: From Homogeneous to Heterogeneous Deployments. *In 2018 14th International Conference on Wireless and Mobile Computing, Networking and Communications (WiMob)*, pages 192–199, Oct 2018. 61

[98] M. N. OCHOA, A. GUIZAR, M. MAMAN et A. DUDA : Toward a Self-Deployment of LoRa Networks: Link and Topology Adaptation. *In 2019 International Conference on Wireless and Mobile Computing, Networking and Communications (WiMob)*, pages 1–7, Oct 2019. 61, 95

[99] Circles Covering Circles. https://www2.stetson.edu/~efriedma/circovcir/, 2015. 65

[100] E. TANGHE, W. JOSEPH, L. VERLOOCK, L. MARTENS, H. CAPOEN, K. V. HERWEGEN et W. VANTOMME : The Industrial Indoor Channel: Large-Scale and Temporal Fading at 900, 2400, and 5200 MHz. *IEEE Transactions on Wireless Communications*, 7(7):2740–2751, July 2008. 66

[101] Arturo GUIZAR, Moises Nunez OCHOA, Valérian MANNONI et Mickael MAMAN : LPWA Deployment for Factory of the Future: LoRa or Turbo-FSK Based Technology? *In 30th IEEE Annual International Symposium on Personal, Indoor and Mobile Radio Communications, PIMRC 2019, Istanbul, Turkey, September 8-11, 2019*, pages 1–6. IEEE, 2019. URL https://doi.org/10.1109/PIMRC.2019.8904355. 66